Exploratory Studies of Photocyclization Mechanisms of Diaryl Derivatives via *o*-Dibenzoquinonemethide Intermediates

by

Cai-Gu Huang
B. Sc., Jiangxi Normal University, 1983
M. Sc., Shanghai Institute of Materia
Medica, Chinese Academy of Sciences, 1986

A Dissertation Submitted in Partial Fulfilment of the
Requirements for the Degree of

DOCTOR OF PHILOSOPHY

in the Department of Chemistry

We accept this thesis as conforming
to the required standard

Dr. P. Wan, Supervisor (Department of Chemistry)

Dr. F. P. Robinson, Departmental Member (Department of Chemistry)

Dr. A. Fischer, Departmental Member (Department of Chemistry)

Dr. L. A. Hobson, Outside Member (Department of Biology)

Dr. J. L. Charlton, External Examiner (University of Manitoba)

University of Victoria

Supervisor: Dr. P. Wan

ABSTRACT

Three classes of new photoreactions were discovered and their reaction mechanisms investigated. These reactions are related in that the same critical *o*-quinonemethide intermediate is involved in the mechanism of each reaction.

The first reaction is the photocyclization of 2-(2'-hydroxyphenyl)benzyl alcohol (**1**) and derivatives to 6*H*-dibenzo[b,d]pyrans (e.g., **7** from **1**), with excellent chemical (>95%) and quantum yields (Φ_p = 0.50 for **7** from **1** in basic solution). Results from investigations of structure-reactivity, pH-effects and fluorescence data suggest that, in neutral solution, the primary photochemical step involves ionization of the phenol moiety to phenolate ion in S_1, which is probably concerted with twisting of the phenyl rings, to give a more planar species in S_1. The subsequent dehydroxylation step of the benzyl alcohol moiety, to give o-quinonemethide **20**, is initiated by a charge transfer from phenolate to the adjacent phenyl ring. The thermal ring closure of **20** competes with nucleophilic solvent (e.g., H_2O or MeOH) capture, to give observed pyran **7** and alcohol **1** (by H_2O) and **5** (by MeOH), respectively. In moderately strong acidic media, acid-catalyzed photosolvolysis occurs, to give carbocation **21** which can also cyclize to afford pyran **7**.

The second photoreaction is the photocyclization reaction of 2-phenoxybenzyl alcohols **22** and **23** to give dibenzo[b,d]pyrans **7** and **29**,

respectively, in aqueous solution. The primary photochemical step is believed to involve initial aryl-O bond homolysis followed by rearrangement to give alcohol **1**, which cyclizes to observed pyran **7** upon secondary photolysis. The *meta*-substituted isomer **24** did not produce cyclized photoproducts, but instead gave isomeric hydroxybiphenyls which are also derived from initial aryl-O bond homolysis followed by simple radical recombination. The photocyclization appears to be general for the *ortho*-phenoxybenzyl alcohol system, in which an appropriate assembly of phenoxy and hydroxymethyl (CH_2OH) functional groups is a necessary requirement. In acidic solution, a competing proton-assisted photosolvolysis reaction, via heterolysis of the benzylic C-OH bond, takes place for all these compounds, to give carbocation intermediates which were subsequently trapped by the solvent.

The last reaction is the photoisomerization of xanthene (**26**) to pyran **7** (~70% yield and Φ_p ~ 0.0035 in aqueous solution). In addition to **7**, 2-benzylphenol (**40**) (Φ = 0.001), 9,9'-bixanthyl (**41**) (Φ < 0.001) and alcohol **1** (Φ < 0.001) were also observed as minor products in the reaction. The photoisomerization is again initiated by aryl-O bond homolysis in S_1, to give a singlet phenyl/phenoxy biradical **48** which undergoes a radical *ipso*-attack on the adjacent phenyl ring, followed by rearrangement to afford *o*-quinonemethide **20**, which cyclizes to form pyran **7** in competition with nucleophilic solvent capture to give **5** (by MeOH). Xanthene derivative **42** also photoisomerizes to the

corresponding pyran derivative **29**, which was obtained in much lower yield due to secondary photochemistry of **29**.

Examiners:

Dr. P. Wan, Supervisor (Department of Chemistry)

Dr. F. P. Robinson, Departmental Member (Department of Chemistry)

Dr. A. Fischer, Departmental Member (Department of Chemistry)

Dr. L. A. Hobson, Outside Member (Department of Biology)

Dr. J. L. Charlton, External Examiner (University of Manitoba)

TABLE OF CONTENTS

LIST OF TABLES

LIST OF FIGURES

LIST OF ABBREVIATIONS

DBD	dibenzo-p-dioxin
ET	electron transfer
GC	gas chromatography
HFIP	1,1,1,3,3,3-hexafluoroisopropyl alcohol
MBA	methoxybenzyl alcohol
MS	mass spectrometry
NMR	nuclear magnetic resonance
μs	microsecond
ns	nanosecond
ps	picosecond
PNBA	*para*-nitrobenzoic acid
Φ_p	product quantum yield
Φ_f	fluorescence quantum yield
Φ_L	quantum yield for loss of starting material
S_1	first singlet excited state
E_T	triplet excited state energy
TLC	thin layer chromatography

Acknowledgement

I would like to thank my supervisor, Dr. Peter Wan, for his guidance and patient encouragement during the course of this work, and his generosity for allowing me to travel and to investigate a wide-range of subjects. I would also like to express my appreciation to colleagues in Wan's group, Eric, Xigen, Pin, Dave, Deepak and more... for their assistance and thoughtful discussions.

Support from my family and my wife made this work possible.

Dedication

To Mother and Father

CHAPTER ONE: Introduction

1.1 General

The photon is a unique and clean reagent. Absorption of a photon by a ground state organic molecule produces an electronically excited state species. This excited species possesses an *excess* energy content and can readily undergo photochemical reactions before deactivating back to the ground state. Developing new photochemical reactions and studying their mechanisms has always been of paramount concern to organic photochemists. Of utmost importance in elucidating photoreaction mechanisms is to understand the nature of the primary photochemical event. There are a limited number of primary photochemical processes available for photoexcited organic molecules; the most commonly encountered being a unimolecular fragmentation process via initial bond homolysis. This process, along with the less common bond heterolysis, will be particularly relevant to this investigation and thus a few additional comments are worthwhile.

$$R\text{-}X \xrightarrow{h\nu} R^{\cdot}\cdot X \longrightarrow \text{radical-derived product} \qquad (1.1)$$

$$R\text{-}X \xrightarrow{h\nu} R^{+}\ X^{-} \longrightarrow \text{ion-derived product} \qquad (1.2)$$

By definition, homolysis is a bond cleavage process which generates a radical pair and subsequently leads to radical-derived products (eq. 1.1), whereas

heterolysis leads to an ion pair, which gives rise to ion-derived products (eq. 1.2). For a given bond, these two processes may occur in competition with one another or one process may predominate or even occur exclusively, depending on the inherent character of the specific bond and the associated chromophore. The nature of the medium may also have a significant impact on these two processes as well as on the fates of the photogenerated radical and ion pairs (i.e., their subsequent thermal reactions). Thus, by varying the solvent system, photoreactions may be modified to follow an otherwise less desirable pathway. For example, use of water - a polar and powerful ionizing solvent - can facilitate the heterolysis process considerably, by increasing the solvation energy of the ion pair.

This thesis is concerned with three classes of highly solvent dependent photochemical reactions, in which either the bond heterolysis or bond homolysis process is involved in the primary photochemical step. One of these photoreactions, initiated via bond heterolysis, is concerned with the photosolvolysis of benzyl alcohols. The other two, initiated by bond homolysis, fall into the category of photorearrangement of diaryl ethers. A review of the literature background of photosolvolysis in general and the photochemistry of diaryl ethers is given below.

1.2 Photosolvolysis

Photosolvolysis proceeds via heterolysis of a carbon-leaving group

$$R\text{-}X \xrightarrow{h\nu} R^{+}\ X^{-} \xrightarrow[HS]{\text{solvent}} RS + HX \quad .. \quad (1.3)$$

(nucleofuge) bond, to generate an ion pair. The solvent, acting as the nucleophile, then captures the carbocation intermediate, to give the solvolysis product **RS** (eq. 1.3). This class of photoreaction has received much less attention compared to those proceeding via photoinduced homolysis. Of all the photosolvolytic reactions studied so far, the benzene chromophore has been frequently used, with the simple benzyl derivatives most extensively investigated. The details of structure-reactivity relationships and substituent, leaving group, solvent and catalytic effects are now well-documented.[1] However, only during the last decade has the use of hydroxide ion as a leaving group been recognized as a useful and unique approach to probe the nature of the photosolvolytic reactions. The photosolvolysis of benzyl alcohols (hereby known as "photodehydroxylation", because the primary step is believed to involve loss of hydroxide ion from substrate) is particularly appealing since these alcohols have demonstrated unique photobehavior in aqueous solution.[2] The topic of photodehydroxylation will be reviewed in section 1.3.

Interest in photosolvolytic reactions dates back to as early as the turn of this century. Lifschitz and Hantzsch[3-5] noted that leuco base **Ia** and its derivatives, upon irradiation with an iron-arc source, underwent C-C bond heterolysis to give

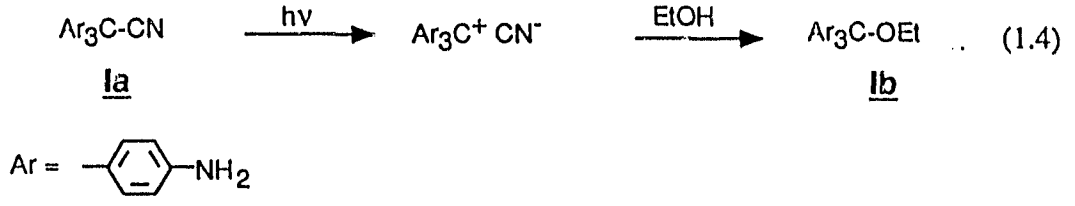

a coloured cation and the cyanide ion. The carbocation can be trapped by a nucleophilic solvent such as ethanol, to give the photosolvolytic product **Ib** (eq. 1.4). In this case, the photogenerated carbocation (in the ground state) is quite long-lived since it is stabilized by the aryl rings substituted with electron-donating amino groups. Subsequent studies of photosolvolysis centred on the photogeneration of stable carbocations while the mechanism of these reactions was not clearly elucidated in most cases.[1]

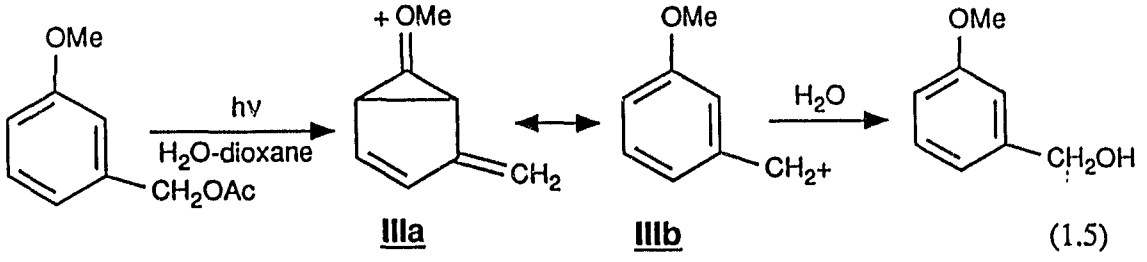

Three decades ago, Zimmerman and Sandel[6] reported what is now regarded as a classical example of a photosolvolysis reaction for simple benzyl derivatives, which impacted greatly on the development of the field of photosolvolysis. They found that irradiation of *meta*- and *para*-methoxybenzyl acetates gave essentially solvolytic products in aqueous dioxane (eq. 1.5), but afforded mainly radical-

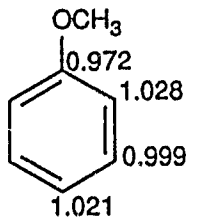

IIa (ground state)

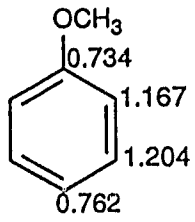

IIb (excited state)

derived products in 100% dioxane. The *meta*-methoxybenzyl acetate (Φ = 0.13) photosolvolyzed about ten times more efficiently than the corresponding *para* isomer (Φ = 0.016). In the ground state, the relative reactivity is *reversed.* As an attempt to rationalize these observations, the authors calculated the electron densities at the aromatic carbons (using LCAO-MO theory) for the ground and first excited electronic states of benzene with substituents capable of donating a lone pair of electrons. In the case of anisole, they found that the aromatic positions with highest electron densities were the *ortho* and *para* positions in the ground state as expected, and were the *meta* and *ortho* positions in the excited states (see **IIa** and **IIb**). They termed this gain of electron density at the *meta* position in the excited state as a "*meta*-electron transmission" effect, now simply known as the "*meta* effect". The authors further indicated that structure **IIIa** was a resonance structure of the benzyl cation **IIIb** in the excited state (eq. 1.5). Although both *meta*- and *para*-methoxybenzyl acetates produced to some extent radical-derived products in aqueous dioxane, 3,5-dimethoxybenzyl acetate gave exclusively the photosolvolysis product, indicating an additive electron-donating effect of two methoxy substituents.

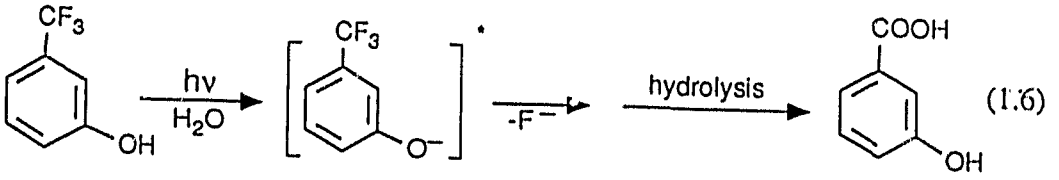

(1.6)

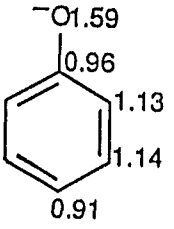

IV (excited state)

The so-called "*meta* effect" has also been observed in photohydrolysis of trifluoromethyl-substituted phenols. Grinter et al.[7] reported that *m*-hydroxy benzotrifluoride in neutral or alkaline solution reacted faster than the *p*-hydroxy isomer, to yield the corresponding acid (eq. 1.6). Wirz and Seiler[8,9] further demonstrated that this photohydrolysis proceeded via the singlet excited state of the phenolate ion, in which the primary step involved loss of a fluoride ion from the benzyl position, to generate an *o*-quinonemethide intermediate. The theoretical calculation for the first excited state phenoxide anion indicated that the electron densities at *ortho* and *meta* positions were again higher than that at the *para* position,[9] as shown in IV. This prediction is consistent with the observation that *meta*-trifluoromethyl phenoxide photohydrolyzed significantly faster than the *para* isomer. In addition, these authors investigated the photohydrolysis of a series of trifluoromethyl-substituted naphthols in aqueous solution (pH = 12-14). These

studies clearly reveal that the phenolic hydroxyl group or the phenoxide anion (phenolate ion) is a powerful electron-donating group, and could be used to promote the photosolvolysis of the strong C-F bond.

As an attempt to study the rearrangement of carbocations generated from the triptycene derivatives (e.g. **Va**), Cristol et al.[10-12] reported that photolysis of deuterium-labelled bromohomotriptycene (**Va**) in aqueous acetone gave a solvolytic product **Vb** and a rearranged product **Vc**. The compound **Vc** is derived from a Wagner-Meerwein rearrangement of the initially formed carbocation (eq. 1.7).

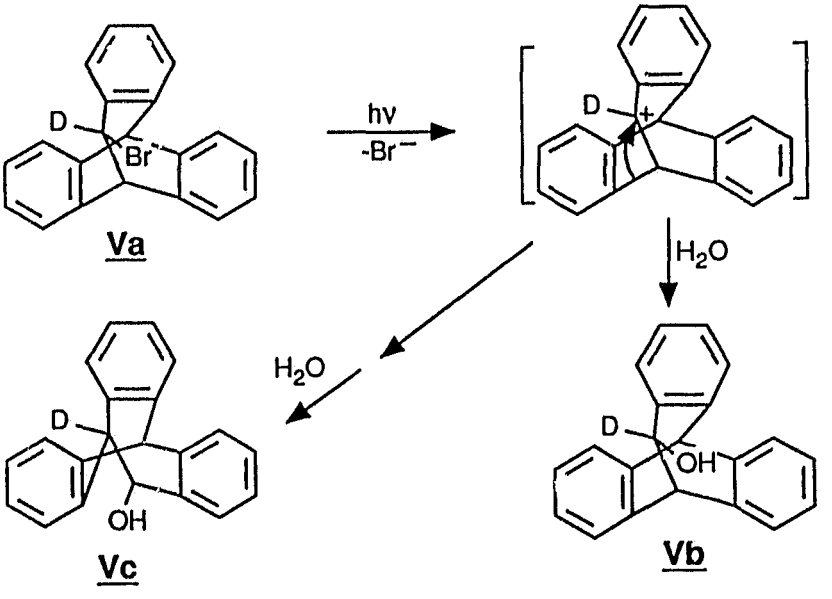

(1.7)

As discussed above, photosolvolyses of numerous benzyl systems have been studied in detail. On the other hand, the first example of photosolvolysis involving carbocations of a β-arylethyl (homobenzyl) system was reported by Jaeger[13a] only in 1976. He found that irradiation of **VIa** in 50% aqueous methanol afforded the

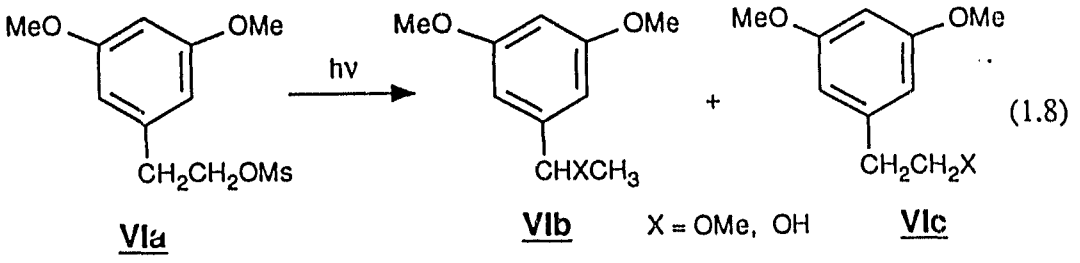

alcohol **VIb**-OH and methyl ether **VIb**-OMe along with a small amount of **VIc**-OH and **VIc**-OMe (eq. 1.8). This photosolvolysis reaction is of particular interest since the substituent OMe can photoactivate a remote functional group (OMs). Thus Cristol[13b] and Morrison[13c] and their respective coworkers have in subsequent studies devoted a considerable effort in elucidating the mechanism of this reaction. Cristol

Scheme 1.1

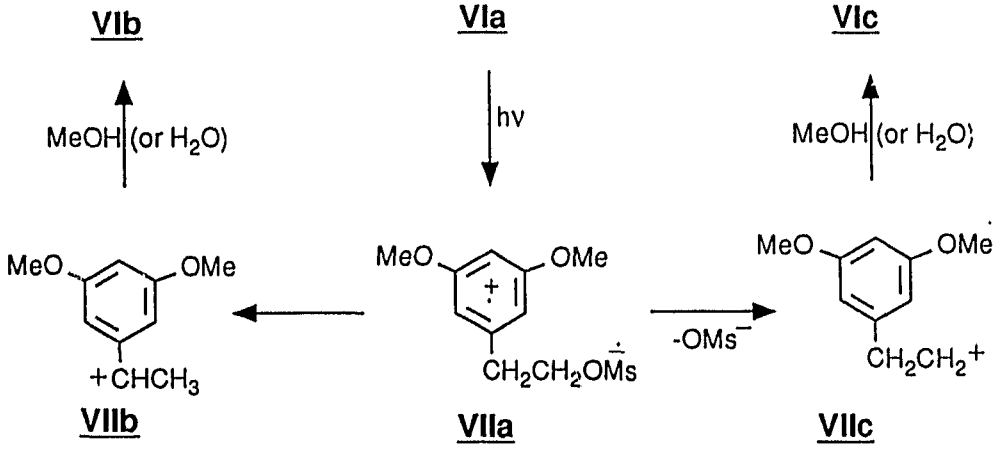

et al.[13b] have proposed that the activation of a remote functional group occurs via intramolecular electron transfer from the photoactivated aromatic ring to the leaving

group (OMs) to produce a zwitterionic biradical **VIIa** (Scheme 1.1). The zwitterionic biradical may suffer two fates. Migration of a hydrogen at the benzyl position, concerted with methanesulfonate loss, may occur, to give the cation **VIIb** which eventually gives rise to **VIb.** Alternatively, **VIIa** could lose methanesulfonate without an attendant migration to give the cation **VIIc**, which leads to **VIc.**

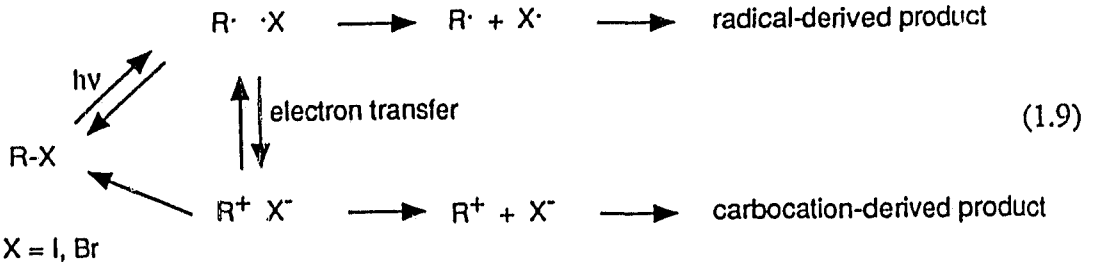

(1.9)

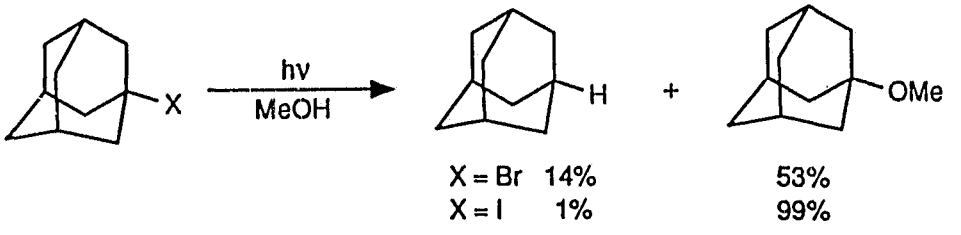

(1.10)

Another class of interesting photosolvolytic reaction involves the photoinduced homolysis of a carbon-halogen bond, followed by electron transfer in the initially formed radical pair, to produce a carbocation intermediate, as shown in eq. 1.9.[14,15] Kropp et al.[15] have shown that irradiation of 1-iodo and 1-bromoadamantane in MeOH affords a mixture of radical and ionic products, with

the latter usually dominating (eq. 1.10). This has been shown to be a convenient and powerful method for the generation of carbocations, including many that are not readily accessible by classical, ground-state procedures, such as bridged cations. The reaction is also of synthetic interest since the ionic-derived products are usually obtained in high yields. Very recently, Kropp et al.[15] further found that by adding hydroxide ion into the solvent MeOH, the ionic photobehavior and good material balances of alkyl bromides (which are less expensive and more readily available) was greatly improved. The authors proposed that the hydroxide ion served as an efficient scavenger for the byproduct HBr while giving minimal competing photoreduction via electron transfer to the alkyl bromide. The alkyl bromides have previously displayed disappointing ionic photobehavior in solution, usually affording lower material balances and substantially higher yields of radical-derived products.[16,17]

1.3 Photodehydroxylation of Benzyl Alcohols

The photodehydroxylation of benzyl alcohols where the hydroxide ion acts as the leaving group in the photosolvolysis has been well-established by Wan's group in the 1980's.[2] The use of hydroxide ion as a leaving group in photosolvolysis provides several advantages: (i) benzyl alcohols are generally more soluble than halogen derivatives in aqueous solution, where heterolysis is generally preferred over homolysis, by lowering the activation energy for heterolytic cleavage

due to stabilization of the ion pair; (ii) catalytic studies due to acid (or base) become feasible since one can work in aqueous solution and the fact the hydroxyl group can interact with solvent water or proton source; (iii) the hydroxide ion has been proven to be an excellent and clean leaving group in the excited state,[2] but is known as a poor one in the ground state. Thus in most cases, the compounds studied are exceptionally unreactive in the ground state, enabling their photosolvolysis to be studied with ease. Wan et al.[18,20,22,23,29] have disclosed several interesting benzyl alcohol systems which undergo efficient photosolvolysis. These include the adiabatic generation of an excited carbocation from 9-phenylxanthene-9-ol (**VIII**),[18] the photosolvolysis of 9-fluorenol (**VIV**) to generate a carbocation believed to possess "aromatic" character in the excited state,[29] and the photosolvolysis of the geometrically flexible biphenyl system **1** (the details of which will be reported in this thesis).[20]

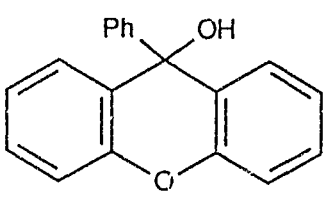

VIII

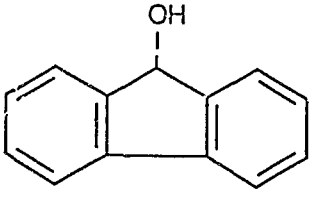

VIV

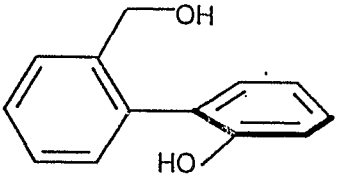

1

Ullman and coworkers[21] reported the first example of photosolvolysis of a benzyl alcohol via initial charge-transfer. They found that photolysis of compound **Xa** in methanol gave methyl ether **Xb** (39%). The reaction occurred even when

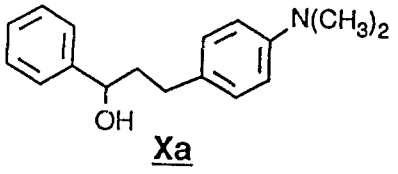

Xa

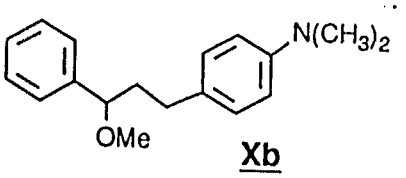

Xb

employing light (>300 nm) that was not significantly absorbed by the phenyl chromophore. The photochemical reaction apparently requires both an electron acceptor (phenyl) and donor (dimethylaminophenyl). The authors proposed the following mechanism to account for their observations. The first step is a

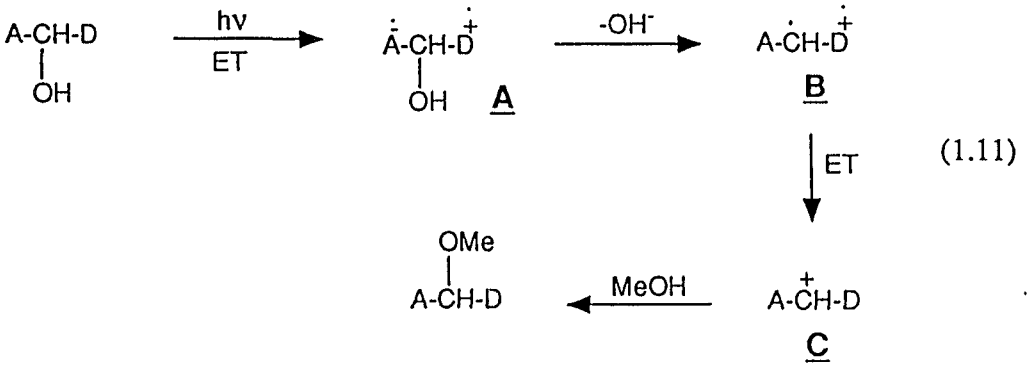

(1.11)

A: electron acceptor, α-phenyl ring group

D: electron donor, dimethylaminophenyl group

photoinduced electron transfer (ET) from the amino group to the α-phenyl-ring (eq. 1.11). The initially formed intermediate A presumably expels the hydroxide ion

to give **B**. This species is reoxidized by the electron deficient donor to give a ground state carbocation **C**. The solvent MeOH then captures carbocation **C**, which results in the formation of solvolytic product, methyl ether **Xb** (eq. 1.11).

Turro and Wan[22] were the first to study the photochemical and photophysical behavior of a number of methoxy-substituted benzyl alcohols in aqueous solution. They found that on excitation to the singlet excited state, the *ortho*- and *meta*-methoxy benzyl alcohols underwent acid-catalyzed (proton-assisted) loss of hydroxide ion (dehydroxylation), to give the corresponding benzyl cations. This was the first demonstration of photosolvolysis with novel catalytic effects due to the hydronium ion. In a subsequent investigation, Wan et al.[23] further investigated structure-reactivity relationships and catalytic effects in the photosolvolyses of several methoxy, dimethoxy and hydroxyl-substituted benzyl alcohols in aqueous solution. The authors found that the primary photochemical event was

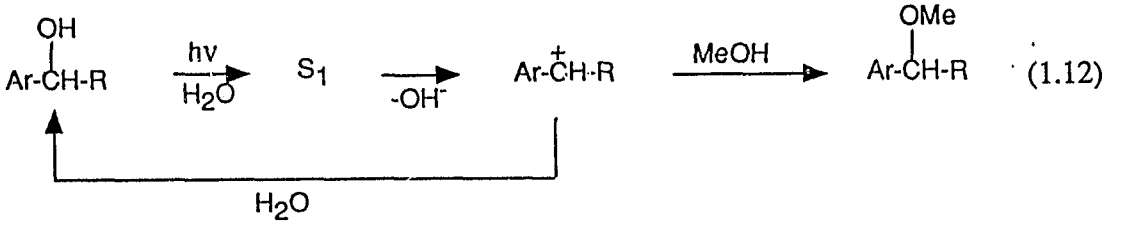

(1.12)

photodehydroxylation, to give a benzyl cation intermediate, which can be trapped by added external nucleophiles such as alcohols or cyanide ion (eq. 1.12). The proposal of singlet state reactivity was based on observation of fluorescence

quenching by acid concurrent with enhanced quantum efficiency for the formation of photosolvolytic product. In these studies, the "*meta* effect" was again observed, that is, *meta*-methoxybenzyl alcohol was found to undergo moderately efficient photosolvolysis, while the *para* isomer exhibited no reaction.[22,23]

Scheme 1.2

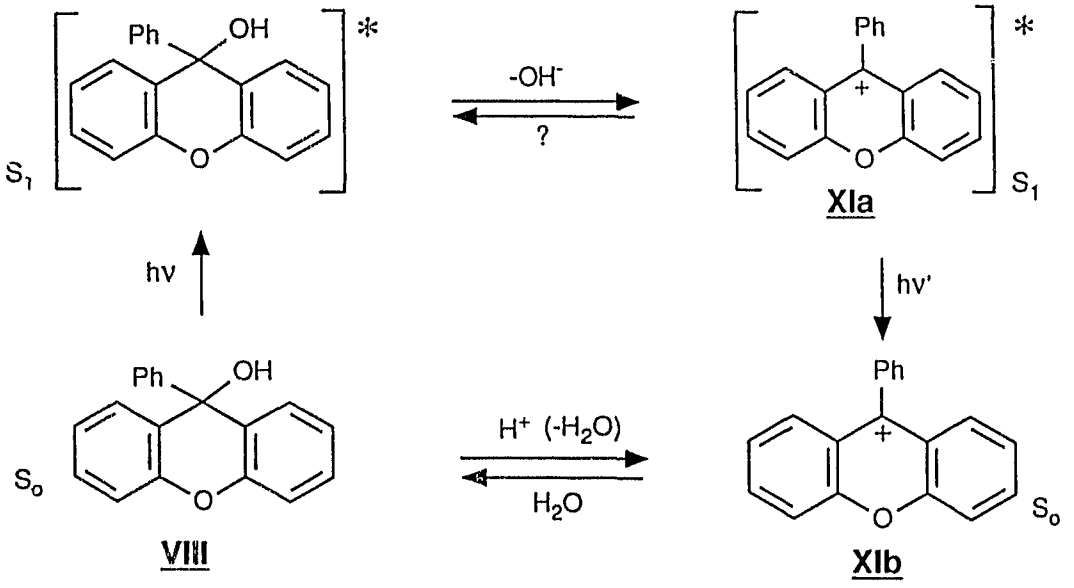

Not addressed in these studies is the question of adiabaticity of the primary photodehydroxylation step, i.e., whether the carbocation so generated is on the S_1 surface (adiabatic process[24]) or is funnelled down to the ground state surface (diabatic process[24]). An approach to detect adiabaticity of photodehydroxylation is to observe fluorescence emission of the *initially* formed carbocation. Since

carbocations generated from simple benzyl alcohols would be expected to be very short-lived, fluorescence emissions from these excited carbocations have not been detected. In an attempt to directly obtain fluorescence emission from a photogenerated excited carbocation, Wan et al.[18,19] used the structurally rigid xanthene system which is known to be highly fluorescent in many examples. They found that the singlet excited alcohol **VIII** (Scheme 1.2) underwent adiabatic photodehydroxylation in aqueous solution to give the excited state carbocation **XIa** with a weak fluorescence emission with a maximium at 507 nm. A mechanistic scheme for photosolvolysis of alcohol **VIII** in aqueous methanol is shown in Scheme 1.2. These authors proposed that the *ortho*-oxygen might play the electron-donating role in the singlet excited state. This is a new class of adiabatic photochemical reactions. Studies of adiabatic photoreactions are particularly interesting since these types of reactions are rare. This discovery stimulated several further investigations of this photoreaction by laser flash photolysis.[25,26] For example, Das et al.[25] observed the transient absorption of the excited carbocation **XIb** generated from parent alcohol **VIII** and found that only a small portion of carbocation (1%) was produced on the excited state surface.[26]

The above adiabatic photoreaction appears to be general for related xanthene-9-ol systems. Very recently, Wan and Shukla[27] studied 9-phenyl-thioxanthene-9-ol (**XII**) and derivatives in aqueous solution. Again, adiabatic photodehydroxylation was observed as indicated by detection of fluorescence

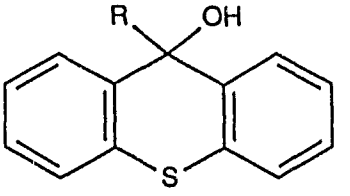

XII

R = Me, Ph

emission from the corresponding excited state carbocation, under conditions where the ground state alcohol was non-reactive.

In an effort to examine photosolvolyses of benzyl alcohols structurally related to the xanthene system, Wan and coworkers[28,29] studied 9-fluorenol (**VIV**) and derivatives. They observed that alcohol **VIV** - which clearly lacked any electron-donating group to drive the photosolvolytic reaction - photosolvolyzed efficiently in aqueous MeOH. The primary photochemical event is believed to be heterolytic cleavage of the benzylic C-OH bond, to give the carbocation **XIIIa**,

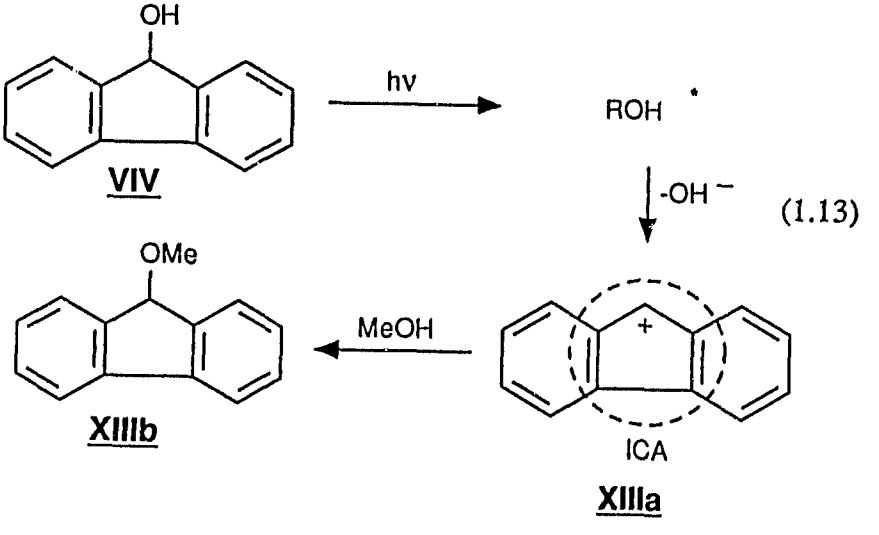

which can be captured by water, or MeOH to afford methyl ether **XIIIb** (eq. 1.13). It was found that 9-fluorenol derivatives photosolvolyzed much more efficiently than any of the related systems. The reactivity trend can be rationalized by simply counting the maximum contributing number of electrons in the internal cyclic array (ICA) in the incipient carbocation (e.g., **XIIIa**). An electron count of four (4) π electrons is the most favourable, and the least reactive system is that in which the incipient carbocation has six (6) π electrons in the ICA. The carbocation with 4 π electron might display somewhat "aromatic" character in the singlet excited state. However, the adiabaticity of this photoreaction could not be confirmed as no fluorescence emission from the excited fluorenyl cation was detected.[29] However, this work has recently attracted the attention of other groups. Thus there has been a number of studies aimed at characterizing the proposed fluorenyl cation intermediate and probing its reactivity by laser flash photolysis.[30-32] Hilinski[31] observed, using picosecond laser flash photolysis, the transient absorption spectrum of this cation with λ_{max} at 515 nm. The lifetime of the fluorenyl cation in 9:1 H_2O-MeOH was estimated to be less than 20 ps. McClelland et al.[32], in an independent investigation, further confirmed that the transient at 515 nm was indeed from the fluorenyl cation **XIIIa**. They also found that this cation is a relatively long-lived species in 1,1,1,3,3,3-hexafluoroisopropyl alcohol (HFIP) (~30 μs) due to the remarkably weak nucleophilicity of HFIP. Additional studies also show that **XIIIa** undergoes electrophilic attack on benzene to give 9-phenylfluorene in competition

with capture by HFIP.[32]

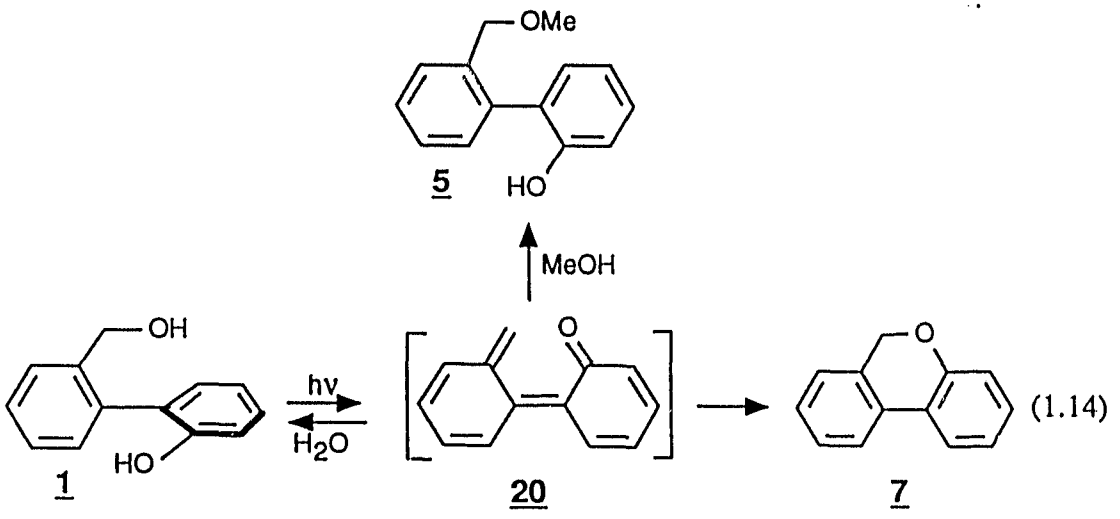

In all of the photosolvolytic studies discussed so far, the substrates examined are either simple benzyl derivatives or possess a structurally rigid backbone. The photosolvolysis of geometrically flexible systems such as biphenyl derivatives has not been reported. Chapter Two of this thesis is concerned with the photosolvolysis of such systems. We show that biphenyl alcohol **1** undergoes efficient photosolvolysis to give methyl ether **5** and 6*H*-dibenzo[b,d]pyran (7) on irradiation in aqueous MeOH (eq. 1.14).[20]

The ground and excited state geometry as well as the photochemistry of 2-substituted biphenyl derivatives are particularly relevant to photosolvolysis of 2-substituted biphenyls in the current investigation. A review of these topics, with attention focused on photocyclization reactions of 2-vinylbiphenyls, is given below.

1.4 Photocyclization of 2-Substituted Biphenyls

Over the last half of this century, there have been numerous studies pertaining to the ground state conformation of the parent biphenyl and substituted biphenyls. In general, ground state biphenyls have large twisted dihedral angles between the two aryl rings in solution and in the solid state.[33a] The parent biphenyl possessing a planar geometry in the *solid state* is an exceptional case.[33b] A variety of methods has been used to probe the geometry of biphenyls, including X-ray diffraction, UV, NMR and dipole moment measurements.[34] For *o,o'*-disubstituted biphenyls, the dihedral angles are estimated as large as 70-80°.[35] Simple molecular mechanics calculations[36] also support the significantly twisted geometry of *o,o'*-disubstituted biphenyls such as alcohol **1** and its derivatives.

However, in the excited state, biphenyls have a tendency to adopt a more planar geometry.[37-42] A simple rationalization for this effect is that the LUMO of biphenyl (assuming a completely planar π-system) has more double bond character between the two atoms joining the two benzene rings than the HOMO. Hoffman et al.[38], using a π-electron SCF and SCF-CI calculation, demonstrated that planar biphenyl in the lowest singlet excited state was of minimum energy, as shown in Figure 1.1. These authors assumed that the H-H interactions were the same in all states, and so the excited state preference was a direct consequence of the lower π-electron energy. That is, on excitation, the 1-1' and 2-3 bonds are

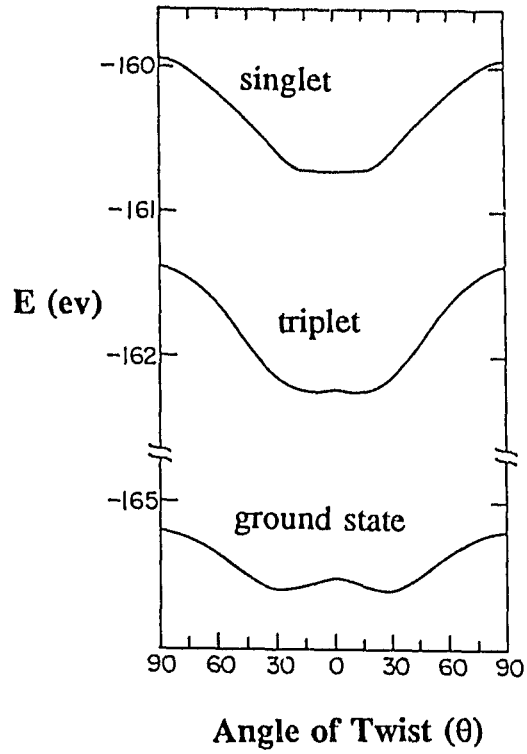

Figure 1.1. Total energy vs angle of twist for the ground state and lowest singlet and triplet excited states of biphenyl. Note the energy scale is interrupted.[38]

strengthened and the 1-2 and 3-4 bonds are weakened. This is apparent in the calculated bond orders and the quinoid valence structure for the excited state shown in **XIV**. In addition, the large Stokes shift and increased vibrational fine structure in the fluorescence emission of biphenyl is also indicative of a more planar geometry.[39]

As mentioned above, excited state biphenyls prefer a more planar geometry. However, only a few photochemical reactions are known which take full advantage of this tendency towards planar conformation. Two such types of photoreactions,

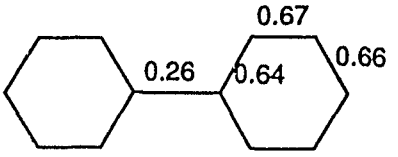

Ground State

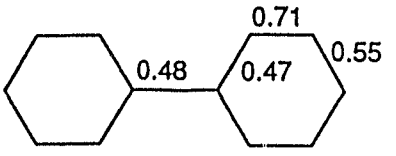

Excited State

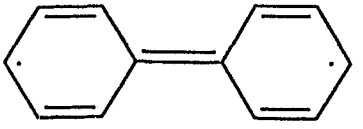

XIV

namely photoracemization of appropriately substituted biphenyls and photocyclization of 2-vinyl biphenyls, which are relevant to the current study will be discussed below.

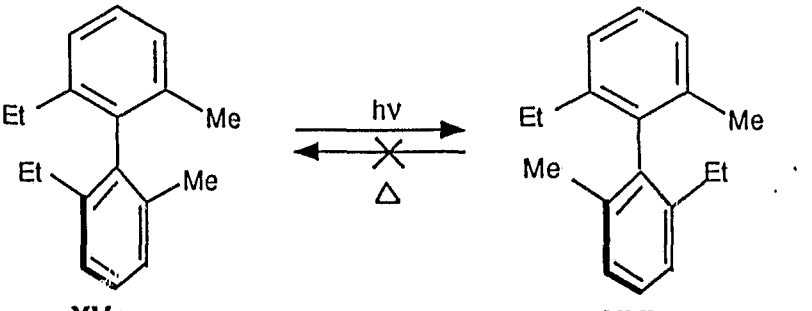

XVa **XVb**

To delineate the importance of geometrical change in the excited state, Zimmerman and coworker[40] accomplished a photochemical racemization of optically active 2,2'-dimethyl-6,6'-diethylbiphenyl (**XVa**). Interconversion of

enantiomers in the excited state (via a "planar" species) is understood on a MO basis as deriving from an enhanced excited state central bond order (e.g., strengthened 1-1' bond and thus more planar geometry). Biphenyl **XVa** was found to be exceptionally stable to thermal racemization.

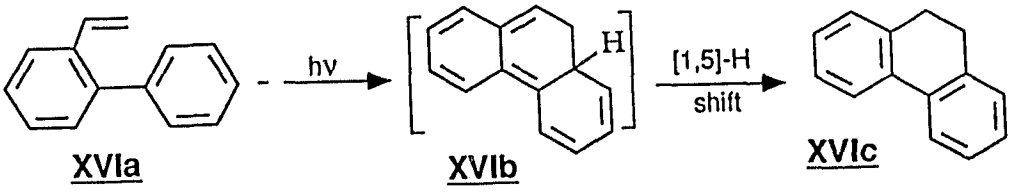

XVIa **XVIb** **XVIc** (1.15)

The photocyclization of 2-vinylbiphenyls has been well studied.[43-53] For example, upon direct excitation, 2-vinylbiphenyl **XVIa** twists rapidly to a planar geometry and then undergoes a 6π electrocyclic ring closure reaction followed by a thermal 1,5-hydrogen shift to give dihydrophenanthrene derivative **XVIc** in quantitative chemical yield (eq. 1.15).[43] This photochemical reaction has been used for the synthesis of cannabinols.[43] A laser flash photolysis study revealed that the first step of the photocyclization was indeed the formation of a cyclic polyene **XVIb**.[44] The quantum yield of the reaction depended greatly on the structure as well as the initial geometry of the biphenyls and can be rather large (e.g., $\Phi = 0.2 - 0.4$). In addition, the photocyclization may occur from either the excited singlet or triplet state.[44-46] The singlet cyclization, occurring exclusively from planar biphenyl, is an anticipated concerted conrotatory 6π electrocyclic ring closure and

hence is stereoselective.[45,46] The triplet cyclization is stereoselective only when occurring from the planar geometry, but could be non-stereoselective when occurring from a fast equilibrium between the planar and perpendicular biphenyl.[45,46] Bonneau et al.[46] reported that, under sensitization by xanthone, the first step of the photocyclization of 2-vinyl biphenyl derivatives was an adiabatic reaction to give the triplet state of the cyclic polyene (e.g., **XVIb**). The triplet of the polyene decays to the singlet ground state with a lifetime of about 550-750 ns. This adiabatic photoreaction is energetically possible because of the relatively high

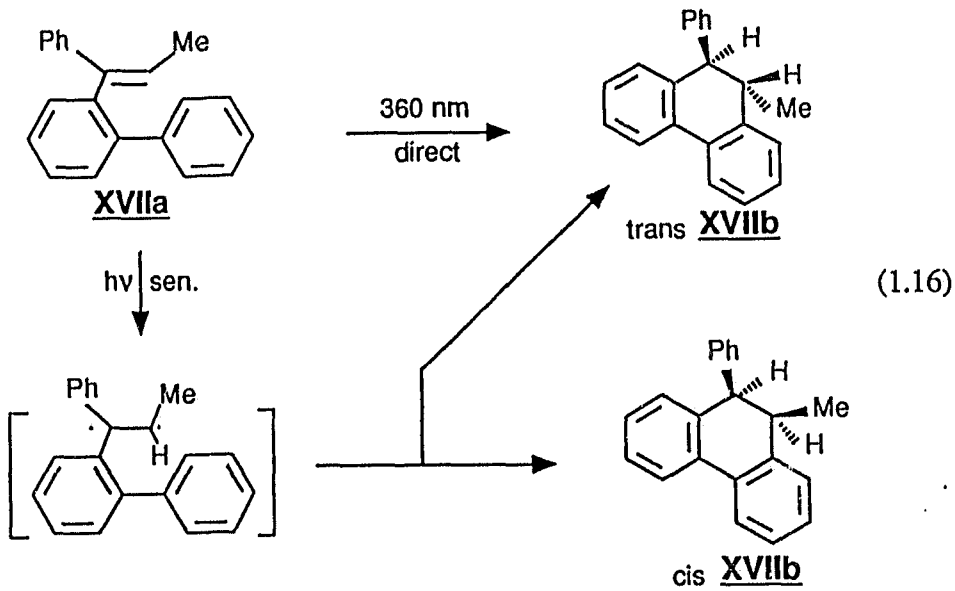

(1.16)

triplet energy of these biphenyls (~65 kcal mol^{-1}) and the low triplet energy of the cyclic polyene (~50 kcal mol^{-1}).[46] Lapouyade et al.[47] found that direct irradiation of compound **XVIIa** (*E*-Me isomer) gave only *trans*-**XVIIb**, whereas the triplet-sensitized photolysis of **XVIIa** (both *E*-Me and *Z*-Me isomers) yielded both *cis*-

and *trans*-**XVIIb** (eq. 1.16). These results are in general agreement with the stereoselectivity of this reaction discussed above.

Scheme 1.3

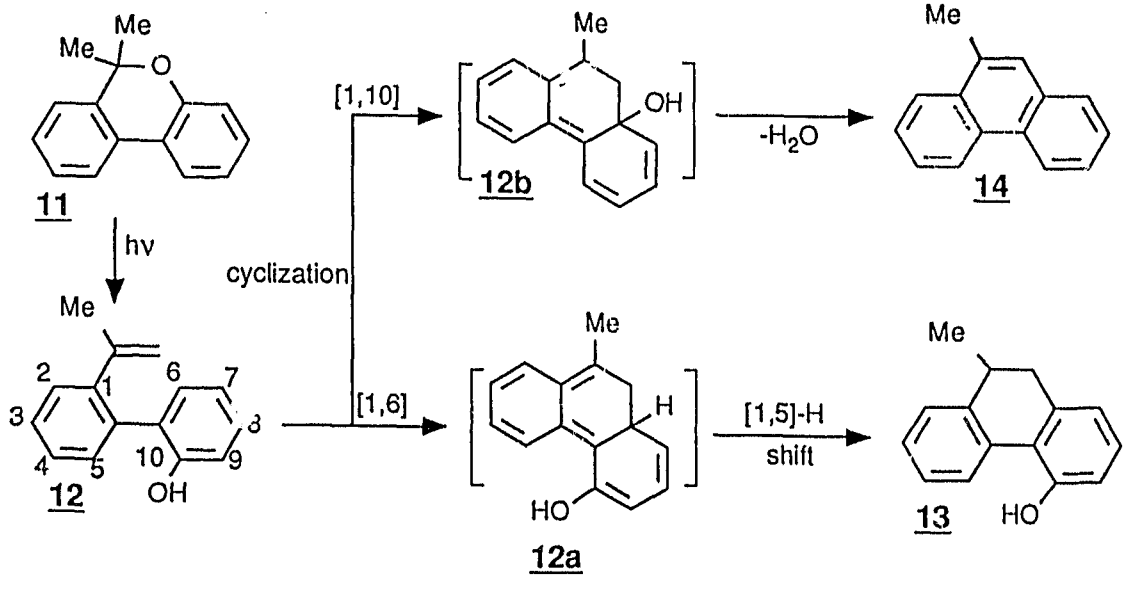

Substituents at the 2'-position are sometimes lost in the overall photocyclization.[48-50] Bowd et al.[48,49] reported that irradiation of **11** in ethanolic solution gave three products **12-14**, as shown in Scheme 1.3. The first photochemical step, an electrocyclic ring opening of dibenzopyran **11**, has an analogue in the photoreaction of 2,2-dimethylchromenes, which will be discussed below. The 2-vinylbipenyl **12** has two possible modes of photocyclization available due to the presence of the 2'-hydroxyl substituent. One mode of electrocyclic reaction occurs between the positions designated 1 and 6, presumably

via an intermediate **12a**, which subsequently undergoes a thermally allowed 1,5-hydrogen shift to give **13**. However an alternative photocyclization route involves the positions designated 1 and 10, via intermediate **12b**, which undergoes 1,2-elimination of water to form **14**.

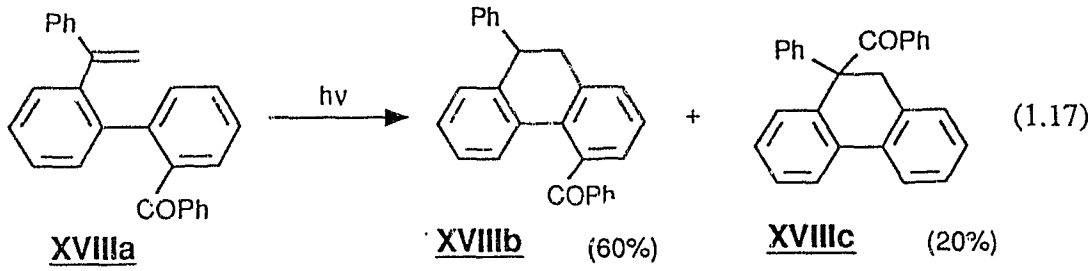

XVIIIa **XVIIIb** (60%) **XVIIIc** (20%) (1.17)

Substituents at the 2'-position may undergo a sigmatropic shift instead of elimination. Padwa et al.[51] reported that irradiation of benzophenone **XVIIIa** in benzene with 365 nm light furnished a mixture of two isomeric ketones **XVIIIb** (60%) and **XVIIIc** (20%) (eq. 1.17). The ketone **XVIIIc** is apparently derived from a 1,5-carbonyl group sigmatropic shift of an initially formed photocyclization product.

Several examples are known of 2-substituted isonitrile or isocyano biphenyls which also form cyclized products on irradiation.[52,53] Swenton et al.[53] studied the effect of biphenyl geometry on the efficiency of the photocyclization reaction of 2-isocyano substituted biphenyls. The authors proposed that the approach to planarity in the excited state biphenyl would favour bond formation between the

ortho position of the biphenyl and an unsaturated *ortho*'-substituent.

1.5 *o*-Quinonemethide Intermediates

As will be demonstrated in the subsequent chapters of this thesis, the photochemical reactions studied all proceed via the same crucial *o*-quinonemethide type of intermediate. A general review of these intermediates is given below.

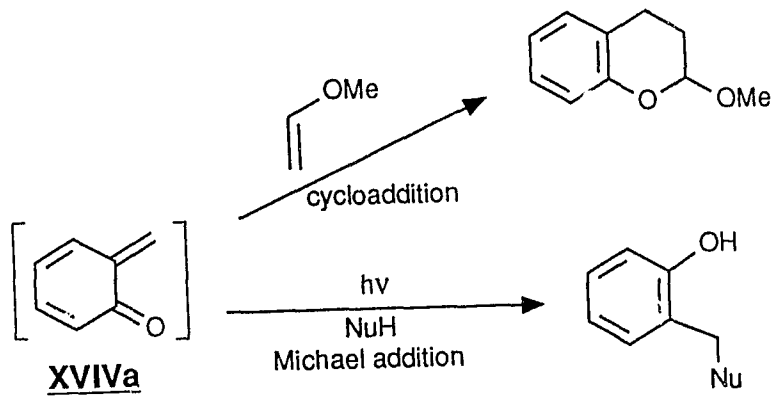

XVIVa (1.18)

The parent *o*-quinonemethide **XXIVa** is believed to be an important intermediate in biological systems.[54a-c] For instance, such an intermediate has been proposed as an alkylating agent generated *in vivo* from appropriately substituted quinones in a bioreductive activation process.[54] A variety of methods has been developed to generate this intermediate from different precursors such as o-(hydroxylmethyl)phenols[55b] or (trimethylsilyl)methyl-1,4-benzoquinones.[55d] The reactivity of such an intermediate is characterized by Michael additions (with nucleophilic reagents NuH)[55d] as well as by Diels-Alder cycloadditions (with

dienophiles)[55c] to the enone moiety (eq. 1.18). The intramolecular Diels-Alder reaction of an *o*-quinonemethide with a dienophile is usually stereospecific and of synthetic interest.[55e]

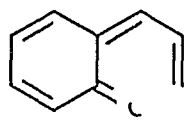

XVIVb

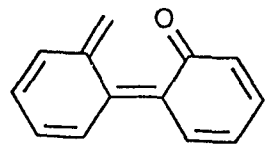

20

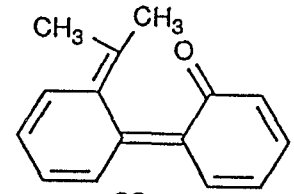

20a

o-Quinonemethides such as **XXIVb** have received less attention than the parent **XXIVa**. It is well known that the 2*H*-chromene readily undergoes electrocyclic ring opening to give *o*-quinonemethide **XVIVb**.[56-60] Padwa et al.[57-59] reported in a series of papers that irradiation of 2,2-disubstituted chromenes gave products derived from an *o*-quinonemethide intermediate, the fate of which depends on the nature of the substituent groups as well as the photolysis conditions. In the case of 2,2-dimethyl system, the solvent MeOH capture of the *o*-quinonemethide to give methyl ethers **XXa**, may compete with a 1,7-hydrogen shift to form **XXb** (eq. 1.19). Becker et al.[60], using nanosecond (about 1 - 800 ns) and microsecond (about 0.5 - 400 μs) laser flash photolysis, obtained the transient absorption spectrum of *o*-quinonemethide **XXI** which is stable in the microsecond time domain (Figure 1.2).

o-(Dibenzo)-quinonemethide 20, structurally related to **XVIVa** or **XVIVb**

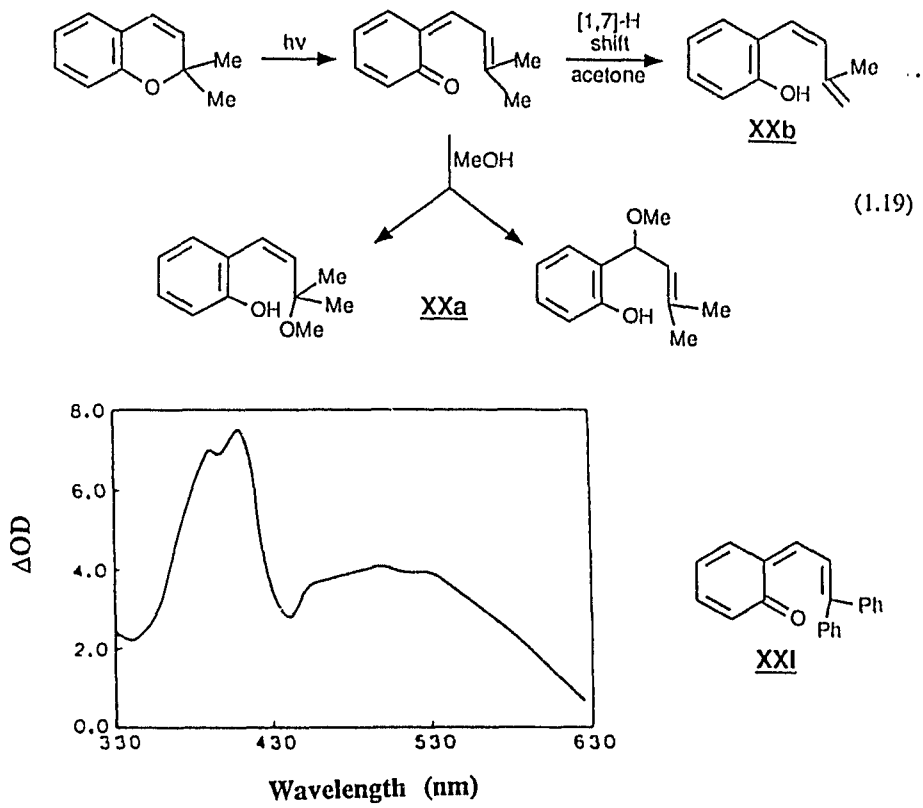

Figure 1.2. Transient absorption spectrum of **XXI** in ethanol (recorded 1 μs after a 266 nm laser flash).

might also be generated by using appropriately substituted precursors. For example, photolysis of **11** gave styryl derivative **12**,[20,48,49] indicating involvement of an *o*-quinonemethide **20a**. However, so far, there has been no precedent study of the intermediates **20** and **20a** in the literature. Unlike other *o*-quinonemethides, the species **20** in aqueous solution might be very short-lived (probably in the picosecond time domain) since it should suffer at least two rapid deactivation processes, intramolecular cyclization to pyran **7** and diffusion-limited capture. In

addition, the lack of aromaticity in the two rings of **20** also indicates its relatively high potential energy and its probable tendency to readily undergo reactions that restore aromatic character.

1.6 Photochemistry of Diaryl Ethers

Photochemical reactions of diaryl ethers, particularly those initiated by the aryl-O bond homolysis will be investigated in Chapters Three and Four. Therefore, a review of photochemistry of diaryl ethers is given below.

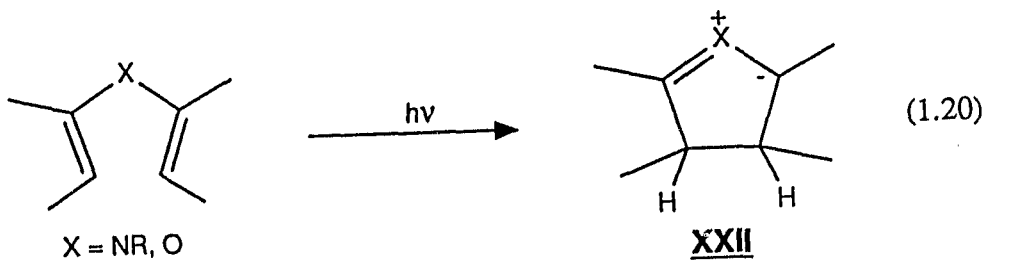

(1.20)

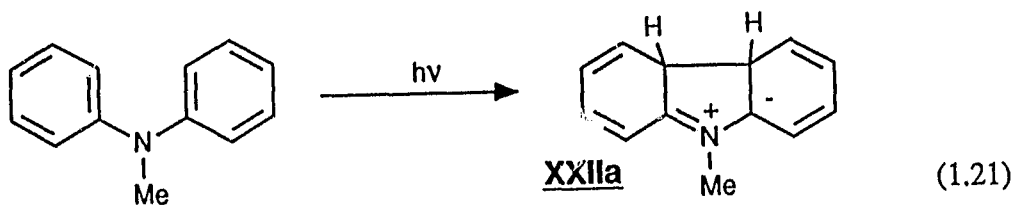

(1.21)

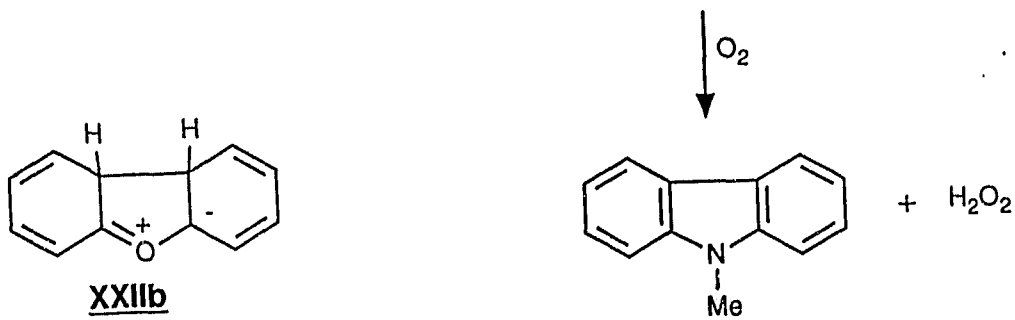

In general, there are two types of photoreactions available for diaryl ethers, namely 6π electrocyclic ring closure and the photorearrangement. The

photochemical electrocyclization of 6π electron systems containing a heteroatom has been well studied.[63] In these systems, the heteroatoms are connected to two carbon-carbon double bonds (eq. 1.20). The photocyclization results in the formation of a reactive ylide intermediate **XXII**, which undergoes rearrangement or dehydrogenation to produce derivatives of pyrroles and furans. Carruthers et al.[64] reported that, in the presence of oxygen or a small amount of iodine, irradiation of a dilute solution (~0.005 **M**) of *N*-methyldiphenylamine in hydrocarbon solvent gave *N*-methylcarbazole in 60-70% yield (eq. 1.21). It is now generally agreed that this photocyclization proceeds exclusively from the triplet state, to give an unstable ylide **XXIIa** in its triplet excited state.[65,66] The ylide intermediate was further characterized by subsequent flash photolysis studies. Rapid relaxation of this triplet state produces the singlet ground state which has two absorption maxima at 370 nm and 610 nm. The decay of the transient of **XXIIa** can be measured in microsecond flash experiments by using 610 nm as the monitoring wavelength.[65,66]

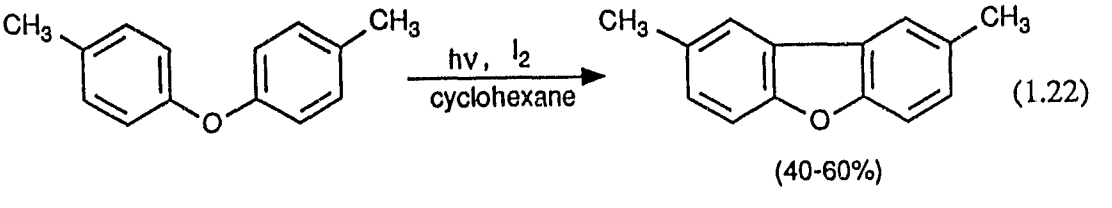

(1.22)

In a similar fashion, the corresponding diaryl ethers should also photocyclize

to the dibenzofuran derivatives on irradiation. Indeed, Zeller and Petersen[67] found that a series of diphenyl ethers underwent photocyclization, to give benzofurans on irradiation in the presence of an equivalent amount of iodine in cyclohexane solution (eq. 1.22). The reaction mechanism is similar to that operative for the amino analogue. From these studies, it is clear that the diaryl ethers have a tendency to undergo 6π electrocyclic ring closure reactions. The primary photochemical step of these reactions is to form an ylide intermediate **XXIIb**, which can be oxidized by iodine or oxygen to give dibenzofurans. However, no direct evidence for the formation of the corresponding ylide **XXIIb** has been obtained. When there is a photo-labile substituent at the *ortho* position, diaryl ethers undergo an eliminative photocyclization. Elix and Murphy[68] found that trace quantities of dibenzofurans were formed by irradiation of *o*-methoxyphenyl *m*-phenyl ether (eq. 1.23). Also, Henderson and Zweig[69] photolyzed *o*-chloro-phenyl-1-naphthyl ether (**XXIIIa**), in the presence of added iodine and oxygen, and

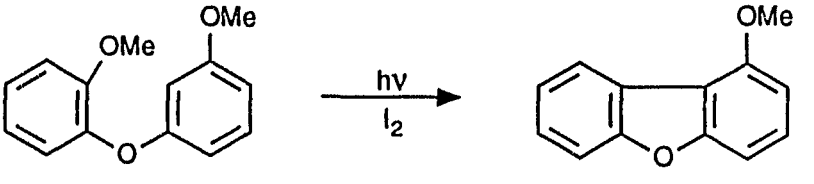

(1.23)

isolated benzo[b]naphtho[2,1-d]furan (**XXIIIb**) in 45% yield (eq. 1.24). This

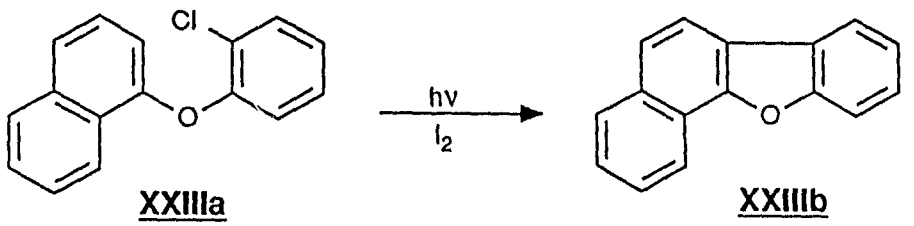

XXIIIa **XXIIIb** (1.24)

photocyclization may involve a radical-induced process.[63]

Another class of photoreaction of diaryl ethers is the photorearrangement initiated by the aryl-O bond homolysis, which has attracted more attention than the 6π electrocyclization.[63] In the absence of an in situ oxidizing reagent, photolysis of diaryl ethers without a photolabile *ortho*-substituent only leads to the rearranged products rather than cyclized dibenzofurans. In most cases, rearranged products, derived from the recombination of the initially formed radical pair, are *o*-hydroxyl and *p*-hydroxylbiphenyls. In general, the quantum yield of this reaction is very low, considerably depending on the nature of the solvent. In non-polar and good hydrogen-donor organic solvents, significant amounts of radical escaped products, such as phenols and benzene derivatives may be formed. Structure-reactivity relationships and substituent and solvent effects have also been investigated.[63]

Four decades ago, Kharasch and coworkers[70] initiated this topic and reported that irradiation of diphenyl ether in 2-PrOH gave phenol and *p*-hydroxybiphenyl. Subsequent studies[71,72] indicated that this preliminary observation was not complete since *o*-hydroxylbiphenyl was also detected (eq. 1.25).

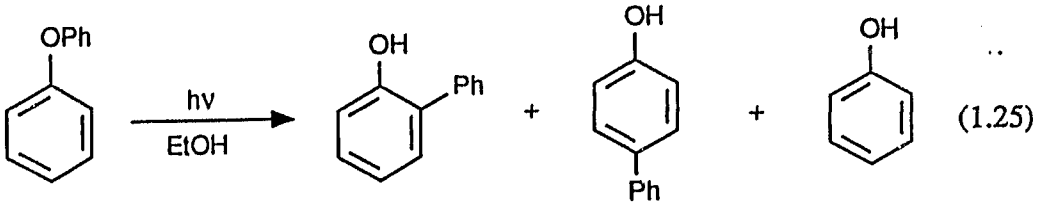

(1.25)

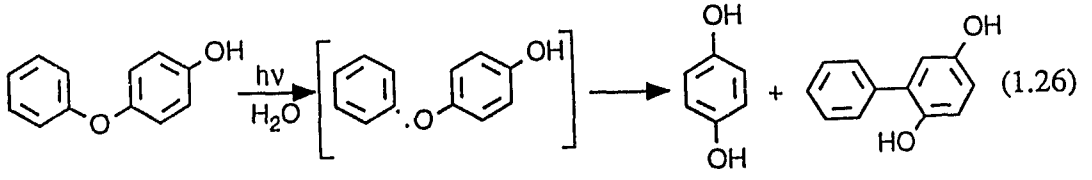

(1.26)

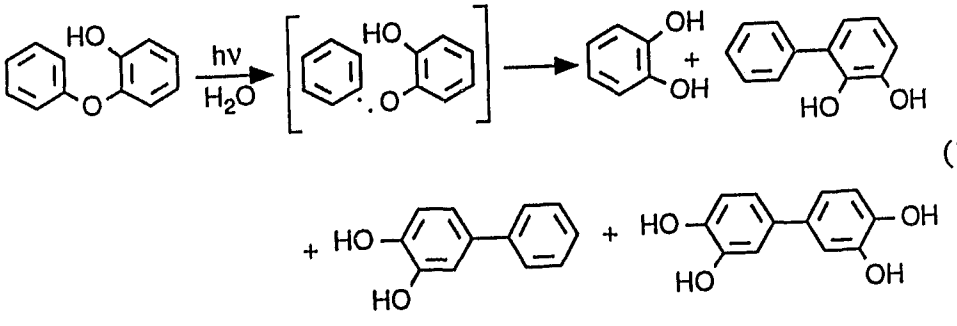

(1.27)

Joschek and Miller[73] carried out a laser flash photolysis study of several aryloxyphenols in water. They found that the primary photochemical step of the rearrangement was the homolysis of an aryl-O ether bond. The phenolic hydroxyl group controlled the regioselective cleavage of the unsymmetrical aryl-O bond, as

shown in eq. 1.26 and 1.27. Thus photolysis of 2- or 4-phenoxyphenol gave rise to radical-derived hydroxybiphenyls, which were formed exclusively from the cleavage of the ether bond (a) (eq. 1.26 and 1.27). The authors argued that the hydroxyl group might stabilize the phenoxy radical.[73] Radical recombination appears to be highly selective and non-random. The products are always those expected from coupling in positions *ortho* or *para* to the oxygen involved in cleavage.

About two decades ago, two independent studies appeared, aimed at elucidating the photorearrangement mechanism of diaryl ethers. Ogata et al.[74] reported that photolysis of several diaryl ethers in organic solvents afforded rearranged hydroxybiphenyls and escaped phenols. They found that piperylene did not quench the reaction. In these studies, results from triplet state sensitization were not conclusive since the triplet energy of the diaryl ethers were higher than that of triplet sensitizers used by these authors. However, they noted that the initially formed radical pair was trapped in the solvent cage and the reaction was an intramolecular rearrangement. In addition, they observed a significant solvent effect on the efficiency of the reaction. That is, hydroxylic solvents enhanced the efficiency of the rearrangement. This solvent effect was found to be unrelated to the viscosity effect. The authors assumed that the formation of H-bonding between solvent alcohols and the oxygen atom in diaryl ethers might assist the aryl-O bond fission (eq. 1.28). The hydroxylic solvents would also stabilize

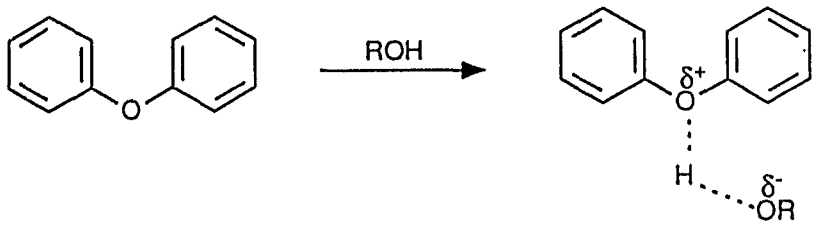

(1.28)

Scheme 1.4

Photorearrangement of Diaryl Ethers

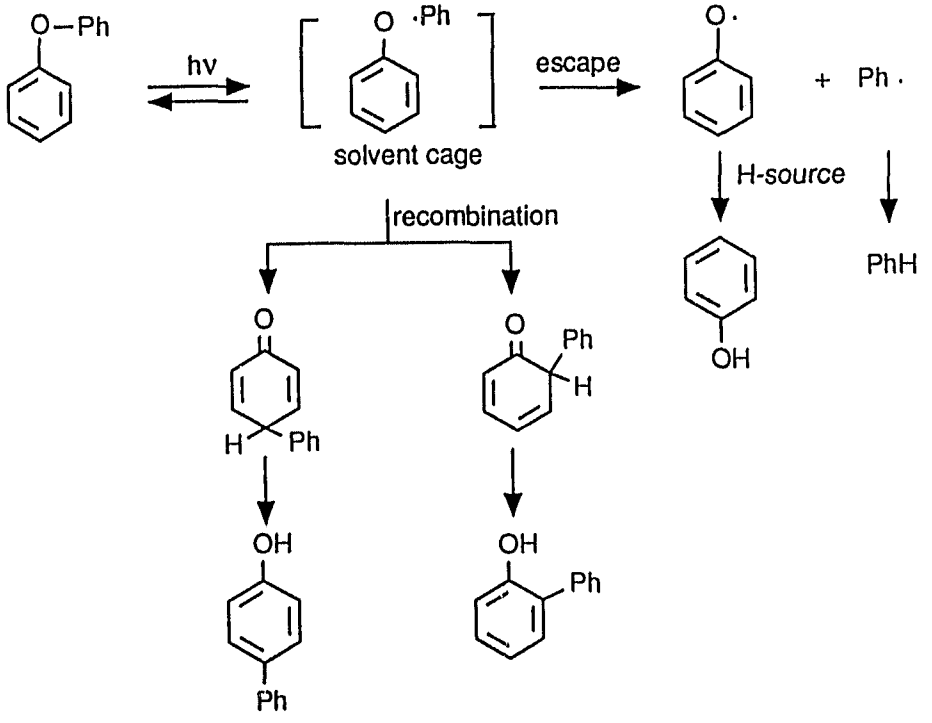

quinoid forms formed in the subsequent steps (Scheme 1.4), and thus facilitate the subsequent rearrangement.

Hageman et al.[75] obtained similar results and proposed the following

mechanism (Scheme 1.4), to account for the observed photochemistry of diaryl ethers. They further found that, on dilution, the amount of *o*-rearranged product was increased at the expense of the *p*-rearranged product. A possible explanation is that the *o*-rearrangement might be the result of some sort of concerted process. The rearrangement to the *p*-position, however, requires the aryl moiety to migrate to the other end of the ring. Alternatively, the *o*-isomer may be partially formed from the dibenzofuran, which could be the intermediary formed via a 6π electrocyclic ring closure reaction on irradiation of diaryl ethers (Scheme 1.5). However, no dibenzofuran was detected under the reaction conditions, and in fact, the dibenzofuran proved to be stable upon irradiation. Therefore, the *ortho* isomer is not from the dibenzofuran. Another intriguing possibility is that the carbonyl ylide **XXIIIb** may rearrange to the benzodihydrofuran (**XXIVa**), which might undergo photorearrangement to *o*-hydroxybiphenyl via the 2,4-cyclohexadienone (**XXIVb**) (Scheme 1.5). While there is no experimental evidence in support of this alternative mechanism for the formation of *o*-hydroxybiphenyl the proposed photorearrangement from **XXIVa** to **XXIVb** is closely related to the rearrangement from **XXVa** to **XXVb** (eq. 1.29). Hageman et al.[76] have observed an interesting *ortho* rearrangement, which is not compatible with this postulated mechanism.

In order to explain the reaction dichotomy (cyclization vs aryl-O homolysis) in diaryl ethers, Elix et al.[68] proposed that a delocalized biradial species **XXVIa** might be formed in the lowest excited state, which could lead to either the

Scheme 1.5

Mechanistic Speculation Concerning Diaryl Ether Photochemistry

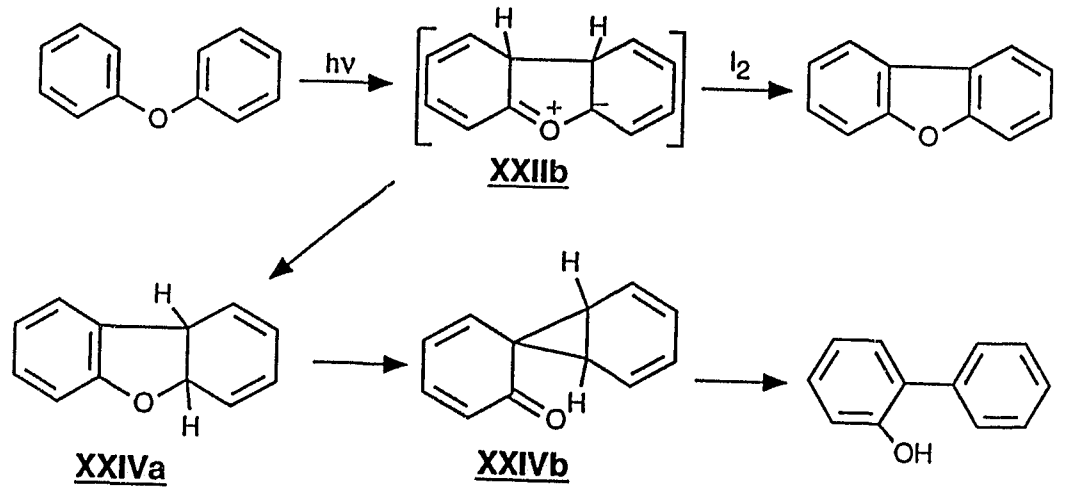

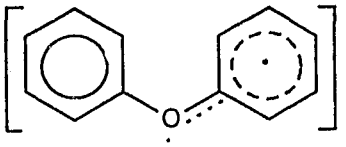

XXVIa

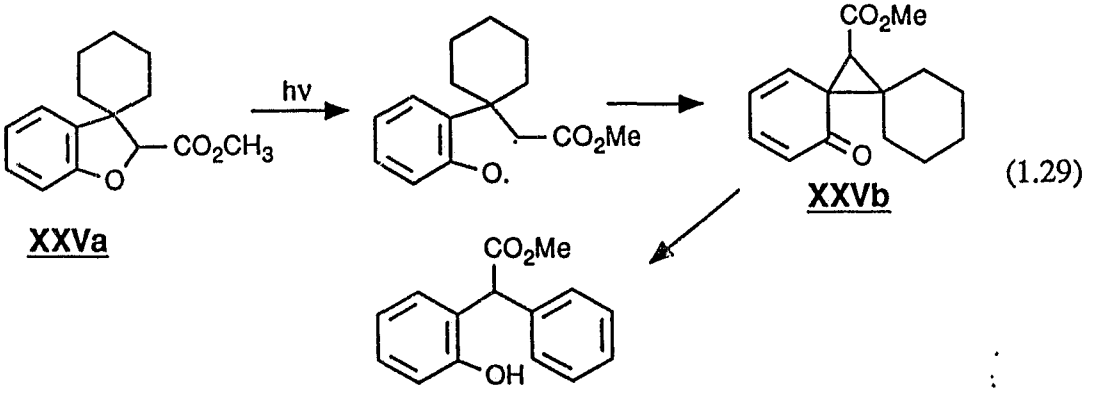

XXVa XXVb (1.29)

ylide **XXIIb** or the phenyl-phenoxy radical pair. However, there is no experimental evidence supporting the existence of such a biradical. Obviously, this mechanism could not account for the enhanced formation of radical-derived photoproducts in hydroxylic solvents. It is clear that the identity of the reactive state as well as the effect of solvent are not fully understood in diaryl ether photochemistry.

1.7 Objectives and Approaches

The initial objective of this thesis was to investigate the photosolvolysis of *o*-phenoxybenzyl alcohol (**22**) in aqueous solution and to examine the possibility of a photoinduced cyclization reaction via a Friedel-Crafts reaction (eq. 1.30), to give xanthene (**26**). However, photolysis of **22** gave only 6*H*-dibenzo[b,d]pyran (**7**) as the major product and xanthene (**26**) was not observed. The detailed mechanistic studies of this photoreaction will be reported in Chapter Three. The extension of this work to xanthene (**26**) and related derivatives will be reported in Chapter Four. During the course of the above mechanistic investigation, it was realized that the crucial step of the mechanism which converted alcohol **22** into pyran **7** involved the photocyclization of biphenyl alcohol **1** to pyran **7**. The details of photocyclization and photosolvolysis of alcohol **1** and derivatives will be reported in Chapter Two.

Approaches to elucidate the mechanisms of the above three classes of

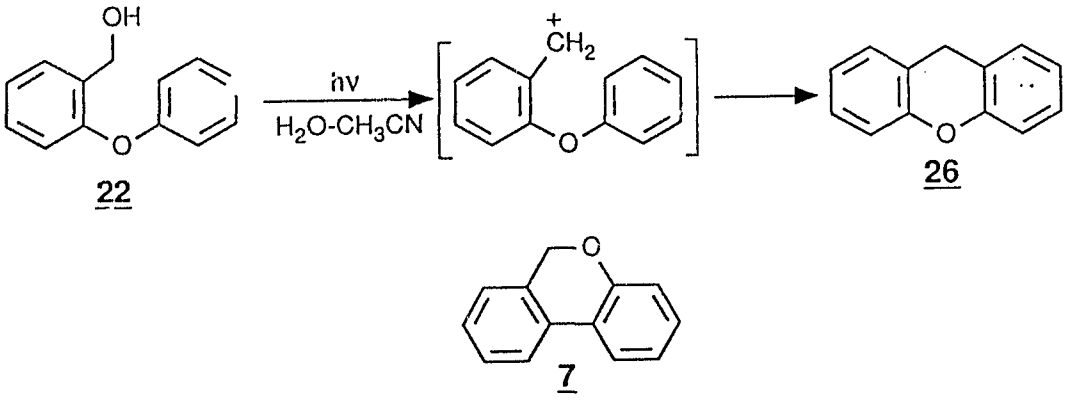

(1.30)

photoreactions include molecular mechanics calculations and X-ray determination of the ground state conformations, product studies, product quantum yield measurements, kinetic photolysis and substrate or solvent isotopic-labelling studies. Fluorescence and lifetime data were also employed to probe photophysical properties of the substrates studied. In addition, the effect of the solvent and pH on the efficiency of these reactions was examined. These studies cover several important areas in organic photochemistry and in physical organic chemistry. For reference, the main compounds studied in this thesis are shown below.

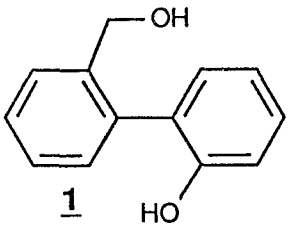

1

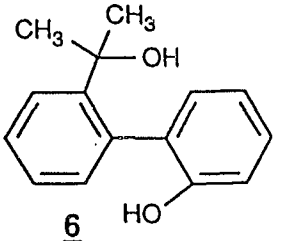

6

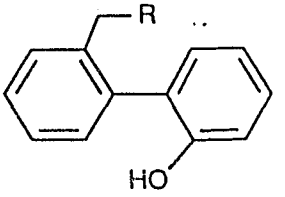

5 R = OMe

19 R = Cl

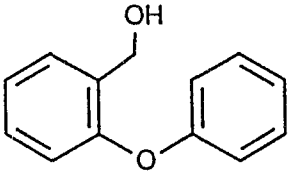

22

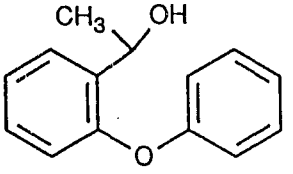

23

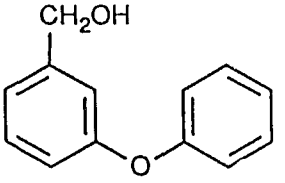

24

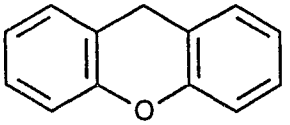

26

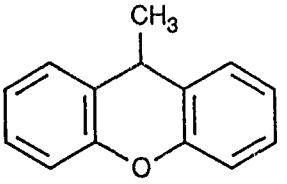

42

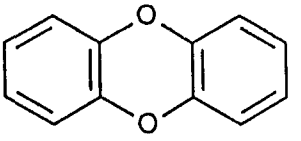

44

CHAPTER TWO: Photocyclization of 2-(2'-Hydroxyphenyl)benzyl Alcohols 1 and 6 and Derivatives 5 and 19

2.1 Introduction

As discussed in Chapter One, the photosolvolysis of a variety of benzyl derivatives has been well documented in the literature. However, no attempt has been made to explore the photosolvolysis of geometrically flexible systems such as biphenyl derivatives. As discussed in Chapter One, it is well known that biphenyls have a tendency to accommodate enhanced planar geometry in the lowest excited states.[37-42] The planar biphenyls would certainly provide an ideal template to impose the electronic effects from one phenyl ring to another as well as to facilitate inter-ring chemistry. The biphenyl alcohol **1**, an intermediate in a photocyclization reaction of **22** (which will be discussed in detail in Chapter Three) was found to photosolvolyze as well as photocyclize efficiently in aqueous MeOH, whereas the corresponding thermal reaction needed harsher conditions (250°C, BF_3-THF).[79] This finding stimulated us to extend photodehydroxylation to biphenyl alcohols. The present chapter is thus concerned with detailed investigations of the photocyclization and photosolvolysis of **1** and derivatives since these reactions are central to the photochemistry to be described in subsequent chapters. The photoreaction of **1** is believed to take full advantage of the more planar geometry of excited biphenyls and the powerful electron-donating ability of the excited

phenolate ion as a driving force, to heterolytically cleave the benzylic C-OH bond and to generate a previously unreported *o*-quinonemethide intermediate **20**. Results suggest that biphenyl alcohols are excellent precursors for examining photosolvolytic reactions via heterolysis of the benzylic C-OH bond.

2.2 Synthesis of *o,o'*-Disubstituted Biphenyls

As shown in Scheme 2.1, the synthesis of these compounds started with the oxidative cyclization of biphenyl-2-carboxylic acid by CrO_3 in aqueous acetic acid, to give 2-hydroxybiphenyl-2-carboxylic acid lactone **8**.[80,81] Although the yield of lactone **8** was only moderate (ca. 50%, calculated by GC and ^{1}H NMR) the starting material can be readily separated from **8**. The lactone **8** then served as a synthetic intermediate, which was converted into biphenyl alcohols **1, 6** and pyrans **7, 11**, respectively, by various reagents. More specifically, the reduction of lactone **8** with $NaBH_4$ in BF_3-Et_2O afforded the 6*H*-dibenzo[b,d]pyran (**7**) in excellent yield (ca. 90%), as reported by Delvin.[79] The lactone **8** was also readily reduced into alcohol **1** using $LiAlH_4$ in THF (ca. 95%). Reaction of **8** with excess Grignard reagent MeMgBr in THF produced alcohol **6** in high yield (ca. 90%). Alcohol **1** was refluxed in MeOH under the presence of a catalytic amount of conc. H_2SO_4 to give 2-(2'-hydroxyphenyl)benzyl methyl ether **5** as a major product (ca. 90%) along with some minor cyclized product **7** (ca. 10%). Refluxing **6** in 30% H_2SO_4-THF, yielded 6,6-dimethyl-6*H*-dibenzo[b,d]pyran (**11**) as the major product.

Scheme 2.1

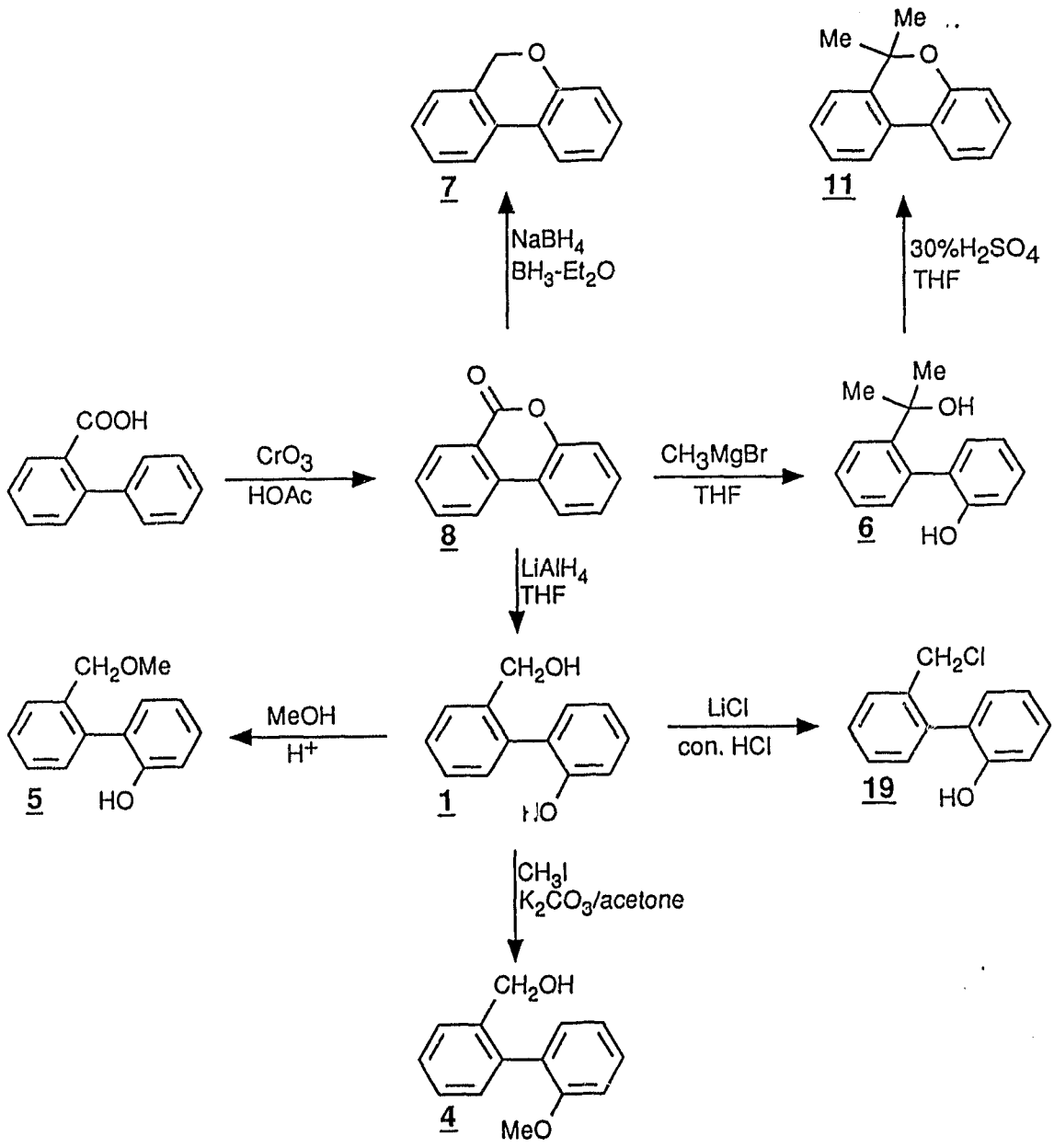

Selective methylation of the phenolic hydroxyl group of alcohol **1** with CH_3I in K_2CO_3-acetone gave product **4**. Chlorination of benzyl alcohol **1** was achieved by a newly developed method.[82] That is, **1** was refluxed in conc. HCl-LiCl to give

product **19** in over 90% yield. No cyclized pyran **7** was observed under these reaction conditions.

2.3 Results

2.3.1 Product Studies

Photolysis of 1 in Aqueous CH_3CN Solution. Photolysis of 10^{-3}-10^{-2} **M** of **1** in aqueous CH_3CN solutions (typically 1:1 or 7:3 H_2O-CH_3CN) in a Rayonet RPR 100 photochemical reactor (254 nm lamps; 0.5-2 h; solution was cooled and argon purged) gave over 95% yield of 6*H*-dibenzo[b,d]pyran (**7**) as the only product by GC and ^1H NMR analyses (eq. 2.1). The structure of **7** was further confirmed by comparison with an authentic sample made by the reduction of

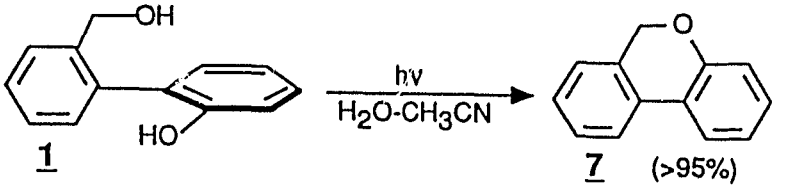

(2.1)

lactone **8**.[79] Under the above reaction conditions but without irradiation, alcohol **1** was stable indefinitely. In fact, it was found that compound **1** did not cyclize under a variety of conditions including reflux in acidic or basic solutions, unless conc. H_2SO_4 was used. This observation is consistent with results obtained by Devlin,[79] who has cyclized the *p*-hydroxy derivative of alcohol **1** to the

corresponding pyran only at 250°C using Lewis acid BF_3, in moderate yield (49%). The markedly high efficiency for the cyclization of **1** upon irradiation might reflect unique geometrical and electronic characteristics of the excited state biphenyl derivative **1**. Closer examination of geometrical and electronic change upon excitation of **1** may provide a vital role in understanding the mechanism of this novel photocyclization. To begin, two approaches, namely X-ray crystallography and molecular mechanic calculations, were employed to probe the ground state conformations of biphenyl derivatives **1** and **6**.

X-Ray Crystallography and Molecular Mechanics Calculations. In order to determine the extent of twisting between the benzene rings of **1** and its derivatives and how the *o,o'*-disubstituents are arranged in the crystalline state, the crystal structures of **1** and **6** were determined by X-ray crystallography from single crystals grown from toluene-MeOH. Crystallographic data are summarized in Table 2.1. Selected bond lengths and angles of **1** and **6** are given in Appendix A. The crystal structures were solved by K. Beveridge of the chemistry department. ORTEP views of **1** and **6** are shown in Figure 2.1. The dihedral angle between the benzene rings was 68° for **1** (angle $C_1C_6C_7C_8$) and 72° for **6** (angle $C_1C_2C_7C_8$), respectively. Furthermore, it is clear that in the solid state of these two compounds, the preferred conformation has the substituents on the two rings *syn* to one another (when viewed along the molecular axis and considering only the non-hydrogen substituents). The *syn* geometry may be preferred due to the formation of an

intramolecular hydrogen bond, which at least is true in the case of **6**. However, the *syn* geometry is also generally observed for *o,o'*-disubstituted biphenyls although the reason for this remains unknown.[83]

Table 2.1. Summary of Crystallographic Data for **1** and **6**.

	1	**6**
formula	$C_{13}H_{12}O_2$	$C_{15}H_{16}O_2$
mol wt	200.2	228.3
crystal system	monoclinic	monoclinic
space group	Cc	$P2_1c$
cell dimensions		
a, Å	13.180(5)	11.973(1)
b, Å	6.448(2)	7.376(2)
c, Å	12.096(4)	7.161(1)
α, deg	90	90
β, deg	96.80(4)	104.13(1)
γ, deg	90	90
V, Å^3	1020.7	613.27
Z	4	2
T	20°C	20°C
λ	Mo Kα (0.71069)	Mo Kα (0.71069)
ρ_{obsd}, g cm^{-1}	1.297	1.2296
ρ_{cald}, g cm^{-1}	1.303	1.236
μ, cm^{-1}	0.93	0.45
$R(F_o)$	0.095	0.0412
$R_w(F_o)$	0.105	0.0429

Molecular mechanics calculations (using IBM-PCMODEL and MMX) for **1** and **6** also indicated a preference for a highly twisted geometry with the dihedral angle of about 70° (for **1**) and 80° (for **6**). The total (or steric) energy of *syn*-

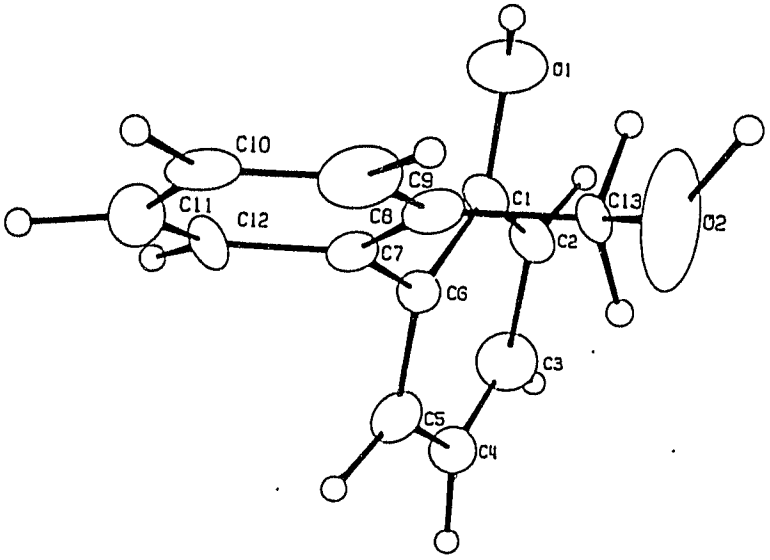

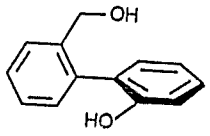

1

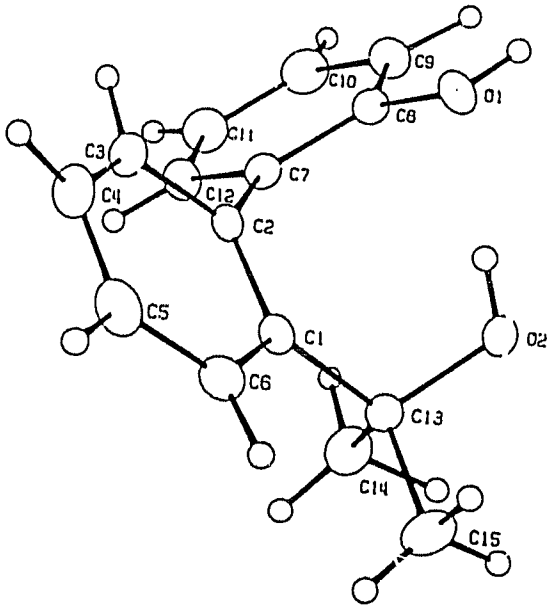

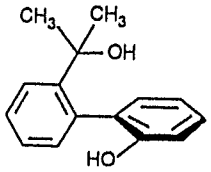

6

Figure 2.1. ORTEP drawings of biphenyl alcohols **1** and **6**. Note that both structures have the *ortho* substituents in the *syn* geometry in the solid state. The dihedral angles (between the two benzene rings) are 68° for **1** and 72° for **6**.

geometry is slightly higher than that of *anti*-geometry for both compounds. The H-bonding was not considered during the energy minimization since the formation of intramolecular H-bonds for these alcohols is unlikely in aqueous (or protic solvents) solution. Although the results of X-ray crystallography and molecular mechanics calculations show a highly twisted geometry of biphenyl derivatives in the ground state, one could not simply infer a solution conformation based on these results. However, Roberts[83] has shown using a ^{13}C NMR spectroscopic technique that the dihedral angles of several biphenyl derivatives, including some o,*o*'-disubstituted systems, have solution dihedral angles which agree well with those measured in the solid state. Therefore, it is reasonable to assume that both **1** and **6** would also have large dihedral angles in solution. Molecular mechanic calculations for **7** also showed that product pyran **7** was essentially a planar molecule, with a slight puckering out of planarity at the oxygen atom. Thus, the overall transformation (eq. 2.1) takes highly twisted **1** to essentially planar **7** (with loss of H_2O from **1**) on irradiation.

UV Absorption Trace Studies. The photocyclization of **1** can be readily followed by UV spectroscopy. As shown in Figure 2.2, photolysis of a deaerated ca. 10^{-4} M solution of **1** in aqueous CH_3CN (1:1 H_2O-CH_3CN or 100% H_2O) resulted in growth of absorption bands at 305 and 265 nm, which can be assigned to pyran **7**. After an exhaustive irradiation, the absorption spectrum observed is essentially identical to that of authentic **7** (see inset of Figure 2.2). Shown in

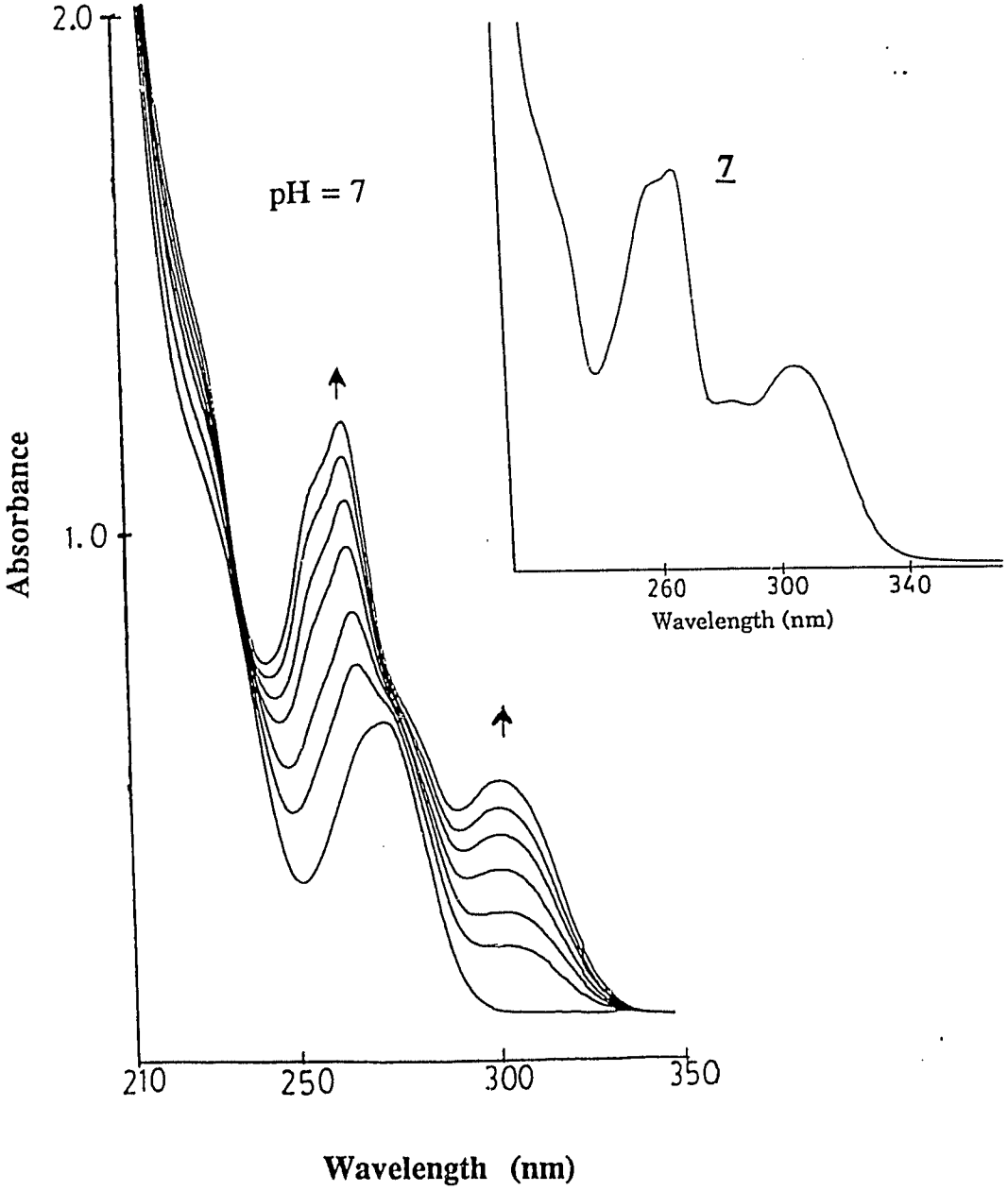

Figure 2.2. UV absorption traces in the photolysis of **1** in 1:1 H_2O-CH_3CN. Each trace represents ca. 15 seconds photolysis at 254 nm inside a Rayonet reactor employing a merry-go-round assembly. The inset is a spectrum of authentic **7** in the same solvent, which matches one obtained from an exhaustively irradiated sample of **1**.

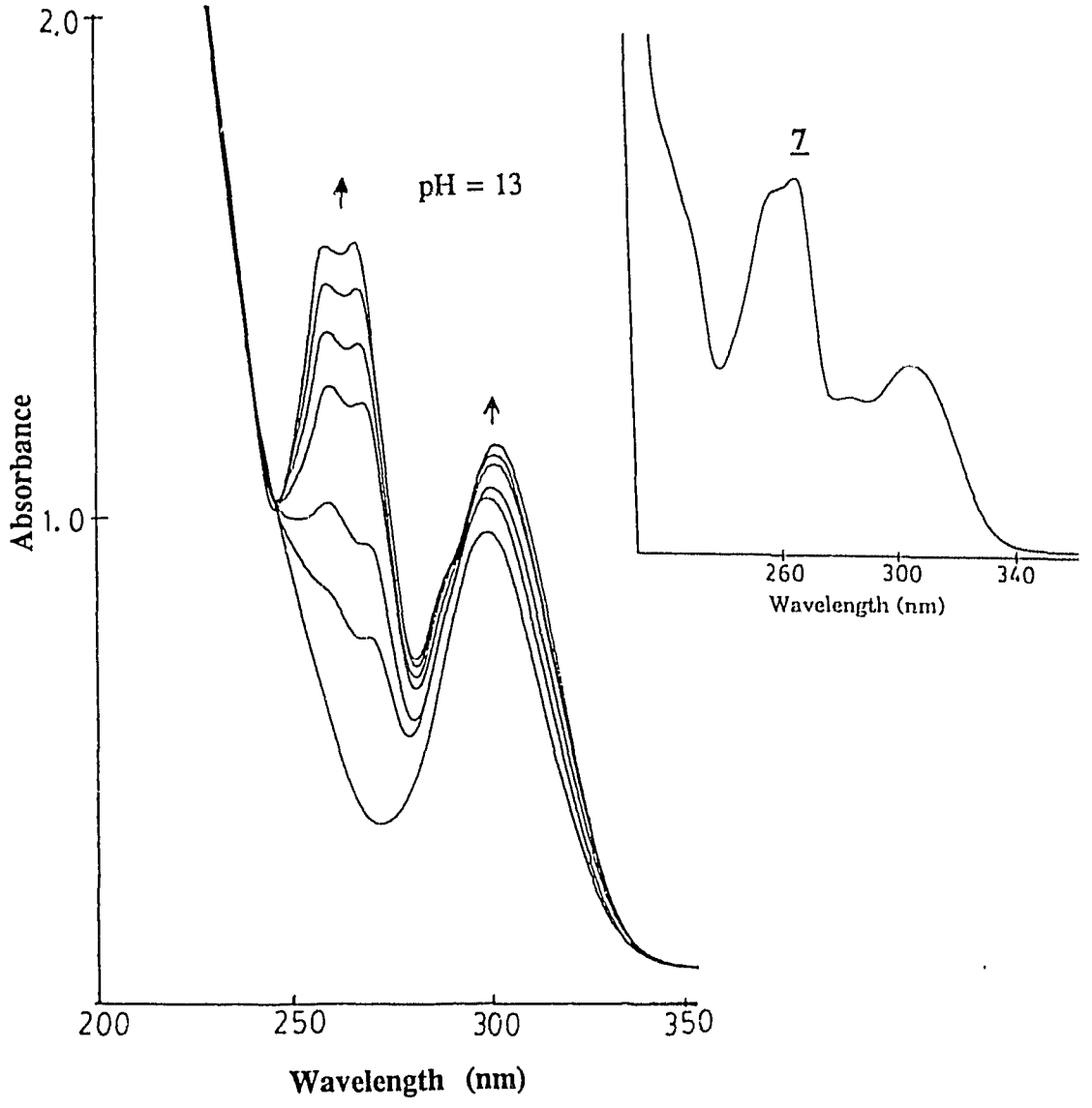

Figure 2.3. UV absorption traces in the photolysis of **1** in 1:1 H_2O-CH_3CN (pH was adjusted to 13). Each trace represents ca. 15 seconds photolysis at 254 nm inside a Rayonet reactor employing a merry-go-round assembly. The inset is a spectrum of authentic **7** in the same solvent, which matches one obtained from an exhaustively irradiated sample of **1**.

Figure 2.3 is the UV absorption change on photolysis of **1** under the above conditions except using a pH = 13 solution (phenol **1** is ionized at this pH). In this case, the absorption bands at 305 and 265 nm grew very quickly and the absorption of the final run essentially resembled that of product 7. From these studies, it is clear that the photocyclization of **1** is qualitatively faster in basic solution than in neutral solution. The effect of pH on quantum yield of the photocyclization will be addressed in a more detail later.

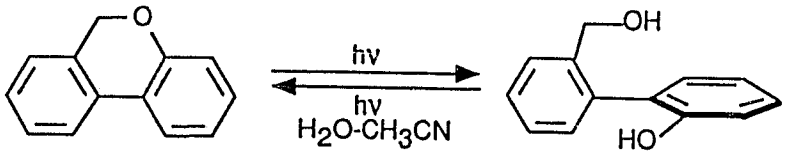

7 (98%) photostationary state ratio 1 (2%) (2.2)

Kinetic Studies of Photolysis of 1 and 7 in Aqueous CH_3CN. Based on the above observations, it would appear that **1** can be converted essentially quantitatively into 7 on irradiation in aqueous CH_3CN. To examine this possibility in more detail, the reaction (in 1:1 H_2O-CH_3CN) was followed by GC as a function of irradiation time (Figure 2.4). It was found that the prolonged photolysis of **1** did not alter the ratio of starting material **1** to product 7 (at 2:98). This indicated that the reaction reached a photostationary state of 98:2 for **7**:**1** (eq. 2.2). The photoreaction overwhelmly favoured the formation of the product 7. The photostationary state was further confirmed by the kinetic photolysis of authentic

7 under the same condition as for **1**, as shown in Figure 2.5.

Kinetic Photolysis of 1 and 7 in MeOH. Photolysis of **1** in 100% MeOH or aqueous MeOH gave the cyclized product 7 and the MeOH trapping product **5**, with the ratio of **5**:7 depending upon the irradiation time as well as the water content of the solution (eq. 2.3). The kinetic photolysis of **1** in 100% MeOH is shown in Figure 2.6. This plot shows that exhaustive photolysis of **1** in 100%

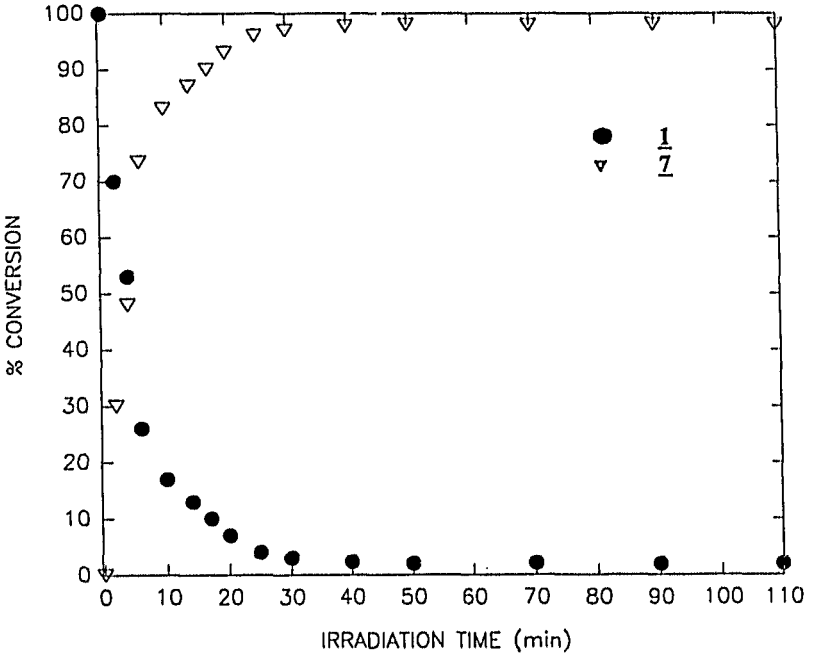

Figure 2.4. Yield of 7 as a function of irradiation time on photolysis of **1** in 1:1 H_2O-CH_3CN as determined by GC.

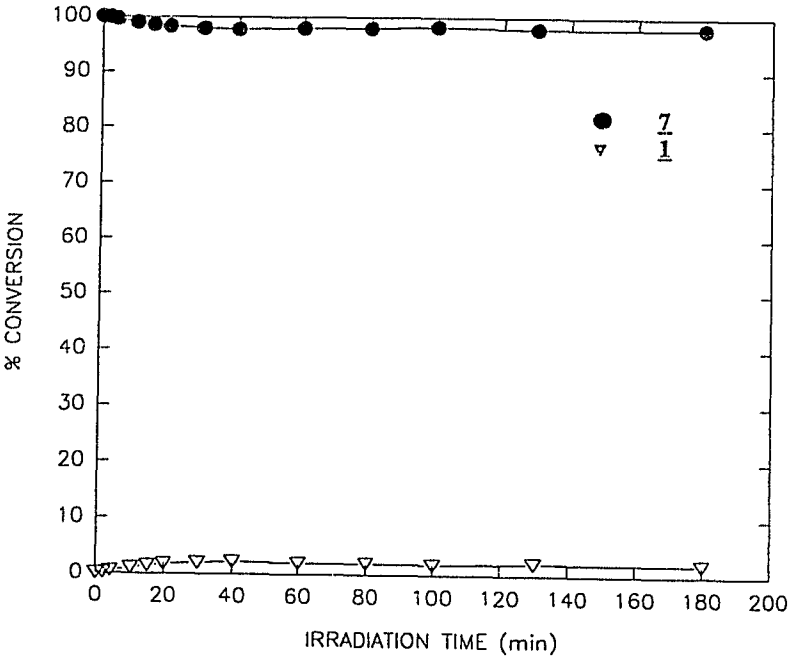

Figure 2.5. Yield of **1** as a function of irradiation time on photolysis of 7 in 1:1 H_2O-CH_3CN as determined by GC.

MeOH gave **5** and 7 in a photostationary state ratio of 45:55. At low conversions (<20%), the ratio of **5**:7 observed was ca. 2:1; that is, there is preference for MeOH attack (resulting in overall photosubstitution at the benzylic position) vs cyclization when **1** is irradiated in 100% MeOH. When an authentic sample of 7 was irradiated in 100% MeOH, the only product observed was **5** and a photostationary state of 45:55 (for **5**:7)(eq. 2.4) was also observed after the exhaustive photolysis. The kinetic photolysis of 7 in 100% MeOH is shown in Figure 2.7, which further confirms the formation of this photostationary state.

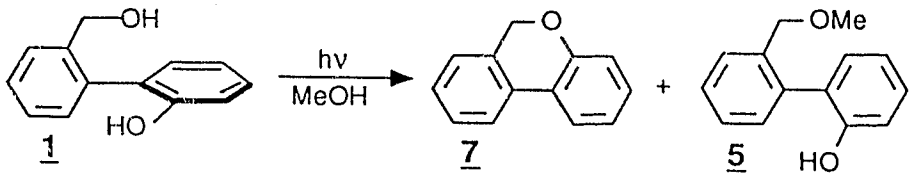

(2.3)

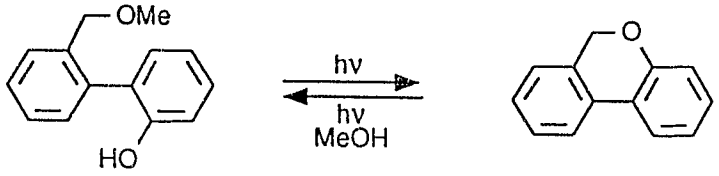

(2.4)

5 (45%) photostationary state ratio 7 (55%)

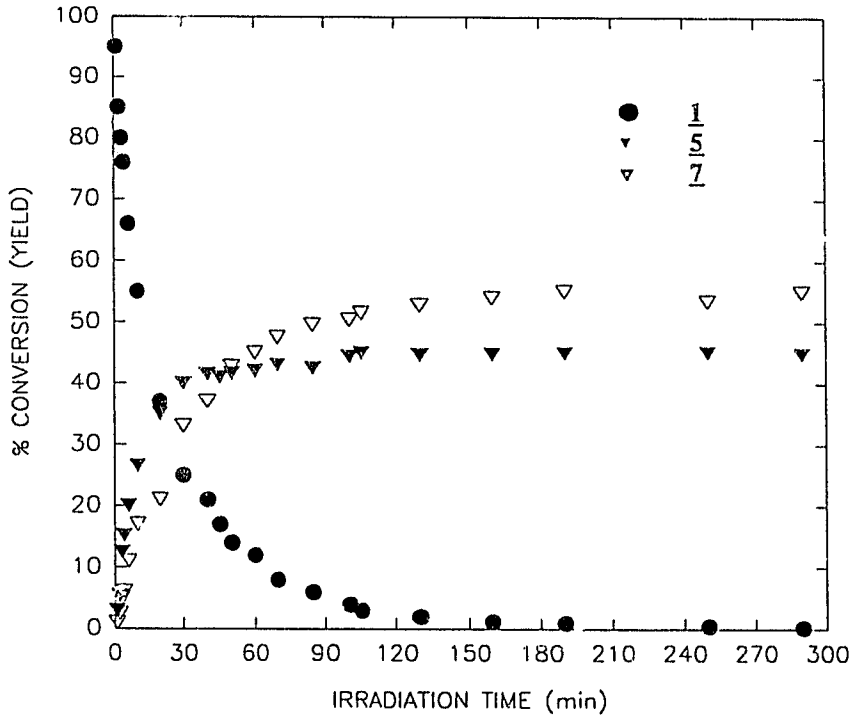

Figure 2.6. Plot of yields as a function of photolysis time on irradiation of **1** in 100% MeOH.

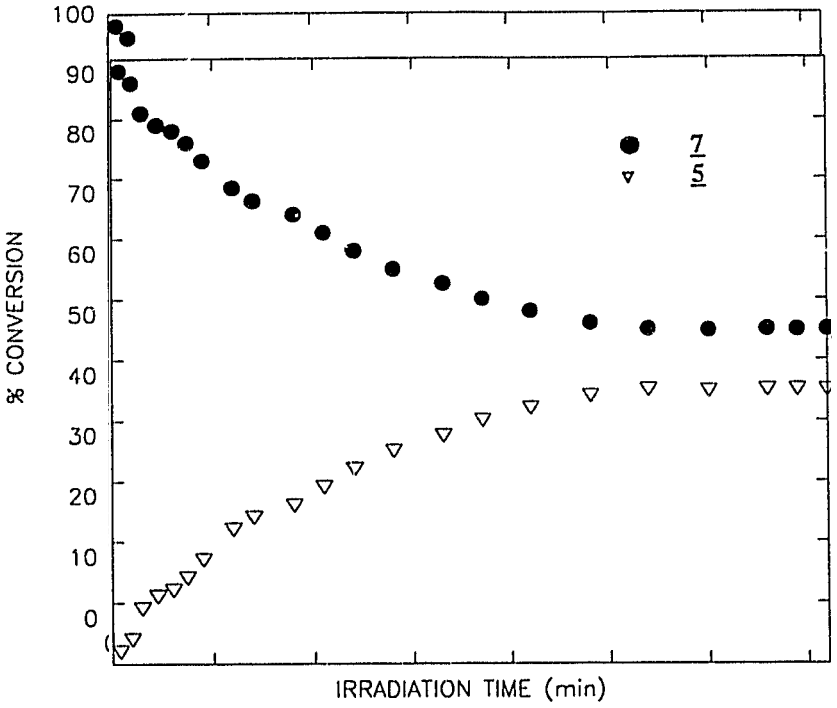

Figure 2.7. Yield of **5** as a function of irradiation time on photolysis of **7** in 100% MeOH.

Photolysis of 5 and 19. The photocyclization of alcohol **1** seems to be general for its derivatives. Photolysis of **5** or **19** in aqueous CH_3CN gave a mixture of **7** and **1** in the quoted ratio (eq. 2.5). The ratio of products was found to be dependent on the photolysis time. The kinetic photolysis of **5** in 1:1 H_2O-CH_3CN is shown in Figure 2.8. A similar plot was obtained on irradiation of **19**. At low conversions (<15%), the ratio of **7**:**1** was 2:1, indicating that the cyclization process (to afford **7**) was faster than the solvolysis pathway (to give **1**).

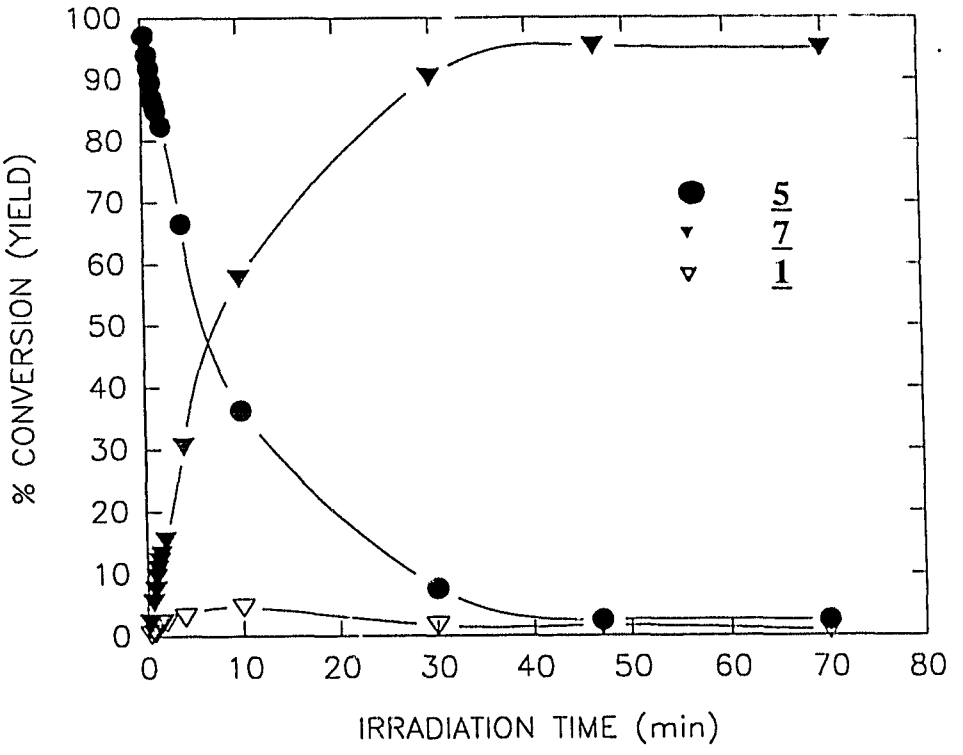

Figure 2.8. Plot of yields as a function of photolysis time on irradiation of **5** in 1:1 H_2O-CH_3CN.

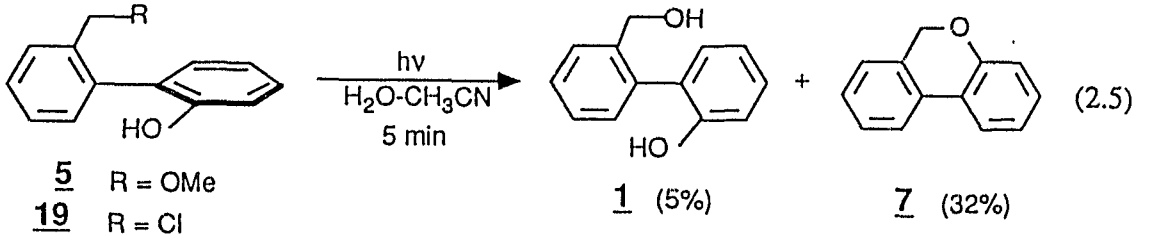

So far, all these results demonstrate that photolysis of **1** in nucleophilic solvents (e.g. water or MeOH) can reach a photostationary state. Results further indicate that use of MeOH in the photolysis of **7** results in a higher yield of the

ring-opened product **5** compared to use of H_2O-CH_3CN, which gave only 1-2% yield of **1**. There are two factors contributing to this higher yield of the ring-opened product **5** in MeOH. First, the efficiency of photocyclization of **1** is higher than that of **5** (*vide infra*). The solvent MeOH is simply a better nucleophile than that of the solvent water.

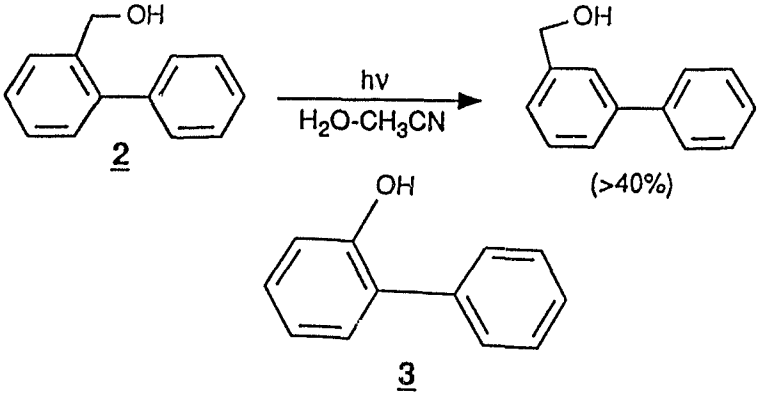

2 **3** (2.6)

Photolysis of 2-4. Additional insights into the mechanism of photocyclization was obtained by studying biphenyl derivatives **2-4**. Above results already suggest that the phenyl moiety in alcohol **1** may play a vital role in the promoting the photocyclization reaction. Indeed, photolysis of methoxyl-substituted

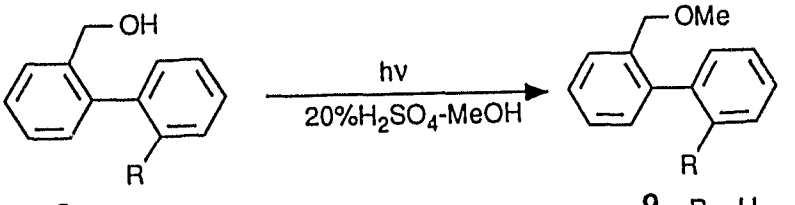

2 R = H
4 R = OMe

9 R = H
10 R = OMe (2.7)

biphenyl **4** in neutral aqueous CH_3CN or MeOH led to the complete recovery of starting material. Furthermore, irradiation of **2** and **3** in both aqueous CH_3CN and

MeOH did not give the cyclized product **7**. There was a possibility that one of the carbon in pyran **7** might have been incorporated from the solvent CH_3CN or MeOH. In fact, 2-phenylphenol (**3**) was found to be photostable, whereas 2-phenylbenzyl alcohol (**2**) photoisomerized to an isomer, namely 3-phenylbenzyl alcohol (eq. 2.6), under the above conditions. However, irradiation of **2** or **4** in 1:1 MeOH-20% H_2SO_4 gave the solvolysis products **9** and **10**, respectively (eq. 2.7). These structure-reactivity studies clearly reveal that the presence of the phenol moiety is a necessary requirement for the photocyclization of **1**.

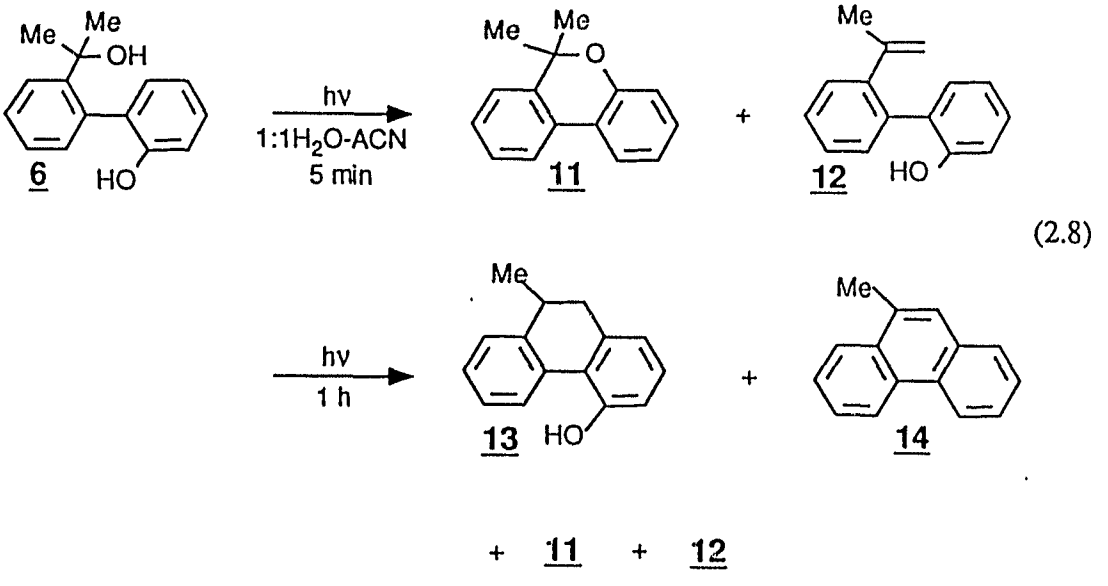

Photolysis of 6. With an attempt to generalize the photocyclization of **1** and to obtain additional insights into the reaction mechanism, the dimethyl derivative **6** was prepared and studied. Photolysis of **6** in 1:1 H_2O-CH_3CN for a short time (5 min) produced the photoproducts **11** and **12**, while for prolonged photolysis, two

more products **13-14** appeared, as shown in eq. 2.8. The yields of these products were dependent upon the photolysis time. The kinetic photolysis of **6** in aqueous CH_3CN was plotted in Figure 2.9. Closer examination of this plot clearly indicates that the pyran **11** and styryl derivative **12** are formed as primary photochemical products. In addition, this plot further indicates that both **11** and **12** are photolabile, and therefore cyclized compounds **13-14** are secondary photoproducts

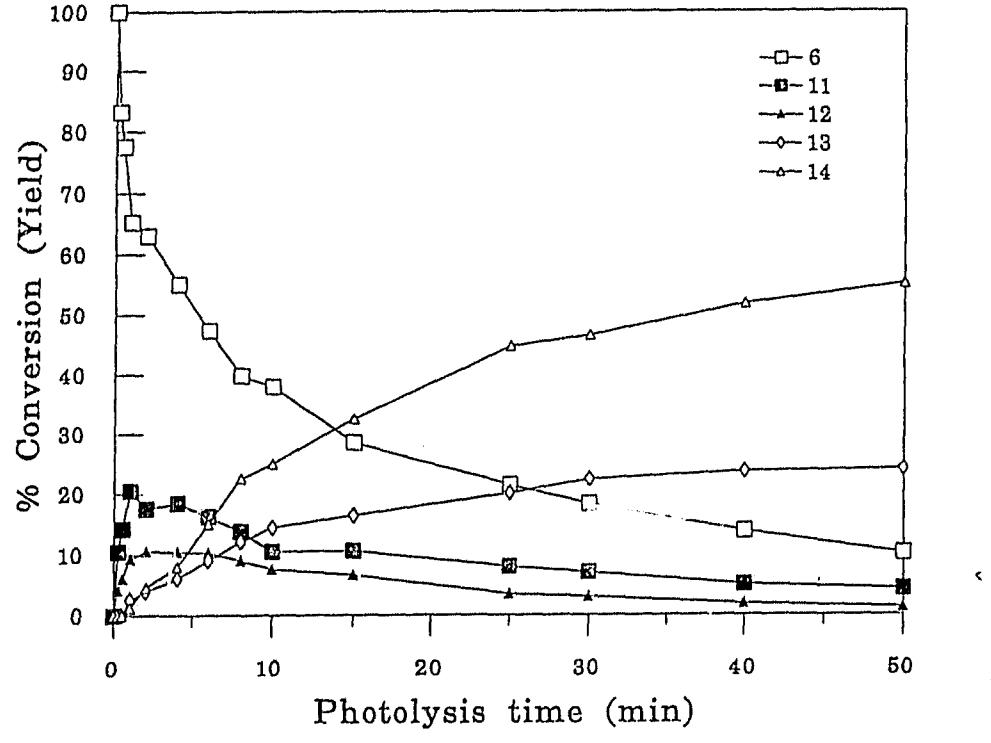

Figure 2.9. Plot of product distributions as a function of photolysis time on irradiation of **6** in 1:1 H_2O-CH_3CN.

from **12**. All of these photoproducts were isolated and characterized by MS and ^1H NMR spectroscopy. The pyran **11** was synthesized and irradiated under the same conditions as for 6, to give **12** and **13-14**. As mentioned in Chapter One, the

photolability of pyran **11** and its derivative has been reported by Turnbull and coworkers.[48,49] They found that photolysis of **11** (in EtOH) gave initially **12**, followed by **13** and **14** as final products (*vide supra*). Their results corroborate the overall photochemistry observed for **6** shown in eq. 2.8. As shown in Figure 2.9, as the starting material 6 was lost, the styryl derivative **12** was initially accumulated and then decreased with the continued growth of the compounds **13-14**. The kinetic photolysis of **11** under the same conditions as for **6** was also carried out, which unambiguously demonstrated that products **13** and **14** were secondary photoproducts of **12**, presumably via an electrocyclic ring-closure reaction. Several groups have shown that 2-vinylbiphenyl derivatives undergo efficient electrocyclic ring closure on photolysis, to give phenanthrene derivatives as final products.[43-53] The same reaction for **12** would be expected to give both **13** and **14**, which are in fact the observed final products.

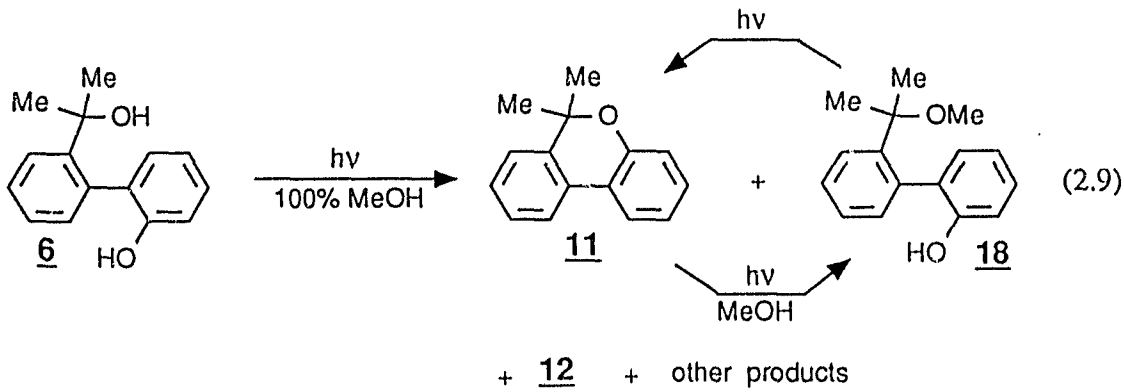

(2.9)

As in the case of **1** and **7**, photolysis of **6** or **11** in 100% MeOH yielded a small amount of the solvent MeOH trapping product, tentatively identified as the

methyl ether **18** (5%), in addition to other photoproducts (eq. 2.9). The low yield of **18** is a combined result of its secondary photolysis (eq. 2.9) and an additional competing pathway available for the reactive intermediate **20a** (1,7-H shift, resulting in the formation of **12**, vide infra).

^{18}O-Incorporation from Photolysis of 1 in $H_2{}^{18}O$. As mentioned before, photolysis of **5** or **19** in aqueous CH_3CN gave the solvent water trapping product **1**. On photolysis of **1**, the solvent water capture product is the starting material **1** (see eq. 2.5). If irradiated in $H_2{}^{18}O$ solutions, **1** should give the ^{18}O-enriched **1**, which can be detected by MS. Unfortunately, our MS instrument (even using CI) failed to show the molecular ion of molecule **1**, the highest peak being pyran **7** (M^+-18, water). Results obtained on photolysis of **5** or **19** suggested that the oxygen in product pyran **7** was not derived from the hydroxymethyl group (-CH_2OH) in **1** and that the oxygen in the pyran product (**7** or **11**) came from the phenol moiety. The final possibility that had to be eliminated was that the pyran oxygen came from solvent H_2O (or solvent CH_3OH when it was used). Photolysis of **1** in 20% $H_2{}^{18}O$-enriched 1:1 H_2O-CH_3CN (taken to >50% conversion to **7**) resulted in no observable incorporation of ^{18}O into pyran **7** (by GC/MS analysis). Therefore, the oxygen in **7** must come from the phenol moiety of **1**.

2.3.2 Quantum Yields

Quantum yields for the formation of photoproduct **7** on irradiation of **1**, **5**,

19 were measured in pure CH_3CN and aqueous CH_3CN, and are listed in Table 2.2. Due to the formation of several products on photolysis of **6**, only the quantum yield for loss of **6** was estimated.

pH-Effect Studies. Quantum yields (Φ_p) for formation of **7** from alcohol **1** have also been measured in 7:3 H_2O-CH_3CN where the pH (H_o) of the aqueous portion was varied over the whole pH range and into moderately strong acidic

Table 2.2. Quantum Yields for Photocyclization of Biphenyl Derivatives **1**, **6**, **5** and **19**.

substrate	condition[a]	Φ[b]
1	100% CH_3CN	0.12 ± 0.01
	1:1 H_2O-CH_3CN	0.21 ± 0.02
	7:3 H_2O-CH_3CN	0.25 ± 0.03
5	100% CH_3CN	0.080 ± 0.003
	1:1 H_2O-CH_3CN[c]	0.13 ± 0.02[c]
6	1:1 H_2O-CH_3CN[d]	0.20 ± 0.03[d]
19	100% CH_3CN	0.05 ± 0.003
	1:1 H_2O-CH_3CN[c]	0.11 ± 0.02[c]

[a] The H_2O portion of these solutions was buffered at pH 7.
[b] Quantum yield for formation of pyran **7** unless otherwise noted.
[c] Predominant product was pyran **7** (95%) with a trace of **1** (5%) in this solvent.
[d] Quantum yield for loss of **6** (pyran **11** is the initially formed product, which was found to be photolabile, see text).

solution. Dark control runs showed that no cyclization was observed without

irradiation in acidic and basic solutions. Φ was found to vary significantly with pH (H_o) (Figure 2.10).

There are two inflection points in the plot, one at pH = 10 and the other at pH = 1.2, and a plateau region between 2 and 9. Above pH > 10, **1** exists in the phenolate ion form in the ground state since the ground state pK_a of **1** was determined to be 9.9 ± 0.2 in H_2O. Excitation of the phenolate ion of **1** resulted in the highest quantum yield for cyclization (Φ = 0.50 ± 0.04). The second inflection point at pH = 1.2 is associated with the excited state pK_a^* of the phenol

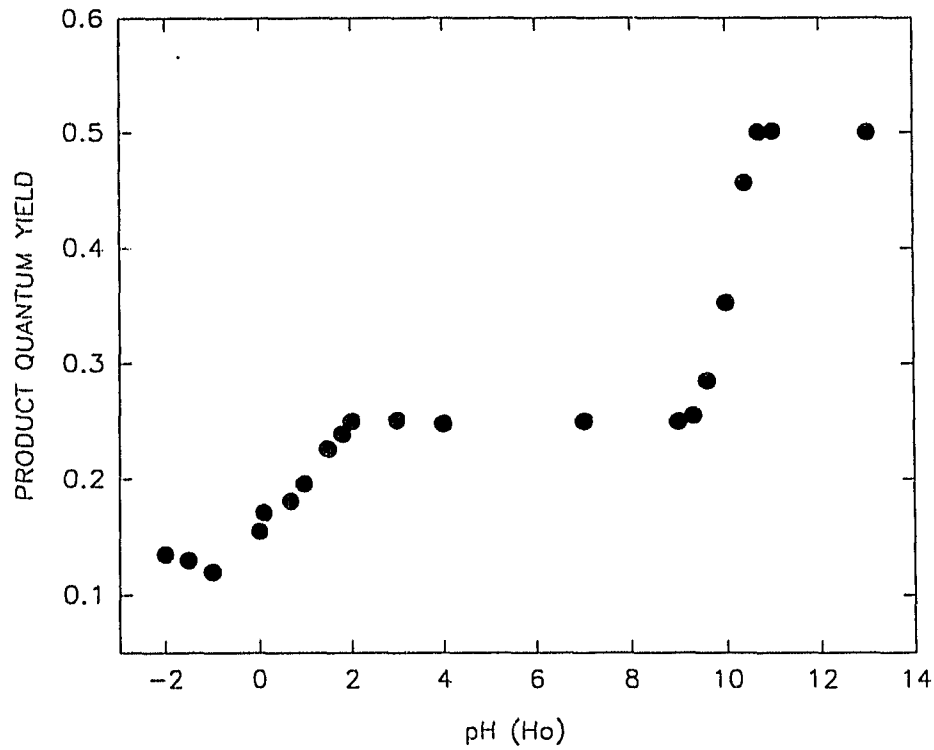

Figure 2.10. Plot of quantum yield (Φ) for formation of **7** on irradiation of **1** as a function of pH in 7:3 H_2O-CH_3CN (quoted pH is of the aqueous portion only).

1. Because the fluorescence emission from **1** was very weak at all pH's (*vide infra*), it was not possible to carry out accurate fluorescence titration of the phenol **1** and to estimate its $pK_a^*(S_1)$. However, the structurally related phenol **3** (which was photochemically non-reactive) was found to be very emissive. Fluorescence titration (*vide infra*, Figure 2.15) of biphenyl phenol **3** gave $pK_a^*(S_1) = 1.5 \pm 0.3$ in 100% water. The expected $pK_a^*(S_1)$ of **1** would be close to this value since the ground state pK_a of **3** was found to be 10.2 ± 0.3, similar to the ground state counterpart of **1**. Phenols of comparable and stronger acidity in S_1 have recently been reported by Tolbert and Haubrich.[85] For example, several appropriately substituted naphthols have $pK_a^*(S_1)$ values approaching zero.[86] Therefore, the presently determined $pK_a^*(S_1)$ of ca. 1.5 for biphenyl phenol **3** and ca. 1.2 for **1** is quite reasonable. In general, phenols are known to become stronger acids in the lowest excited states compared to the ground state counterparts.[86-90]

The plot further indicates that the inflection of Φ at pH = 0-2 does not follow a normal titration curve similar in shape to the pH = 9.5-10.5 region, and does not go to zero in more strongly acidic media, as might be expected since all excited states in this acidity region would remain protonated. In contrast, Φ even slightly increased as the media became more acidic. Obviously, there is an additional photocyclization pathway available at these higher acidities, also leading to the formation of **7**. In acidic medium, biphenyl alcohols **2** and **4** were found to undergo efficient photosolvolyses (*vide supra*). In addition, acid-catalyzed

photosolvolysis (via a carbocation intermediate) of a number of benzyl alcohols has been well established.[22,23,29] The same acid-catalyzed photosolvolysis may also apply to the alcohol **1**. Indeed, irradiation of **1** in 1:1 20% H_2SO_4-MeOH (v/v) provided solvolytic product **5** and cyclized pyran **7**, respectively, where no dark reaction was observed.

Light Intensity Effects. The possibility that a mechanism requiring two or more photons to transform 1 into **7** needs to be addressed. For example, there might be a case, where on absorption of the first photon, a reactive intermediate

Table 2.3. Quantum Yields for Photocyclization of **1** to **7** at Different Light Intensities.[a]

light intensity[b]	Φ[c]
80 x 10^{-7}	0.19 ± 0.03
2.30 x 10^{-7}	0.20 ± 0.03
2.90 x 10^{-7}	0.25 ± 0.03

[a] Quantum yields in 7:3 H_2O-CH_3CN (water portion at pH = 7)
[b] In einstein min^{-1}. Exciting wavelength = 280 nm; light intensity was varied by changing the slit width of the exit monochromator. Intensity monitored by potassium ferrioxalate actinometry. Estimated error ± 5% of quoted value.
[c] Measured by GC.

was photogenerated (e.g. phenolate ion or other reactive intermediates). This

intermediate might have had a significant lifetime, leading to product on absorption of a second photon. However, there is no transient absorption (limit of detection, $\tau_{1/2}$ = 3 min) observable by UV-Vis spectrophotometry and ^{1}H NMR under the reaction conditions. In order to rule out the above possibility in a more rigorous manner, quantum yields for photocyclization of **1** at several different light intensities (λ_{ex} = 280 nm) (Table 2.3) were measured. No considerable dependence of Φ on light intensity over a 4 fold change in light intensity was observed. Therefore, the possibility that overall photocyclization of **1** involves a two-photon process can be ruled out.

Solvent Effects. The solvent water can considerably enhance the product quantum efficiency of this photocyclization reaction. The quantum yields for formation of **7** on irradiation of **1** in aqueous CH_3CN is shown in Figure 2.11. It is interesting to find that only a small amount of water can significantly increase the photocyclization efficiency. An overall ca. 2 fold enhancement of Φ was observed on going from 100% CH_3CN to over 50% water content in CH_3CN. Photolysis of **1** in a non-polar solvent such as hexane also gave the pyran **7** as the to the only product, but with slightly lower quantum yield than that obtained in aqueous CH_3CN according to the control runs. This suggests that the photocyclization of **1** might not require solvent(s) as a necessary driving force, in contrast to photosolvolyses of other benzyl alcohols.[22,23,29] This special photobehaviour of **1** may again reflect unique properties of its molecular structure.

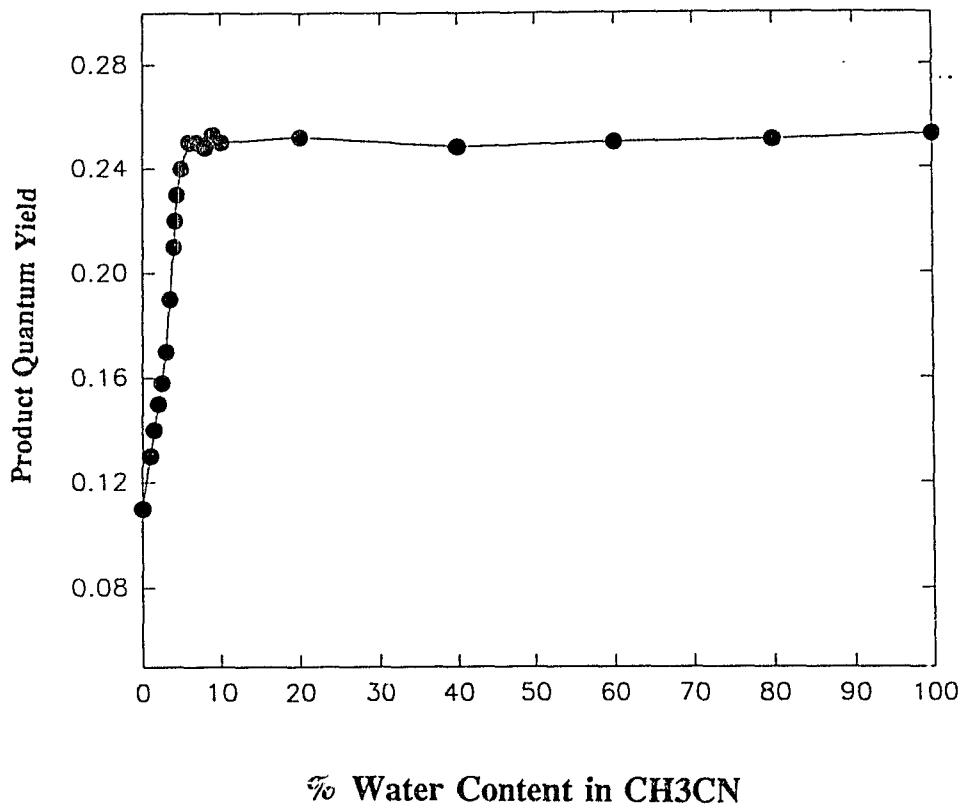

Figure 2.11. Quantum yields for formation of 7 on photolysis of **1** vs water content in CH_3CN.

Results obtained from X-ray diffraction showed that the single crystal structure of **1** was intermolecularly associated via a hydrogen bond. This observation stimulated us to photolyze **1** in the solid state. Although the efficiency of the cyclization is much lower than that in solutions, photolysis of **1** in the solid state (the substrate **1** was absorbed on the surface of a quartz tube) did lead to the formation of 7! It is well known that irradiation of phenols prompts an adiabatic generation of the corresponding excited state phenolate ion and solvated proton.[86-90]

In other words, phenols in the excited state become much stronger acids. It has been shown that the adiabatic deprotonation can occur even in the solid state.[91] The photogenerated proton would certainly act as an acid to catalyse the solvolysis of the benzylic C-OH bond in a similar manner as demonstrated in solutions.[22,23,29] The details of the solid state photochemistry of **1** was not further investigated in this thesis.

2.3.3 Steady-state and Transient Fluorescence Measurements

Steady state fluorescence spectra (uncorrected) of **1** were taken in aqueous CH_3CN (1:1 or 7:3 H_2O-CH_3CN, water portion at pH = 7; buffered solution) with λ_{ex} = 270 nm. The compound **1** was very weakly fluorescent in aqueous solution, as shown in Figure 2.12, with λ_{max} = 335 nm and a weak shoulder at 405 nm. When the fluorescence emission was taken in basic solution, where **1** exists as a phenolate form, two comparable bands at 335 nm and 405 nm were observed, as shown in Figure 2.13. The band at 335 nm in this case is from the emissions of the phenol form (ca. 0.001%) and product **7** which was quickly formed due to the highly efficient photocyclization of **1** in aqueous solution. This is further confirmed by time-dependent fluorescence studies. As shown in Figure 2.14, the product **7** emission appears very quickly, overlapping with the emissions from phenol and phenolate ion forms of **1**. It was concluded that the band at 335 nm and the shoulder at 405 nm shown in Figure 2.12 were primarily due to the

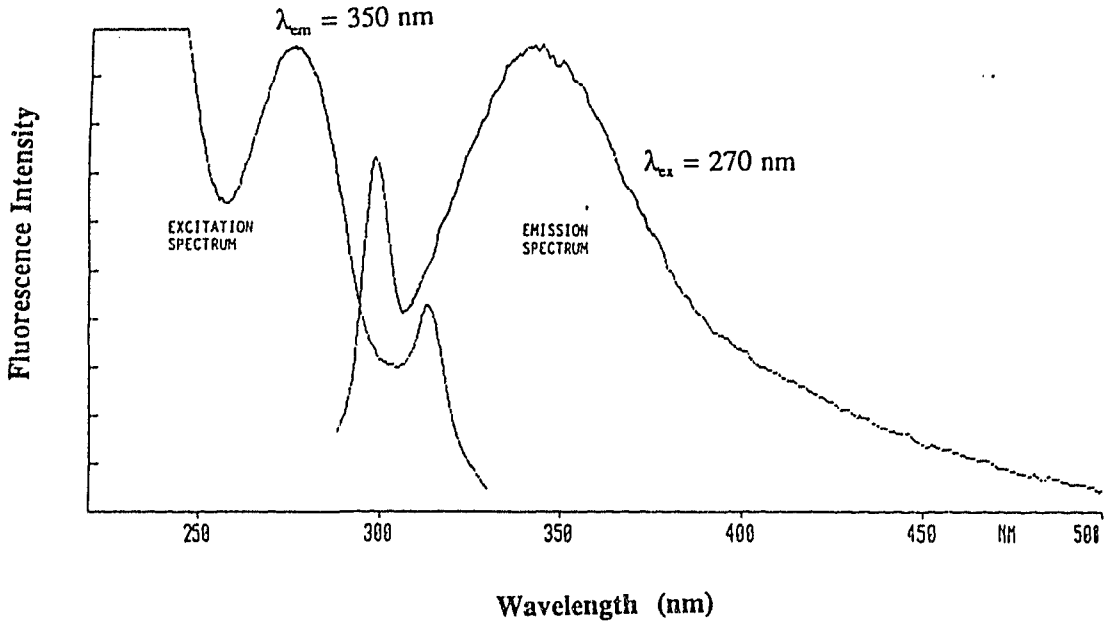

Figure 2.12. Excitation and fluorescence emission spectra of alcohol **1** in 1:1 H_2O-CH_3CN (water portion at pH = 7, buffered solution, excited at 270 nm).

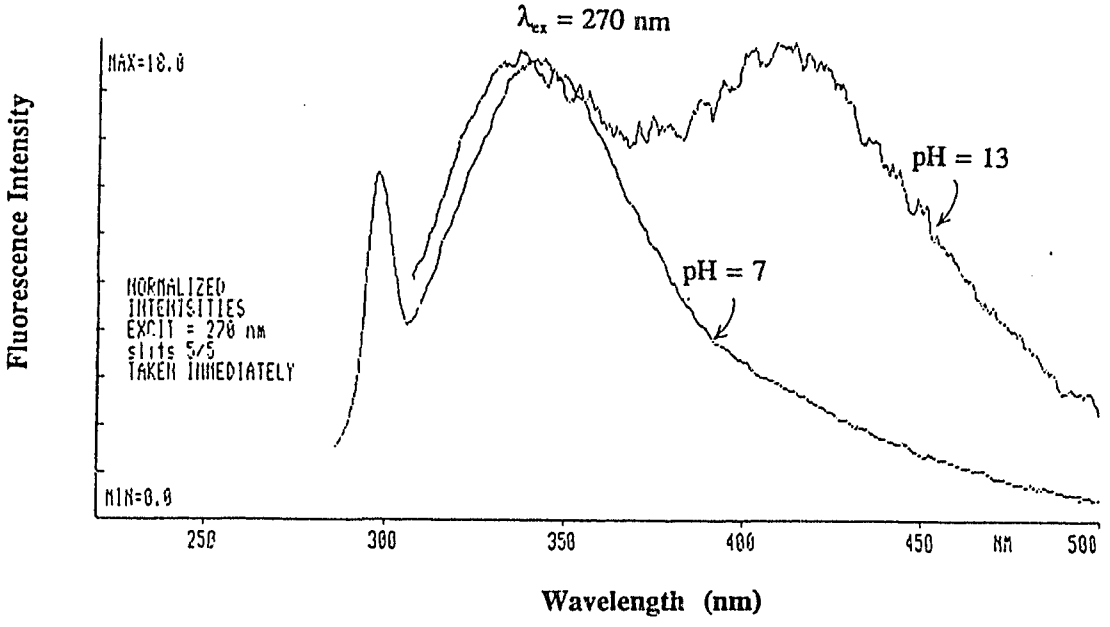

Figure 2.13. Fluorescence emissions of alcohol **1** in 1:1 H_2O-CH_3CN solutions with pH = 7 and 13, respectively (excited at 270 nm).

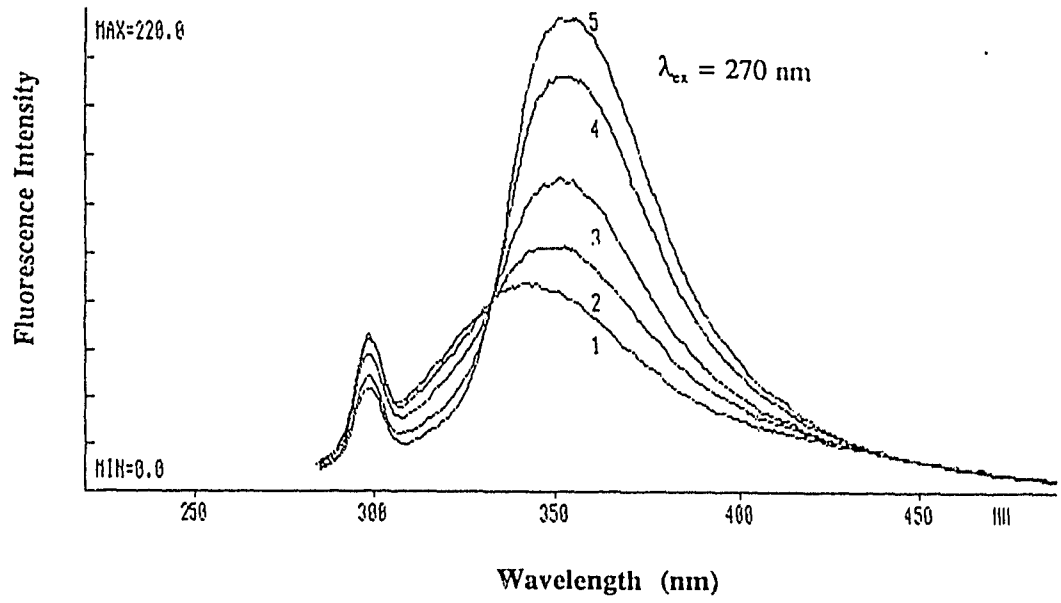

Figure 2.14. Time-dependent fluorescence emissions of alcohol **1** in 7:3 H_2O-CH_3CN (excited at 270 nm).

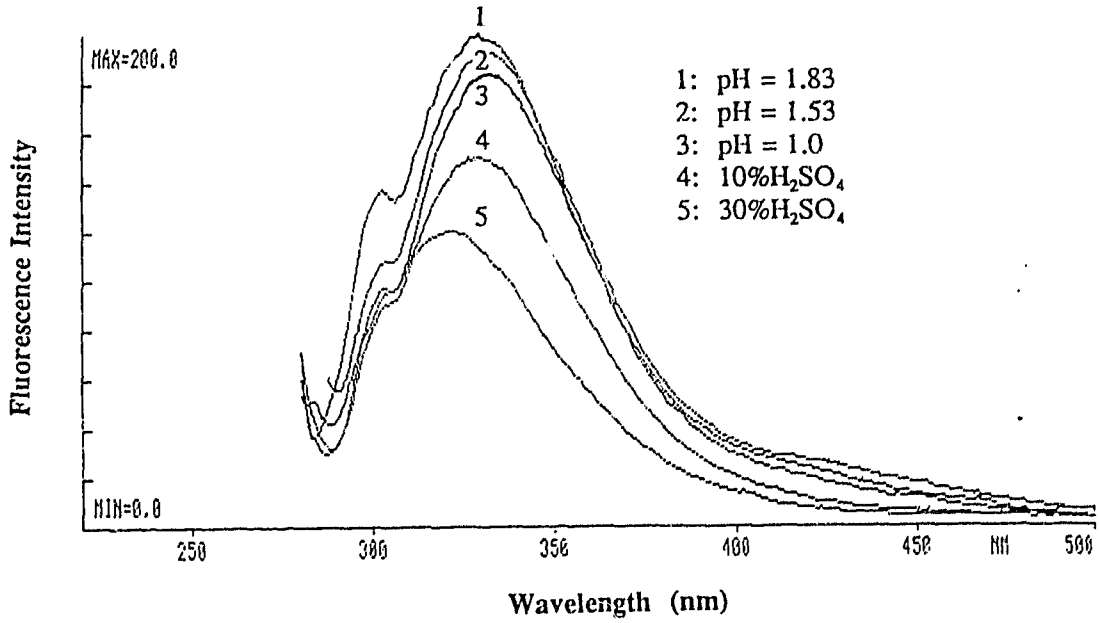

Figure 2.15. Fluorescence emission quenching of **1** in 7:3 H_2O-CH_3CN by added acid (excited at 270 nm).

emissions from phenol and phenolate ion forms of **1**, respectively. Furthermore, the fluorescence emission of phenol moiety could be quenched significantly by added acid, as indicated in Figure 2.15. This acid quenching might indicate that acid-assisted photosolvolysis of **1** does occur as observed in other benzyl alcohols.[22,23,29] These observations are also consistent with previous pH-dependent product quantum yield studies.

The correlation of fluorescence emissions of phenols at various pH-values can be used to determine the singlet excited state $pK_a^*(S_1)$ of the phenols.[92] Unfortunately, in this particular case, the fluorescence emission of phenol **1** was too weak to accurately measure. In order to estimate the pK_a^* of phenol **1**, biphenyl phenol **3** was chosen as a structurally related model compound of **1**. The fluorescence spectrum of **3** in 7:3 H_2O-CH_3CN is shown in Figure 2.16. It is clear from Figure 2.16 that biphenyl phenol **3** is very emissive compared to that of phenol **1**. There are two emission bands of comparable intensity observed for **3** (λ_{max} = 345 nm and 425 nm). The short wavelength band is assumed to be the emission of the phenol form of **3**. Its emission efficiency (Φ_f) was determined to be 0.25 (bandwidth 300-385 nm) in 7:3 H_2O-CH_3CN, using naphtnalene as secondary fluorescence standard. The fluorescence lifetime of this band was found to be τ = 1.2 ns. The longer wavelength band (425 nm) is from the emission of phenolate ion generated from the adiabatic deprotonation of phenol 3. Its emission efficiency (Φ_f) was estimated to be 0.14 (bandwidth 385-500 nm, relative to Φ_f of

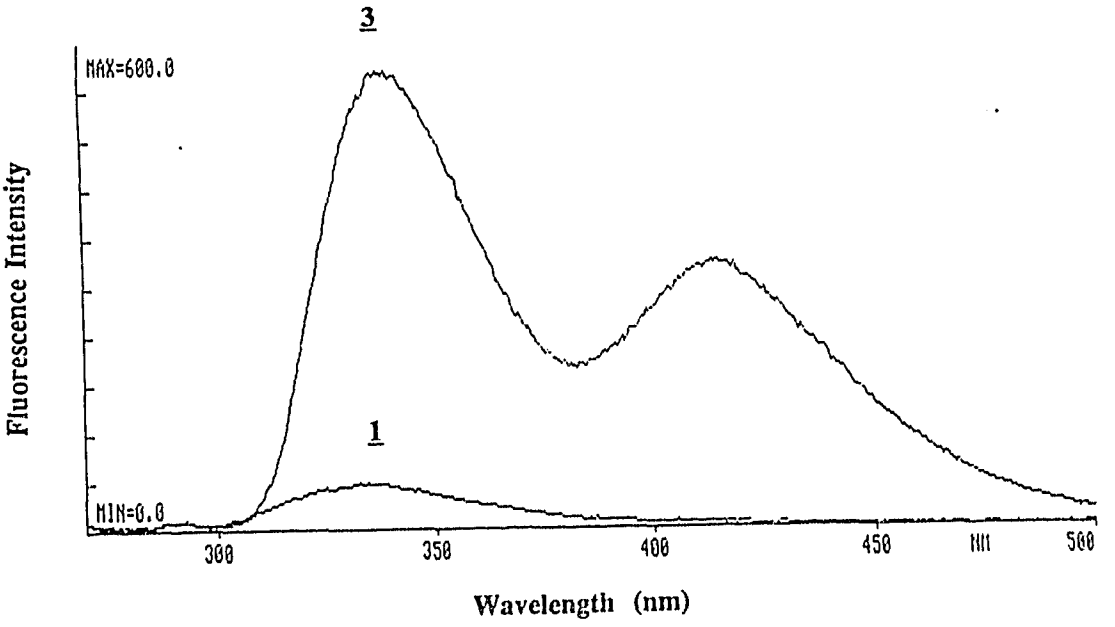

Figure 2.16. Comparison of fluorescence emissions of phenols **1** and **3** in 7:3 H_2O-CH_3CN (excited at 260 nm). Optical densities at 260 nm were matched prior to measurement.

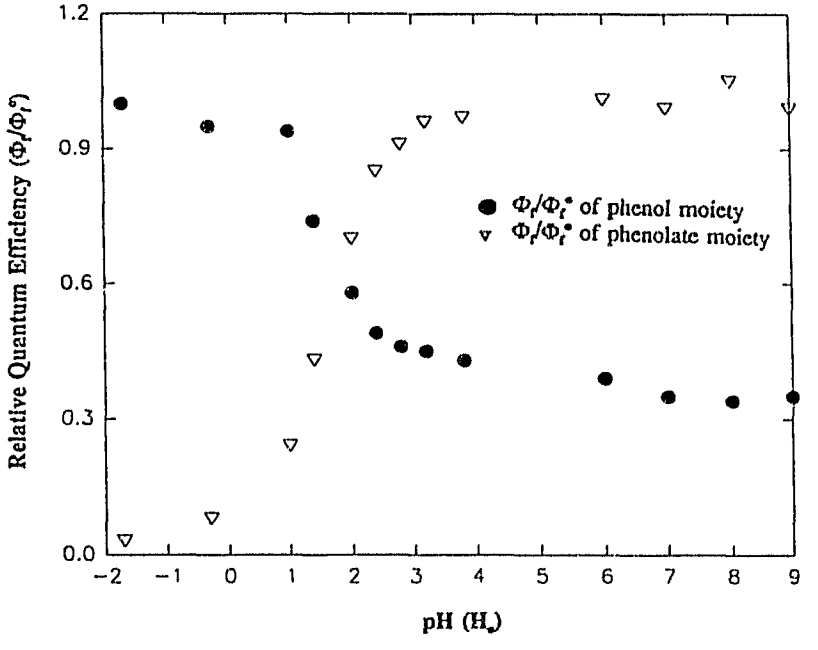

Figure 2.17. The relative emission quantum yields (Φ_f/Φ_f°) of **3** in 7:3 H_2O-CH_3CN (v/v) solutions at various pH-values (quoted pH values are of water portions).

phenol form in **3**) in 7:3 H_2O-CH_3CN. This emission was found to show biexponential decay, τ_1 = 4.2 ns (82%) and τ_2 = 1.2 ns (18%). These observations show that there is adiabatic deprotonation of the phenol **3**, which is a similar to other phenols.[86-90] The relative emission efficiencies of phenol and phenolate moiety of **3** in 7:3 H_2O-CH_3CN were plotted against the pH-values of solutions, as shown in Figure 2.17. Therefore, the singlet excited state $pK_a^*(S_1)$ of phenol **3** was determined to be 1.5 ± 0.2 by this fluorescence titration. This value agrees reasonably well with that of phenol **1**, which was obtained from the quantum yield studies (see Figure 2.10).

Because of the weakness of the emission in aqueous CH_3CN, the fluorescence quantum yield of phenol **1** can only be estimated (Φ_f = 0.02, bandwidth 300-400 nm, relative to Φ_f of the phenol form in **3**). Also, the corresponding lifetime (τ) could not be measured (<0.5 ns) using the single photon counting system available. The weak emission of the phenolate ion of **1** at both pH = 7 and 13 suggests that the phenolate ion is the reactive species responsible for the photocyclization and photosolvolysis. That is, almost all of phenolate forms generated at pH 7 appears to be removed efficiently. However, the phenolate ion form of **3** is photochemically unreactive and thus very emissive.

2.3.4 Triplet-State Sensitization

The fluorescence studies already suggest that the photocyclization is via S_1.

In order to examine the possibility of triplet contribution directly, triplet sensitization of **1** and **6** (E_T = 65 kcal mol^{-1}, estimated on the base of E_T = 64 kcal mol^{-1} for 4-hydroxybiphenyl)[93] with sodium 4-acetylbenzensulfonate (E_T = 74 kcal mol^{-1})[93] and 2-benzophenone-benzoic acetate (E_T = 69 kcal mol^{-1})[93] were carried out. These photolyses at 350 nm in 1:1 or 7:3 H_2O-CH_3CN (pH = 7.0 of water portion) yielded no photoproducts, and the substrates **1** and **6** were recovered unchanged. Thus the triplet excited states of these alcohols are nonreactive under these conditions and it is the singlet excited state that is responsible for the photocyclization and photosolvolysis of **1** and **6**. This conclusion is consistent with results obtained in other benzyl alcohol systems.[22,23,29]

2.4 Discussion

The above results show that the mechanism of the photocyclization of **1** is dependent upon the pH of the medium. There are three distinctly mechanistic regimes, which will be discussed in detail below. In addition, the photogeneration and photochemistry of *o*-quinonemethide type intermediates, along with the secondary photolysis of photoproducts will also be briefly discussed.

2.4.1 Mechanism of Photocyclization

At pH = 2 - 9. The photocyclization mechanism operative in the pH region 2-9 is shown in Scheme 2.1, using alcohol **1** as a model compound. In this acidity

region, **1** exists as a phenol form in the ground state. Excitation of **1** leads to an excited singlet state which is much more acidic than the ground state counterpart and undergoes an efficient deprotonation (which is usually a very fast process,[87-90] $k \sim 10^{10}\ s^{-1}$) to give the phenolate form, which remains on the excited singlet state surface. At the same time, the excited state biphenyl **1** has a tendency to rotate into a more planar geometry. This geometrical relaxation process would also be very fast ($k > 10^{11}\ s^{-1}$) since it is only a torsional motion. These two processes, adiabatic deprotonation and geometrical twisting, might occur simultaneously. As already discussed in Chapter One, it is well established that biphenyl derivatives have a tendency to accommodate more planar forms in the excited state.[37,38] Also, a large number of phenols and related compounds are known to undergo efficient adiabatic ionization of the phenolic hydroxyl groups to give excited state phenolate ions.[86-90] Therefore, the assumption of an adiabatic loss of proton, perhaps concerted with the torsional motion of biphenyl phenol **1** is reasonable. However, the twisting of the *o*,*o*'-disubstituted biphenyl such as **1** can in principle result in *cis* and *trans* isomers, the relative amount of which is unknown. As shown in Scheme 2.2, the subsequent step is *charge transfer* of the phenolate ion to the adjacent benzyl alcohol ring, which results in overall dehydroxylation, to generate two (*cis* and *trans*) *o*-quinonemethide type intermediate **20**. The proposed charge transfer only occurs from the excited phenolate ion since the ground state counterpart fails to undergo the cyclization reaction without irradiation. However,

Scheme 2.2

Mechanistic Scheme of Photocyclization of 1 in pH 2 - 9 Region

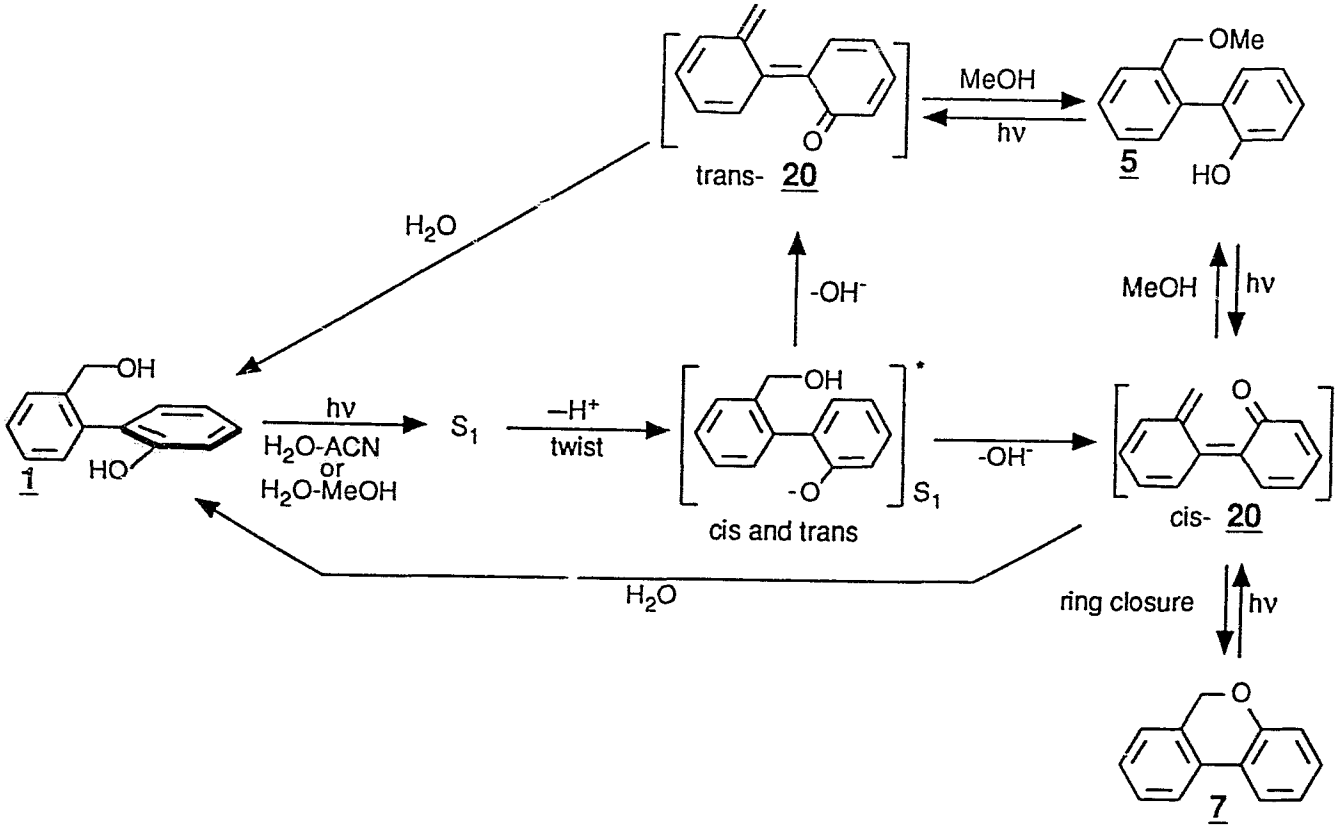

this overall step probably leads into electronic deactivation, crossing back to the ground state surface. Excited state phenolate ions have a very electron-rich character and powerful electron-donor ability, even better than the corresponding phenolic hydroxy and methoxy groups. The methoxy group, proven to be an excellent electron-donor, has been shown to efficiently facilitate the photodehydroxylation (photosolvolysis of a C-OH bond) on irradiation of 2- or 3-methoxybenzyl alcohols.[22,23] The excited state phenolate ion or phenolic hydroxyl group has also been used to promote photosolvolysis.[8,9] It is not surprising that the excited state phenolate ion could assist the photodehydroxylation, particularly in the fully conjugated system such as excited planar biphenyls. Therefore, this proposed dehydroxylation step, a key to cyclized pyran 7, is quite reasonable in terms of the above arguments, and is in fact supported by the experimental results as well. The structure-reactivity studies (*vide supra*) indicate that a necessary requirement for the photocyclization and photosolvolysis (i.e., photosubstitution observed at the benzylic carbon in competition with photocyclization) is *the presence of the phenol moiety in 1*. In addition, the plot of photocyclization quantum yield vs pH for 1 (Figure 2. 10) is strong evidence for the involvement of the phenol moiety. In fact, Figure 2.10 implicates the involvement of the excited state phenolate in the photocyclization mechanism. Furthermore, fluorescence studies indicate that the excited phenolate ion is the reactive species since its emission is very weak, contrary to other photochemically stable phenols. Therefore, it is the excited

phenolate ion that activates the cleavage of the benzylic C-OH bond (through charge transfer). The outcome of the solvolysis of the benzylic C-OH bond from the phenolate ion is the formation of the *cis* and *trans* *o*-quinonemethide intermediates **20** (Scheme 2.2). Again, the ratio of the *cis* and *trans* forms is unknown. However, both forms may be trapped by external nucleophiles (H_2O or MeOH) at the cationic benzylic carbon; only the *cis* form can cyclize to give the pyran **7**. The solvent water capture of intermediate **20** gives back starting material **1**. The trapping of other *o*-quinonemethides by solvent nucleophiles (water or MeOH) has been observed in other studies as discussed in Chapter One (see eq. 1.19).[57-59] It is important to point out that the intermediate **20**, having electrophilic character at benzylic carbon position, is distinctly different from the corresponding carbocation **21**, which can only be generated from photolysis of alcohol **1** in acidic media (*vide infra*).

At pH > 10. In the pH region above 10, **1** exists exclusively as the phenolate ion (phenoxide anion) in the ground state (pK_a = 9.9 ± 0.2 of **1**). Excitation of this form leads to an excited state phenolate ion, which need only twist to reach the precursor to the *o*-quinonemethide **20**. The lower quantum yield (Φ = 0.25) observed at pH = 7 compared to that (Φ = 0.50) at pH > 10 can readily be explained because the quantum efficiency of the deprotonation (from the phenol form to the phenolate form) is not unity. In other words, at pH > 10, there are now fewer non-productive deactivation pathways which the phenolate ion has

to compete with in order to reach the essential reactive intermediates (viz. *o*-quinonemethide **20**). Again, the weak emission ($\Phi_f \sim 0.01$) from the excited phenolate form of **1** is consistent with the high quantum yield for the formation of product **7**. The subsequent reaction pathways are similar to those in the pH 2-9 region.

At pH (H_o) < 0. In the acid region below $H_o = 0$, Φ does not reach zero.

Scheme 2.3

The Mechanistic Scheme for Photocyclization of **1** for the pH < 0 Region

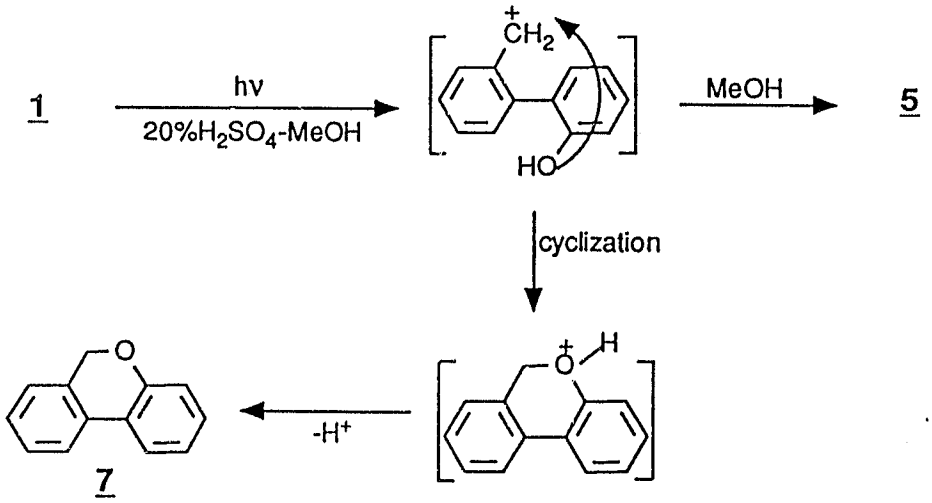

In fact, as the media becomes more acidic, Φ slightly increases (Figure 2.10). In addition, the sluggish inflection between pH = 0-2 indicates that an additional pathway is already making a contribution to the formation of product **7**. Clearly

another distinct mechanistic pathway for the photocyclization is operative at these acidities. Although the phenol moiety no longer undergoes deprotonation in S_1 at these acidities (recall $pK_a^*(S_1) = 1.2$), the so-called acid-catalyzed photodehydroxylation becomes possible due to the presence of moderately strong acid. The acid-catalyzed photosolvolysis of many benzyl alcohols has been well established by Wan and coworkers.[22,23,29] In fact, benzyl alcohols **2** and **4** , structurally related to alcohol **1**, have also been shown to undergo efficient acid-catalyzed photosolvolysis in acidic media, that is, the corresponding methyl ether products were observed on irradiation in MeOH-H_2SO_4 mixtures. Similarly, the acid-catalyzed photosolvolysis of **1** may generate a carbocation intermediate **21**. This carbocation can be trapped by MeOH, to give the photosolvolysis product, methyl ether **5**, which is observed. Due to the presence of the adjacent phenol moiety, the intramolecular cyclization of carbocation **21** occurs, resulting in the formation of pyran **7**. A reasonable mechanism operative for the pH < 0 region is shown Scheme 2.3.

The photocyclization of alcohol **6** probably follows the same mechanism as described for that of alcohol **1**. However, in this case, the photoproducts are not photostable and readily undergo secondary photolysis, leading to a complex of product distribution after exhaustive irradiation of **6**. A distinct feature observed from photolysis of **6** is the formation of styryl derivative **12** as a primary photochemical product, as shown in Figure 2.9. This observation is indicative of

the involvement of *o*-quinonemethide intermediate **20a**, an analogue of **20**, in the

Scheme 2.4

Mechanistic Scheme of Photochemistry of **6**

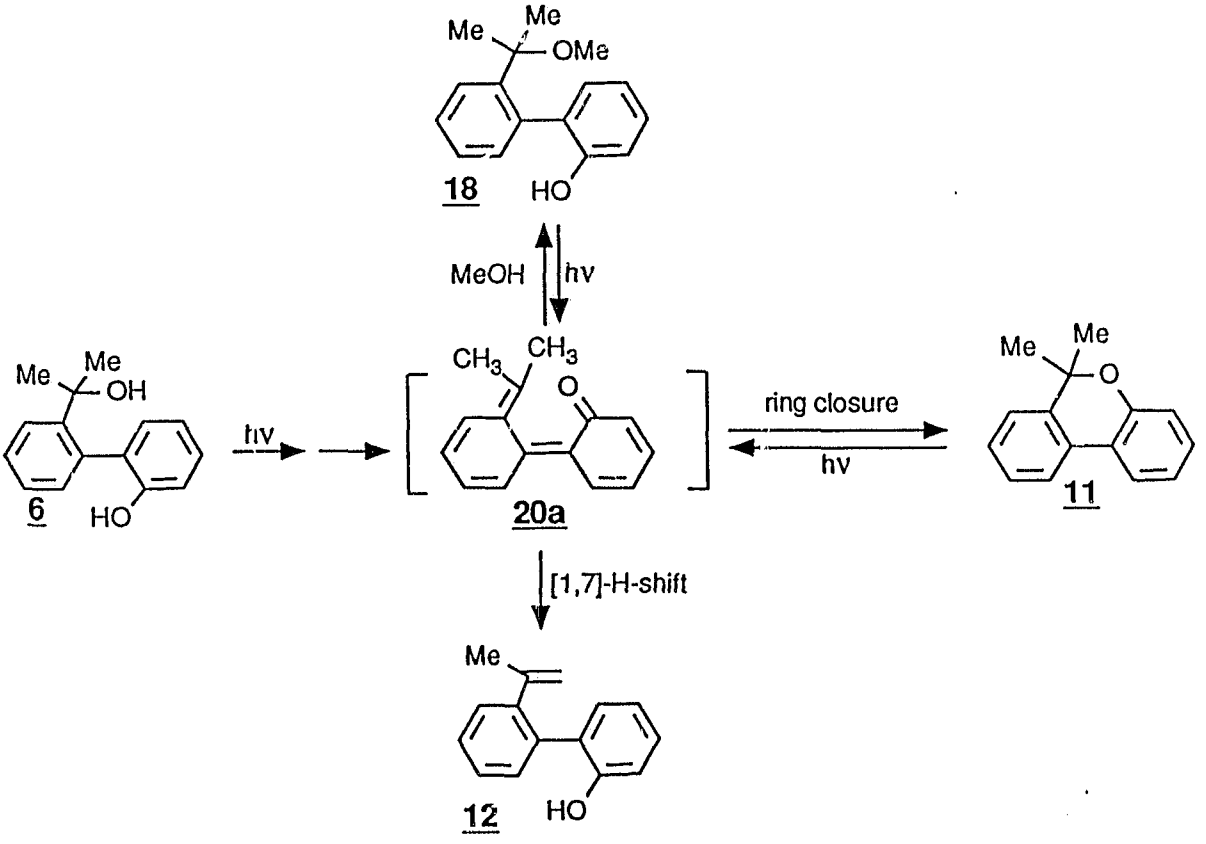

photocyclization reaction (Scheme 2.4). Obviously, apart from cyclizing to pyran **11**, the intermediate **20a** also undergoes a sigmatropic 1,7-hydrogen shift to give styryl **12**. In addition, like **20**, **20a** can also be captured by nucleophile solvents

such as MeOH to yield **18**, which is observed. As discussed in Chapter One, a variety of o-quinonemethides has been well studied[54-60] and their transient absorption spectra in solution have been obtained in some cases.[60] However, *o*-(dibenzo)-quinonemethide type intermediate such as **20** or **20a** have not been reported in the literature. These *o*-quinonemethides, with two destroyed aromatic rings, would be inherently very reactive. In addition, at least two fast deactivation processes, namely intramolecular cyclization to pyrans and diffusion-controlled capture by nucleophiles would account for their short lifetimes. In order to directly obtain their transient absorbtion spectra, a picosecond spectroscopic technique might be needed.

2*H*-Chromenes (2*H*-benzopyrans) are known to undergo 6π electrocyclic ring opening reactions to give *o*-quinonemethide intermediates, as mentioned in Chapter One. It is not surprising that the pyrans **7** and **11**, derivatives of 2*H*-chromenes, are photolabile and undergoes electrocyclic ring opening to give intermediate **20** and **20a**, respectively. The species **20** readily undergoes ring closure to give back starting material pyran **7**, leading to no net photochemistry. When the photoreaction is carried out in nucleophilic solvents such as H_2O-CH_3OH, solvents capture this intermediate, to give alcohol **1** or methyl ether **5**, as observed in photolysis of **7** or **1** in aqueous MeOH. In this situation, a photostationary state is reached after an exhaustive irradiation (see Figure 2.4 and 2.5). However, In the case of **20a**, an additional reaction pathway, the sigmatropic 1,7-hydrogen shift, is

available, resulting in the formation of photoproduct **12**.

The formation of compounds **13-14** on irradiation of **6** is apparently due to the secondary photolysis of styryl derivative **12**. This is clear from the kinetic photolysis of **12**, as shown in Figure 2.9. As discussed in Chapter One, Bowd et al.[48,49] obtained similar results on irradiation of **11** in ethanolic solution (see Scheme 1.3). The photocyclization reactions of 2-substituted biphenyls have also been well established.[43-53] The 2-vinylbiphenyl **12**, with two possible modes of cyclization due to the presence of 2'-hydroxyl group produces ultimately two cyclized photoproducts **13** and **14**. Mechanisms of these photocyclization reactions have already been discussed in Chapter One (see Scheme 1.3).

2.5 Conclusions

In the current chapter, a new photochemical cyclization of alcohol **1** and derivatives **5**, **6** and **19**, to dibenzo[b,d]pyrans **7** and **11** respectively, has been disclosed. The chemical and quantum yields of the photocyclization are very high in aqueous solution. The reaction is proposed to proceed via the excited singlet state. The reaction efficiency is found to be dependent upon the solvent polarity as well as the pH of the media. There are three mechanistic modes operative at acidic, neutral and basic solutions, respectively. Results obtained from structure-reactivity, quantum yield vs pH and fluorescence data suggest a mechanism, in neutral solution, involving initial adiabatic deprotonation from the phenol moiety

to give excited phenolate ion. This step is perhaps concerted with the geometrical relaxation of twisted biphenyl to give a more planar form. The subsequent dehydroxylation of the excited phenolate ion is initiated by charge transfer from the electron-rich phenolate ion to the benzyl alcohol ring, to produce a previously unreported *o*-quinonemethide **20**. In basic solution, the reaction mechanism is similar to that in neutral solution except that the phenolate ion now is directly promoted to an excited species, which has fewer deactivation pathways and thus shows higher product quantum yield. In acidic media, the acid-catalyzed photosolvolysis occurs, to give carbocation **21** which can also cyclize to pyran **7** due to the presence of the adjacent phenolic hydroxy group. The structure-reactivity studies reveal that the phenol moiety (phenolic hydroxyl group) is a necessary requirement for the photocyclization. The reaction appears to be general in similar systems, but secondary photolysis does occur, the extent of which depends on the structure of pyrans. The important implication of this investigation is that the geometrically flexible biphenyl system is another class of precursors for photosolvolytic studies, which has largely been an unexplored area.

2.6 Experimental

2.6.1 General

Preparative or semi-preparative photolyses were carried out using Rayonet RPR 100 photochemical reactors equipped with 254 nm lamps (or 300 and 350 nm

lamps for sensitization experiments). ^{1}H NMR were taken on a Perkin-Elmer RS32 (90 MHz) or a Bruker WM 250 (250 MHz) instrument, in $CDCl_3$ unless otherwise noted. Gas chromatography was carried out on a Varian 3700 instrument with a Hewlett-Packard 3390A integrator and a DB-5 capillary column. Mass spectra were taken on a Finnigan 3300 instrument. UV spectra were taken on a Perkin-Elmer Lambda 4B or Pye-Unicam 800 spectrophotometer. IR spectra were recorded on NaCl plates using a Perkin-Elmer 283 instrument. Fluorescence spectra were performed at ambient temperature using a Perkin-Elmer MPF 66 instrument. Fluorescence lifetimes were measured using standard single photon counting techniques on a Photon Technology International LS-100 instrument. All samples for fluorescence measurements were deaerated by argon purging prior to measurement. Melting points were obtained on a Koefler hot stage microscope and are uncorrected.

2.6.2 Materials

Crystal Structure Analysis. The experimental details are listed in Table 2.1. A Nonius diffractometer using $\omega/2\gamma$ scan was used to collect the data for **1**. A total of 900 reflections were collected and 699 ($I > 1.5\sigma(I)$) used in the structure refinement. A Picker four-circle diffractometer using $\gamma/2\gamma$ scan was used to collect the data for **6**. A total of 1156 reflections were collected and used for structure refinement. Both structures were solved using MULTAN[94] and refined using least

squares using SHELX-76.[95] Illustrations were drawn using ORTEP.[96]

2'-Hydroxybiphenyl-2-carboxylic acid lactone (8). This substance was prepared via the procedure provided by Kenner.[80] To a stirred solution of biphenyl-2-carboxylic acid (10 g, 50.5 mmole) in acetic acid (150 mL) was carefully added a suspension of chromic anhydride (CrO_3) (40 g, 400 mmole) in 80 mL distilled water. The reaction mixtures were refluxed at 95 - 105°C for 45 min and then poured into 200 mL cooled water. The combined extracts (by 3 x 150 mL CH_2Cl_2) were washed with saturated aqueous $NaHCO_3$ to remove the unreacted starting material and then dried over $MgSO_4$. Removal of organic solvents under reduced pressure gave a white solid powder. The recrystallization of this powder from EtOH afforded a white crystal (3.96 g, 40%), mp 90 - 92°C (lit.[80] 92.5°C); ^{1}H NMR δ 7.25-8.35 (m, 8H, Ar-H); MS (EI) m/z (relative intensity) 196 (M^+) (100), 168 (M^+-CO) (38), 139 (44); IR (cm^{-1}) (in mineral oil on NaCl plates) 3050 (w), 1720 (s), 1598 (m), 1550 (m), 1500 (m), 1300 (m). The ^{1}H NMR and MS data are consistent with those reported by Kenner.[80]

2-(2'-Hydroxyphenyl)benzyl alcohol [2'-hydroxy-(1,1-biphenyl)-2-methanol] (1). A suspension of **8** (3.2 g, 16.3 mmole) in THF (200 mL) was added over 5 min to a stirred solution of lithium aluminum hydride (2 g, 52 mmole) in THF (80 mL) at room temperature. The reaction mixture was heated

under reflux for 1 h and then cooled to 0°C. Ethyl acetate (100 mL) was cautiously added over 10 min, followed by aqueous 6 N sodium hydroxide solution (150 mL). The tetrahydrofuran-ethyl acetate phase was removed and discarded. The aqueous alkaline solution was cooled by the addition of ice (150 g), acidified with 4 N hydrochloric acid, and extracted with ether (3 x 150 mL). The combined ether extracts were dried over $MgSO_4$ and evaporated under reduced pressure. The residual oil became solid overnight, giving **1** (2.28 g, 70%). The solid was further recrystallized from toluene to yield colourless needles, and from toluene- MeOH to give rise to single crystal of **1**. mp 134-135 °C (lit.[79], 137°C from benzene). ^{1}H NMR (1:2 acetone-d_6:$CDCl_3$), δ 8.17(s, 1H, exchangeable with D_2O, Ar-OH), 7.60-6.80 (m, 8H, Ar-H), 4.48 (d, J = 6.0 Hz, 2H, -CH_2O), 4.05 (t, J = 6.0 Hz, 1H, exchangeable with D_2O, -OH). Mass spectrum (CI and EI) m/z (rel int) 182 (M^+ - H_2O) (14), 181 (182 - H^+) (100), 171 (10). The ^{1} NMR and MS data agree with the those reported in literature.[79] This compound was further characterized by X-ray crystallography (see text).

2-(2'-Methoxyphenyl)benzyl alcohol (4). To a stirred suspension of potassium carbonate (K_2CO_3) (1.4 g, 10 mmole) and methyl iodide (1.4 mL, 15 mmole) in dried acetone (20 mL) was added alcohol **1** (2 g, 10 mmole). The reaction mixture was refluxed for 3 h and then cooled to room temperature. The cooled solution was filtered by gravity and the solvent acetone was removed under

reduced pressure to provide a colourless oil residual which was purified by column chromatography (20 g silica gel, CH_2Cl_2). ^1H NMR δ 7.61-6.93 (m, 8H, Ar-H), 4.42 (s, 2H, $-CH_2O$), 3.70 (s, 3H, $-OCH_3$). Mass spectrum (EI) m/z (rel int), 214 (M^+) (10), 181 (16), 165 (8), 108 (12), 32 (100).

2-(2'-Hydroxyphenyl)benzyl methyl ether (5). To a stirred solution of **1** (0.5 g, 2.5 mmole) in MeOH (100 mL) was carefully added 2 mL con. H_2SO_4. The reaction mixture was refluxed overnight and quenched with 20 mL of 1 M NaOH. The solution was adjusted to neutrality (pH = 7) and then extracted with CH_2Cl_2 (3 x 100 mL). The combined extracts were dried over $MgSO_4$ and evaporated under reduced pressure to give a colourless oil, which was further purified by preparative TLC (silica, CH_2Cl_2). ^1H NMR δ 7.51-6.95 (m, 8H, Ar-H), 5.12 (broad, exchangeable with D_2O, 1H, Ar-OH), 4.26 (s, 2H, $-CH_2O$), 3.32 (s, 3H, -OMe). Mass spectrum (EI) m/z (rel int) 214 (M^+, 12), 181 (100).

2-(2'-Hydroxyphenyl)-α,α-dimethylbenzyl alcohol (6). Methyl magnesium bromide reagent was prepared from methyl bromide (8 mL, 16 mmol) and magnesium (2 g, 83.5 mmole) in 30 mL anhydrous ether with a few crystal of I_2 under nitrogen. This solution was added dropwise over 30 min to a stirred solution of **8** (4 g, 20 mmole) in 150 mL THF. The reaction was heated under reflux for 3 h and quenched with aqueous KH_2PO_4 (200 mL). The combined extracts (3 x

150 mL CH_2Cl_2) were dried over $MgSO_4$ and evaporated to give a solid, which was recrystallized from toluene to afford colourless crystals of **6**. mp 124-125°C. Yield 70% (3.2 g). ^{1}H NMR (1:1 $CDCl_3$-DMSO), δ 7.82 (broad, 1H, exchangeable with D_2O, Ar-OH), 7.70-7.60 (m, 1H, Ar-H), 7.40-6.90 (m, 7H, Ar-H), 3.81 (broad, 1H, exchangeable with D_2O, -OH), 1.57 (s, 3H, $-CH_3$), 1.32 (s, 3H, $-CH_3$). Mass spectrum (CI) m/z (rel int) 210 (M^+-H_2O) (100), (EI) 196 (130), 195 (100), 115 (8), 63 (7). IR (cm^{-1}) (mineral oil) 3290 (s, broad), 3050 (w), 1580 (m), 1400 (m), 1380 (s), 1200 (s), 1152 (s).

6*H*-Dibenzo[b,d]pyran (7). This compound was prepared from 2'-hydroxybiphenyl-2-carboxylic acid lactone (**8**) according to the procedure of Delvin.[79] ^{1}H NMR δ 7.68 (m, 2H, Ar-H), 7.40-6.90 (m, 6H, Ar-H), 5.08 (s, 2H, $ArCH_2O$); MS (EI) m/z (rel int) 183 (M^++1) (10), 182 (M^+) (78), 181 (M^+-1) (100), 152 (25), 115 (7), 76 (9). The ^{1}H NMR and MS data are identical to those reported by Delvin.[79]

6,6-Dimethyl-6*H*-dibenzo[b,d]pyran (11).[49] A suspension of lactone **8** (4 g, 20 mmole) in THF (100 mL) was added over 10 min to 40 mL of a solution of 1 M methyl magnesium bromide in THF. The reaction mixture was heated under reflux for 3 h. The reaction solution was cooled and poured into a mixture of 30% sulfuric acid (15 mL) and ice (100 g) with vigorous stirring. The aqueous phase

was refluxed for 2h and then extracted with ether (3 x 100 mL). The combined ether extracts were dried over $MgSO_4$ and evaporated to give a colourless oil which was purified by column chromatography (50 g silica, hexanes). Yield 3.5 g (83%). ^1H NMR δ 7.80-7.70 (m, 2H, Ar-H), 7.35-6.95 (m, 6H, Ar-H), 1.59 (s, 6H, 2 x -CH_3); MS (EI) m/z (rel int), 210 (M^+) (6), 196 (15), 195 (M^+-CH_3, 100), 165 (11), 32 (17). The ^1H NMR and MS data were identical to that reported by Bowd et al.[49] for this compound.

2-(2'-Hydroxyphenyl)-α-α-dimethylbenzyl methyl ether (18). To a stirred solution of **6** (0.2 g, 0.9 mmole) in 100 mL MeOH was added 20 mL pH = 1 (H_2SO_4) solution and left stirring overnight at room temperature. The reaction was quenched by adding cold water and extracted with 2 x 150 mL CH_2Cl_2. On evaporation of the solvent, GC and ^1H NMR analysis showed ca. 5% of **18**, the rest being **6** and pyran **11**. The methyl ether **18** could not isolated due to its low yield and was tentatively identified by GC/MS and ^1H NMR (partial) δ 1.25 (s, 6H, CH_3), 3.05 (s, 3H, OCH_3); GC retention time (t_r) (column temperature at 180°C) 4.83 min for **18** and 4.74 min for **6**, respectively; MS (CI) m/z (rel int) 210 (M^+-MeOH) (100).

2-(2'-Hydroxyphenyl)benzyl chloride (19). This substance was prepared from alcohol **1** using a method developed by Masada and Murotani.[82] To a

solution of 20 mL conc. HCl was added a mixture of alcohol **1** (0.5 g, 2.5 mmole) and lithium chloride (1 g) at 0°C. After addition, the reaction mixture was warmed up to 50°C and stirred until the solid materials completely dissolved. After heating at 60°C for 6 h, the reaction was quenched with 100 mL of distilled water. The combined organic extracts (3 x 100 ml CH_2Cl_2) were washed with ethylene glycol (3 x 50 ml) to remove the hydrochloric acid and dried over $MgSO_4$, which on evaporation under reduced pressure gave **19** as a colourless oil (0.4 g, 73%). This was purified by prep TLC (silica, CH_2Cl_2). ^{1}H NMR, δ 7.63-6.90 (m, 8H, Ar-H), 5.0 (broad, 1H, exchangeable with D_2O, Ar-OH), 4.41 (s, 2H, -CH_2Cl); MS (CI) m/z (rel int) 182 (M^+-HCl) (100).

2.6.3 Product Studies

In general, 20-200 mg samples were dissolved in the appropriate solvent or solvent mixture (3-200 mL) and irradiated in one of (i) 3.0 mL Suprasil quartz cuvettes, (ii) 20 mL quartz tubes or (iii) 100 or 200 mL quartz tubes, depending on the scale of the experiment. For analytical scale runs by GC, only the 3.0 or 100 mL volume were employed, whereas for preparative runs, the 200 mL tubes were used. Photolyses using the 100 or 200 mL tubes were cooled using a cold-finger (tap water) along with continuous purging with a stream of argon via a long fine metal needle. Photolyses using the smaller 20 mL tubes or cuvettes were carried out using a merry-go-round apparatus and were cooled by air. These

samples were purged with a stream of argon and sealed with Teflon stoppers or stop-cocks prior to photolysis.

Dark Reactions. None of the compounds studied in this work showed any tendency to react in the dark under photolysis conditions. Shown here is a typical experimental procedure for a preparative dark reaction. A solution of 100 mg compound in 200 mL of solvents used for photolysis was stirred in the dark at room temperature for the appropriate irradiation time. The reactions were worked up by saturating the solution with NaCl and extracting with CH_2Cl_2. The isolated materials were analyzed by ^1H NMR and GC. Starting materials were recovered unchanged.

Photolysis of 1 in 1:1 H_2O-CH_3CN. Preparative photolysis of **1** was carried out in the following fashion. A solution of substrate **1** (200 mg) in 1:1 aqueous CH_3CN (200 mL) was irradiated at 254 nm for 1.5 h. After photolysis, an additional 200 mL of distilled water was added and the solution was saturated with NaCl (3 g). The solution was then extracted by 3 x 150 mL CH_2Cl_2. The combined organic extracts were dried over $MgSO_4$ (3 g) and solvents evaporated under reduced pressure. Product analysis was carried out using ^1H NMR and GC. Final product identification was achieved by isolation via prep TLC (silica, CH_2Cl_2) to yield 150 mg (82.5 %) of **7**.

In an analytical scale experiment, a solution of about 20 mg **1** in 1:1 H_2O-CH_3CN (100 mL) in a 100 mL quartz tube was irradiated. At intervals, 1 mL of

the irradiated solution was taken out and then treated with 2 mL of distilled water and 1 mL of stock solution of xanthene (**26**) in CH_2Cl_2, saturated with NaCl. The mixture was then extracted with CH_2Cl_2 (3 x 1 mL) and the organic layer was separated and dried over $MgSO_4$. The condensed solution (~0.2 mL) was subjected to the GC analysis at 180°C. The conversion and yields were calculated and photoproducts identified by comparing their retention times with those of authentic samples. The GC retention times (t_r) were 4.53 and 5.34 min for **7** and **1**, respectively (column temperature at 180°C).

*Photolysis of **1** in 100% MeOH.* A solution of 200 mg of **1** in 200 mL MeOH was photolyzed at 254 nm for 2 h. After irradiation, the solvent MeOH was removed and the photolysate analyzed by ^{1}H NMR and GC, which indicated only **7** and **5** as photoproducts, in a 55:45 ratio. To confirm their structures, they were separated by prep TLC (silica, CH_2Cl_2) and identified by comparison with authentic samples. Analytical runs were carried out as described above, using GC for analysis.

*Photolysis of **2,3 or 4** in 1:1 H_2O-CH_3CN.* Solutions of 100 mg of **2**, **3** or **4** in 1:1 H_2O-CH_3CN were irradiated at 254 nm for 2 h. After photolysis and the same work-up procedure described above was followed. The product mixture was analyzed by GC/MS and ^{1}H NMR. In the case of **3** and **4**, no photoproducts were detected and starting materials recovered completely unchanged. In the case of **2**, a photoisomerization product was formed and identified as *m*-phenylbenzyl alcohol.

^{1}H NMR δ 7.60-7.30 (m, 9H, Ar-H), 4.71 (s, 2H, -CH_2O), 1.85 (broad, 1H, exchangeable with D_2O, -OH) and MS (EI) m/z (rel int) 184 (M^+) (100), 165 (32), 155 (70), 152 (31), 77 (23). The ^{1}H NMR and MS data are consistent with those of an authentic sample.

Photolysis of 2 and 4 in 1:1 H_2O-MeOH (H_o = -2). Solutions of **2** and **4** (~100 mg) in 1:1 MeOH-20% H_2SO_4 (200 mL) were irradiated for 2h, respectively. After neutralizing the solutions with 1 **M** NaOH, the general work-up procedure already described was used. The corresponding methyl ethers were isolated by prep TLC and were the only products. Dark control reactions indicated no thermal solvolysis. (2-Phenylbenzyl) methyl ether was formed from **2** (~30%), ^{1}H NMR δ 7.50-7.25 (m, 9H, Ar-H), 4.25 (s, 2H, -CH_2O), 3.25 (s, 3H, -OMe), and 2-(2'-Methoxyphenyl)benzyl methyl ether was formed from **4**, ^{1}H NMR δ 7.55-6.95 (m, 8H, Ar-H), 4.30 (s, 2H, -CH_2O), 3.25 (s, 3H, OMe). The ^{1}H NMR data of these products were compatible with those of corresponding authentic samples.

Photolysis of 5 in 100% MeOH. A solution of 100 mg of **5** in 200 mL MeOH was irradiated at 254 nm for 2 h. After photolysis, the solvent was removed directly. The product mixture showed formation of **7** (50%) and substrate **5** (50%). The extended photolysis (>3 h) increased the yield of **7** to a maximum of 55%, with recovered **5** (45%). This ratio (determined by GC) is believed to be the photostationary state, as confirmed by photolysis of **7** in 100% MeOH described below.

Photolysis of 6 in 1:1 H_2O-CH_3CN. For preparative photolysis, a solution of 200 mg of **6** in 1:1 H_2O-CH_3CN (200 mL) was irradiated at 254 nm for 2 h. After the general work-up described above, the product mixtures were separated by prep TLC (silica, 1:1 hexanes-CH_2Cl_2). Four photoproducts were isolated and identified by GC/MS and ^1H NMR as: **11** (10%), t_r = 4.57 at 180 °C, the spectroscopic data are consistent with the authentic sample; **12** (7%), t_r = 3.82 at 180 °C, ^1H NMR δ 7.30-6.80 (m, 8H, Ar-H), 5.05 (m, 2H, $=CH_2$), 1.68 (s, 3H, $=C-CH_3$), MS (CI) m/z (rel int) 211 (M^+ + 1) (100); **13** (25%), t_r = 7.38 at 180 °C; ^1H NMR δ 7.35-6.8 (m, 7H, Ar-H), 5.38 (broad, exchangeable with D_2O, 1H, -OH), 2.90-2.50 (m, 3H, $-CH-CH_2$), 1.24 (d, J = 8.0 Hz, 3H, $-CH_3$), MS (CI) m/z (rel int) 211 (M^++1) (100); **14** (40%), t_r = 8.00 at 180 °C, ^1H NMR δ 8.75 (m, 2H, Ar-H), 8.15 (m, 1H, =CH-), 7.80-7.60 (m, 6H, Ar-H), 2.74 (s, 3H, $-CH_3$), MS (CI) m/z (rel int) 193 (M^+ + 1) (100). The yields were calculated on the base of integrations of ^1H NMR and GC. All ^1H-NMR data of photoproducts **12-14** are consistent with those reported by Bowd et al.[49]

(ii): For analytical runs, a solution of 20 mg of **6** in 1:1 H_2O-CH_3CN (100 mL) was irradiated. After the normal work-up mentioned above, the product mixture was analyzed by GC at 180°C. Relative yields of the various products were calculated from uncorrected GC integration areas with the total area normallized to 100. Since all the products have the same number of carbons, this would not introduce any significant errors in the product ratios. The photoproducts

were further identified by GC/MS and by comparing their retention times with those of authentic samples.

*Photolysis of **6** in 100% MeOH.* A solution of 100 mg of **6** in 100 mL MeOH was photolyzed at 254 nm for 5-10 min. After photolysis, the solvent MeOH was removed and the product mixture analyzed by ^{1}H NMR. In addition to the formation of products **11** and **12** (and subsequently **13** and **14**), the MeOH trapping product **18** was also observed in low yield (<6%) (as identified by GC/MS (t_r = 4.83 at 180°C) and its methoxy singlet at δ 3.05 ppm).

Photolysis of 7 in 100% MeOH. A solution of 20 mg of 7 in 100 mL MeOH was irradiated. At interval, a 2 mL portion of the irradiated solution was taken out and condensed to 0.5 ml. The product mixture was subjected to GC analysis at 180 °C. The photoproducts were identified by comparing the data of GC/MS and retention times with those of authentic samples. After exhaustive photolysis, the ratio of **7** (t_r = 4.52 min) to **5** (t_r = 4.40 min) was constant at 55:45.

Photolysis of 7 in 1:1 H_2O-CH_3CN. A solution of 20 mg of 7 in 1:1 H_2O-CH_3CN (100 mL) was irradiated. After standard work-up as described above, the product mixture was analyzed by GC at 180°C. The photoproducts were identified by comparing the GC/MS data and retention times with those of authentic samples. After exhaustive photolysis, the ratio of **7** (t_r = 4.53 min) to **1** (t_r = 5.34 min) was constant at 98:2.

*Photolysis of **11** in 1:1 H_2O-CH_3CN.* A solution of 20 mg of **11** in 1:1 H_2O-CH_3CN (100 mL) was irradiated. After work-up, the product mixture was analyzed by GC at 180°C. The photoproducts **12-14** were observed and identified by comparing the GC/MS data and retention times with those of authentic samples.

*Photolysis of **11** in 100% MeOH.* A solution of 100 mg of **11** in 100 mL pure MeOH was irradiated for 15 min. After the standard work-up, the product mixture was analyzed by GC and ^{1}H NMR. In addition to the formation of products (**12-14**), product **18** was also detected in low yield (5%) by GC (t_r = 4.83 min at 180°C) and by ^{1}H NMR (partial) δ 3.05 (s, 3H, OMe).

*Photolysis of **19** in 1:1 H_2O-CH_3CN.* A solution of 50 mg of **19** in 1:1 H_2O-CH_3CN (100 mL) was photolyzed for 30 min. Following the standard work-up, the product mixture was analyzed by GC (three peaks, t_r = 4.94 min for **19**, t_r = 4.52 min for 7 and t_r = 5.34 min for **1**) and ^{1}H NMR. The conversion was 60%, calculated on the base of integrated areas of GC and ^{1}H NMR peaks.

2.6.4 Triplet State Sensitization

In a typical experiment, 20 mg of **1** or **6** and 3 g of sensitizer (sodium 2-benzoylbenzoic acetate or sodium 4-acetylbenzenesulfonate; purchased from Aldrich) was dissolved in 1:1 H_2O-CH_3CN (100 mL) (pH was adjusted to 7.0). The solution was irradiated at 350 nm for 1 h with argon purging before and throughout the photolysis. At 350 nm, only the sensitizer absorbed irradiation.

After photolysis, the solution was saturated with NaCl (2 g) and extracted with CH_2Cl_2 (3 x 150 mL). The combined organic layers were then washed with sodium bicarbonate solution (3 x 100 mL) to remove residual sensitizer and evaporated and the residue analyzed by GC and ^1H NMR. In all runs, no photoproducts were formed and the starting materials recovered completely unchanged.

2.6.5 Quantum Yield Measurements

Quantum yields were measured using 280 nm excitation from the output of an Oriel 200 W Hg lamp filtered through an Applied Photophysics monochromator and a 254-400 bandpass filter. Stock solutions (10^{-3} M) were prepared and 3.0 mL were put into 3.0 mL quartz cuvettes and purged with a stream of argon prior to photolysis. Potassium ferrioxalate was used for chemical actinometry.[97] The details of this technique are described in Appendix C. After photolysis, the solution was saturated with NaCl and extracted with CH_2Cl_2 (3 x 3 mL). The combined organic layers were dried over $MgSO_4$ and condensed to a 1 mL solution which was analyzed by GC at 180 °C. The conversions were kept low (10-15%). Excellent material balances were observed, as indicated by ^1H NMR spectroscopy and determined by adding xanthene (**26**) as an internal standard. GC responses of starting materials and products were essentially identical. This was done by co-injecting 1:1 ratio (in mole) of substrate **26** and each of products (using authentic

samples). The ratio of integrated areas of **26** and any of products was determined to be 47-53%, except for the ratio of **26:41** (= 0.48).

2.6.6 Fluorescence Measurements

Fluorescence emission spectra (uncorrected) were taken in 3.0 mL quartz cuvettes at about 10^{-4} M using a Perkin-Elmer MPF 66 spectrophotometer at ambient temperature. Standardized HCl or H_2SO_4 solutions were used for acid quenching experiments. The fluorescence quantum yields of **1** and **3** in neutral 1:1 H_2O-CH_3CN were measured relative to naphthalene (Φ_f = 0.23 in cyclohexane[99]) as secondary fluorescence standard. Optical densities at λ_{ex} = 260 nm were matched prior to measurement. Fluorescence lifetimes were measured at room temperature on a standard single photon counting instrument (PTI LS-1 spectrofluorimeter equipped with single photon electronics) using a hydrogen spark lamp as excitation source. Decays were analyzed using software supplied by PTI.

CHAPTER THREE: Photocyclization of 2-Phenoxybenzyl Alcohols 22, 23 and Derivative 25

3.1 Introduction

As discussed in Chapter One, methoxybenzyl alcohols are subject to acid-catalyzed photosolvolysis.[22,23] Our initial attempt was to study 2-phenoxybenzyl alcohol (**22**), which might photosolvolyze in moderately strong acidic medium, to generate a carbocation. The carbocation would then undergo an intramolecular Friedel-Crafts alkylation reaction, to give xanthene (**26**). Such a photochemical process might prove useful in the synthesis of xanthene derivatives. However, preliminary photolysis of **22** in aqueous solutions led to the formation of cyclized product **7** as mentioned in Chapter One.[61] It was then found that the predominant reaction pathway in neutral aqueous solution proceeded via an initial aryl-O bond homolysis.[62] This unexpected photocyclization promoted us to further investigate the photochemistry of **22** and related compounds **23-25** in various media. As discussed in Chapter One, the photorearrangement of diaryl ethers via initial aryl-O bond homolysis has been studied.[63,75,76] However, the nature of the excited state and the effect of hydroxylic solvents on the efficiency of photorearrangement have not been fully clarified.[63] In this chapter, we present the development of a novel photocyclization reaction of 2-phenoxybenzyl alcohols and the elucidation of the corresponding reaction mechanism. These results show that an assembly of *ortho*-

substituted phenoxy and hydroxymethyl (CH_2OH) groups on the benzene ring can induce previously unexplored photochemical cyclization reactions, which are initiated by aryl-O bond homolysis.

3.2 Results

3.2.1 Product Studies

Photolysis of 22 in Neutral Solution. Photolysis of a 10^{-3} **M** solution of **22** in 1:1 or 6:4 H_2O-CH_3CN (Rayonet RPR 100 reactor; 40 min; 254 nm; solution was cooled and purged by argon) gave 6*H*-dibenzo[b,d]pyran (**7**) and several minor

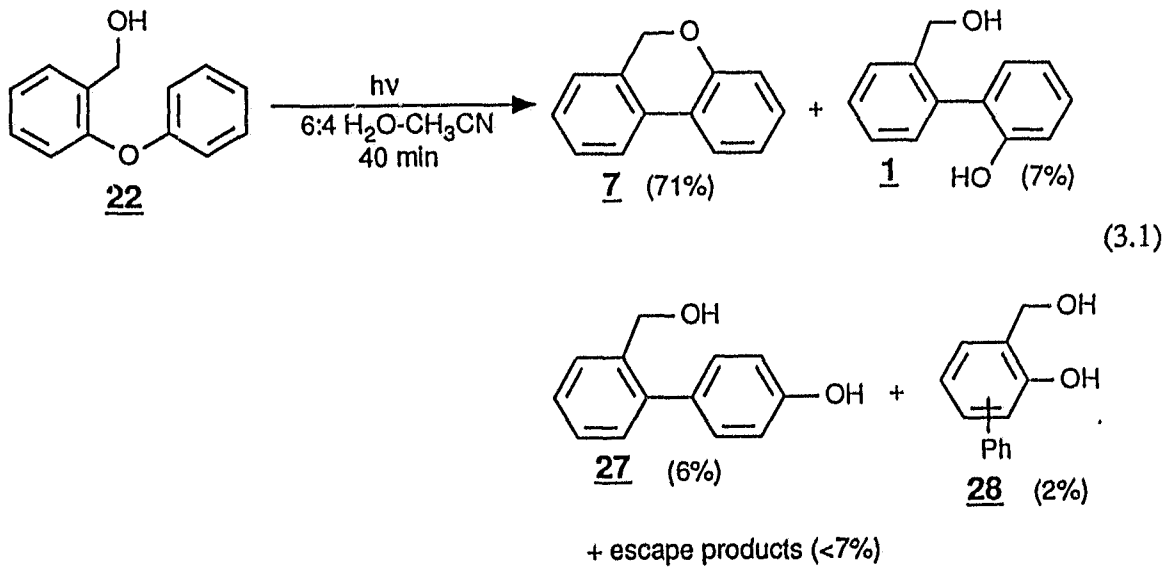

(3.1)

hydroxybiphenyls **1**, **27** and **28** in the quoted yields (eq. 3.1). In addition, small amounts of phenol and benzyl alcohol were also detected, which accounts for a total of 7% yield on prolonged irradiation. These products arise from fragmentation of **22**, via radical escape (*vide infra*). They were not quantitatively

monitored in subsequent product studies. The photoproducts **1**, **7** and **27** were isolated and characterized by ^{1}H NMR and MS. Although not isolated due to their low yields, hydroxylbiphenyls **28** were only tentatively identified by GC-MS (two peaks at r_t = 5.21 and 7.20, respectively, with molecular weight = 200) and by ^{1}H NMR (two singlets at δ 4.50). Separation of nonpolar **7** from starting material and polar hydroxybiphenyls was readily accomplished by chromatography due to the large difference in their retention times. Conversions obtained by GC analysis were further confirmed by ^{1}H NMR spectroscopy. No products were observed without photolysis and the starting material was recovered unchanged.

In order to explore the photocyclization mechanism, a kinetic study of the photolysis of **22** in aqueous CH_3CN (analysis by GC) was carried out and shown in Figure 3.1. It is clear from this plot that the yields of hydroxybiphenyls (**1**, **27** and **28**) remained more or less constant while that of pyran **7** continued to grow as the starting material was lost. Thus pyran **7** was formed as the major product in moderately high yield. A closer examination of Figure 3.1 (see inset) showed that the 2-(2'-hydroxyphenyl)benzyl alcohol (**1**) was formed in higher yield than the pyran **7** at earlier stages (<5% conversion) of the reaction. This observation suggests that pyran **7** is a *secondary* photoproduct of alcohol **1**. Indeed, independent photolysis of **1** under the same conditions as for **22** gave only **7** with high yield (over 95%), as discussed in Chapter Two (see eq. 2.1).

When irradiated in 100% CH_3CN and 100% MeOH, **22** produced the same

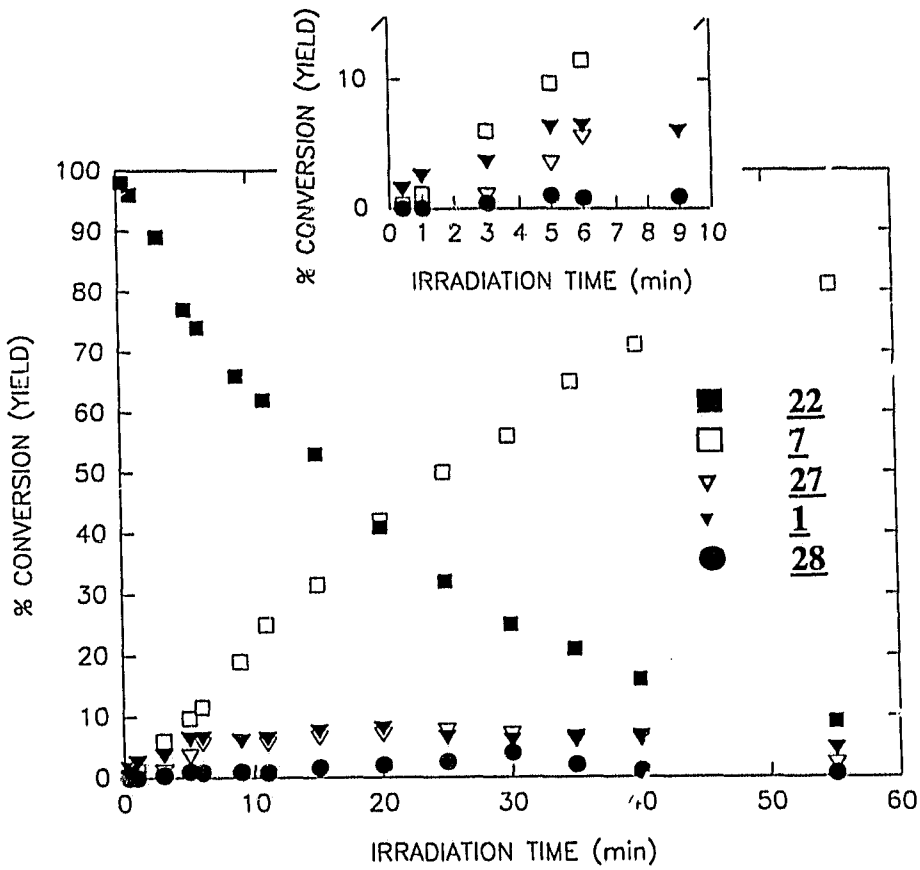

Figure 3.1. Plot of conversion of **22** and product yields as a function of photolysis time on irradiation of alcohol **22** in 6:4 H_2O-CH_3CN (the inset is a partially enlarged plot).

product mixture as obtained in aqueous solution, but the conversions in these cases were considerably lower (by a factor of ca. 4). In addition, yields of escaped products (i.e., phenol and benzyl alcohol) were higher than those formed in aqueous solution due to the fact that MeOH and CH_3CN are better hydrogen-donors than H_2O (the C-H bond of MeOH and CH_3CN is substantially weaker than the O-H bond of H_2O).

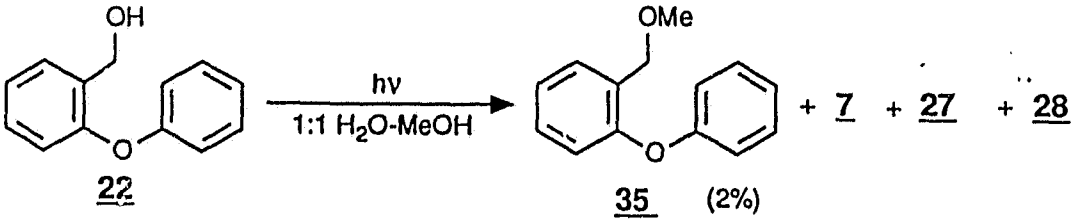

(3.2)

+ escape products

Irradiation of **22** in 1:1 H_2O-MeOH resulted in the formation of a trace amount of the photosolvolytic product, namely 2-phenoxybenzyl methyl ether (**35**), along with the same product mixture as obtained in aqueous CH_3CN (eq. 3.2). These results demonstrate that the expected photosolvolysis of **22** in neutral solution is only a minor process and that the aryl-O bond homolysis occurs predominantly (*vide infra*), resulting in the formation of rearranged photoproducts, pyran **7** and biphenylphenols **1**, **27** and **28** (eq. 3.1).

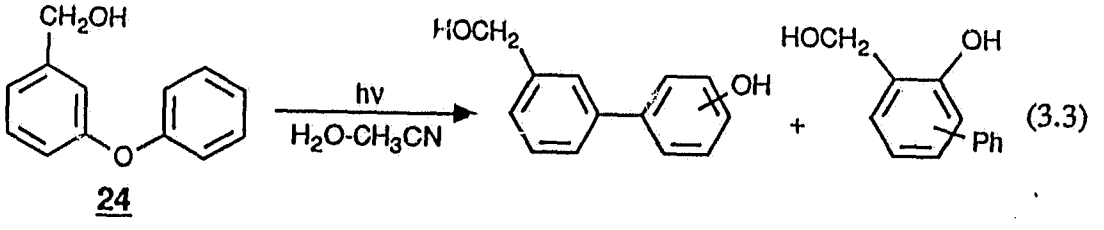

(3.3)

Photolysis of 24 in Neutral Solution. The photocyclization of **22** to **7** seems to be due to a unique assembly of *ortho*-phenoxy and -CH_2OH functional groups. In order to explore a structure vs reactivity relationship for the photocyclization of **22**, 3-phenoxybenzyl alcohol (**24**), the *meta* isomer of **22**, was studied under the same conditions. Photolysis of **24** in aqueous or 100% CH_3CN gave mainly

hydroxybiphenyls with higher conversion in aqueous solution (eq. 3.3). The hydroxybiphenyls were only tentatively identified by GC/MS (four peaks) and ^{1}H NMR further (four hydroxymethyl -CH_2OH signals at around δ4.5). These products were not isolated since they are not interesting in this study. However, these observations clearly show that placing the phenoxy group at the *ortho*-position is a necessary requirement for the photocyclization reaction of diaryl ethers such as **22**.

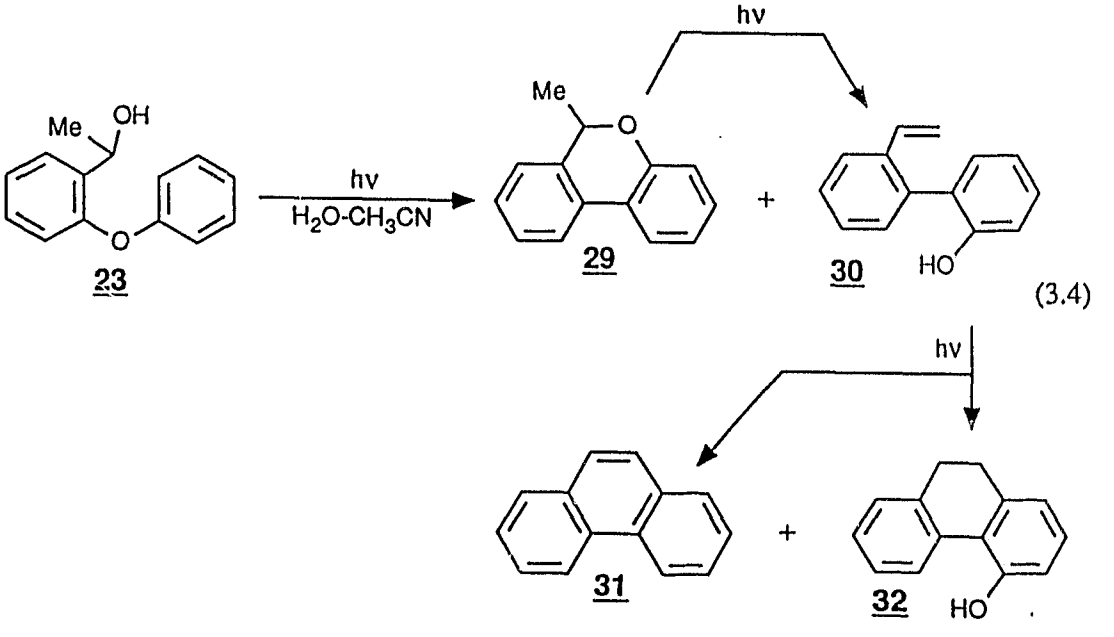

Photolysis of 23 in Aqueous CH_3CN. It appears that the photocyclization can be generalized for other 2-phenoxybenzyl alcohol derivatives. On irradiation of **23** in 1:1 or 2:1 H_2O-CH_3CN for 5-10 min, 6-methyl-6*H*-dibenzo[b,d]pyran (**29**) was formed as the major product (10%). On further photolysis, the yield of pyran **29** decreased with concurrent formation of three other products phenanthrene (**31**)

and two compounds **30** and **32** (eq 3.4), whose structures were proposed on the basis of their GC/MS data and a ^{1}H NMR spectrum of a mixture of **30**, **31** and **32**. The isolation of these products is very difficult due to the complexity of the photoproducts. Photolysis of authentic sample of **29** under the same conditions as for **23** also gave rise to styryl derivative **30** and compounds **31** and **32**. These results indicate that **30-32** are secondary photoproducts of the initially formed pyran **29**. The low yield of pyran **29** is due simply to its photolability. The pyran **29**, a derivative of 2,2'-dimethyl chromenes, probably undergoes an electrocyclic ring-opening reaction. As mentioned in Chapter One, a similar ring-opening photoreaction for the 6,6'-dimethyl-6*H*-dibenzo[b,d]pyran system has been observed by Turnbull and coworkers.[49,56-60] Compounds **31** and **32** are apparently derived from the photolysis of styryl derivative **30**. The photocyclization of a 2-vinylbiphenyl derivative structurally related to **30**, via a 6π electrocyclic ring closure as discussed in Chapter One, has also been reported.[43,49] In addition, we found that the compound **29** was not stable to exposure to air and slowly oxidized (the unidentified material changed from am oil to a crystalline material after several weaks, the ^{1}H NMR of which showed no starting material), a process which was also observed by Cavill and coworkers.[100]

Photolysis of 25 in Aqueous CH_3CN. The above results demonstrate that homolysis of the aryl-O bond (to give rearranged products, to be substantiated in

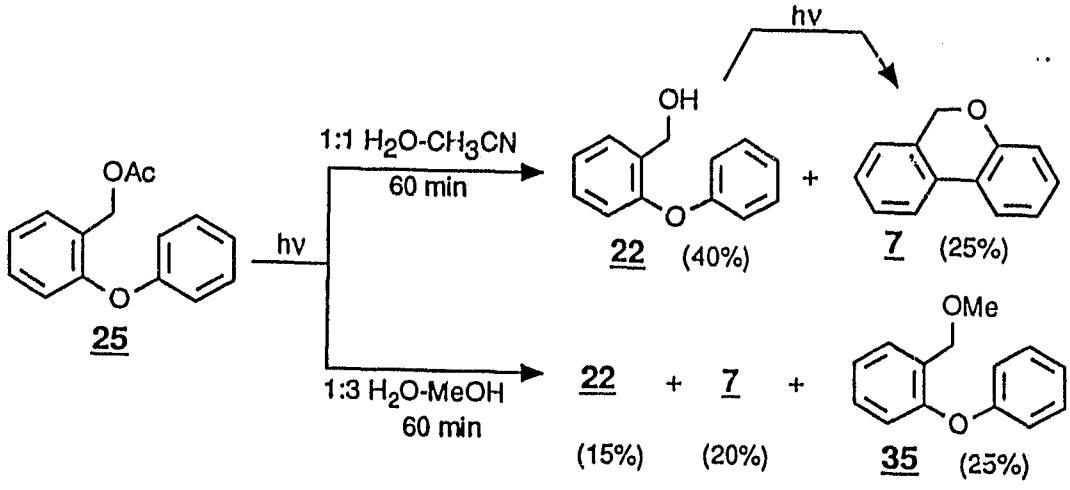

(3.5)

the discussion section) on irradiation of alcohol **22** is the predominant pathway in neutral aqueous solution. The anticipated photosolvolysis of the benzylic C-OH bond is only a minor process (1-2%). Therefore, in order to efficiently generate a carbocation from **22** in the excited state, a better leaving group (e.g -OAc) may be required since -OH is regarded generally as a poor leaving group (relative to -OAc). Thus the corresponding acetate **25** was prepared and studied. Photolysis of **25** in aqueous CH_3CN (1:1 H_2O-CH_3CN) yielded alcohol **22** and pyran **7** (eq. 3.5). When irradiated in 1:3 H_2O-MeOH, **25** gave the photosolvolysis products, methyl ether **35** (by MeOH) and alcohol **22** (by H_2O) along with the cyclized product pyran **7** (eq. 3.5). The kinetic photolysis of **25** in aqueous CH_3CN is shown in Figure 3.2, which clearly indicates that the pyran **7** comes from secondary photolysis of alcohol **22**. In all these studies, there was no trace of xanthene (**26**) detectable at all conversions. However, several hydroxybiphenyls were observed

in low yields (<10%), which were probably derived from secondary photolysis of alcohol **22** (*vide supra*). These results indicate that using a better-leaving group in such as acetate results in photosolvolysis via the corresponding carbocation, which can be trapped by solvent water or MeOH, but *does not* undergo Friedel-Crafts reaction to give xanthene (**26**).

Photolysis of 22 and 24 in Acidic Solution. As discussed previously, Wan et al.[22,23] have shown that the photosolvolysis of many benzyl alcohols is subject

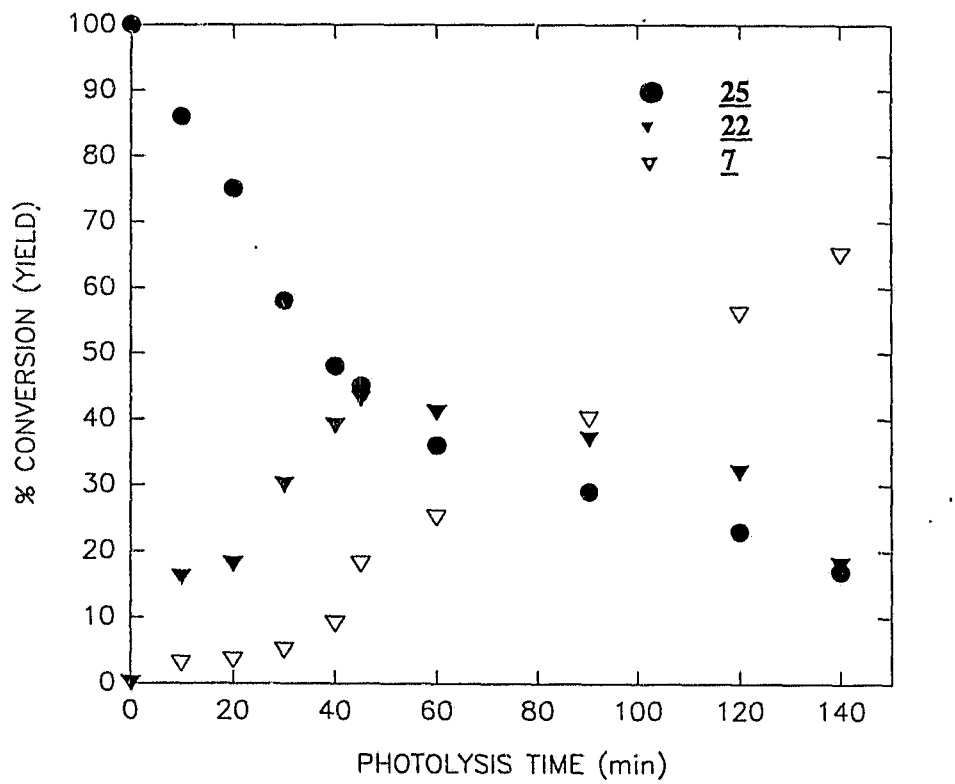

Figure 3.2. Product yield distributions as a function of photolysis time on irradiation of **25** in 1:1 H_2O-CH_3CN. A small amount of hydroxybiphenyls (~10%) was not included for clarity.

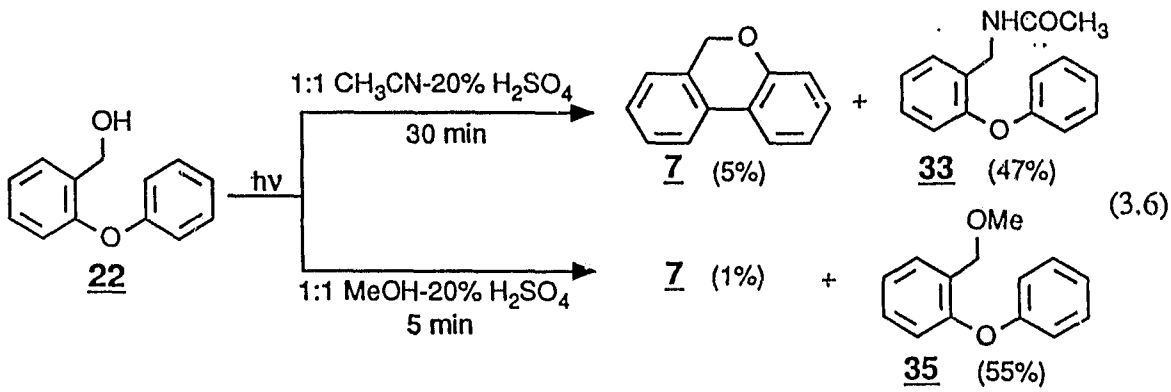

(3.6)

to acid-catalysis. This suggests that the acid might also catalyse the photocleavage of the benzylic C-OH bond of **22** and **24**. Photolysis of **22** and **24** in 1:1 20% H_2SO_4-MeOH indeed resulted in the almost exclusive formation of photosolvolytic products, methyl ethers **35** and **36** (shown for **22** in eq. 3.6). The formation of only a trace amount of photoproducts derived from homolysis of the aryl-O bond at these acidities indicates that the solvolysis now becomes an overriding process. When irradiated in 1:1 20% H_2SO_4-CH_3CN, **22** and **24** produced amides **33** and **34**, respectively (eq. 3.6). A pH-dependent study of the photolysis of **22** in 7:3 H_2O-CH_3CN is presented graphically in Figure 3.3. It is clear from this plot that the overall reactivity of substrate **22** is reduced with increasing acidity (relative Φ vs pH, see Figure 3.3). In acidic medium (pH <1), the efficiency for the formation of pyran **7** and hydroxybiphenyls **1**, **27** and **28** was diminished while the solvolysis of benzylic OH group was enhanced. A portion of the solvolysis of **22** in aqueous CH_3CN gives back starting material (trapping carbocation by solvent water), which

would result in overall reduced observed reactivity of **22** in acidic medium. A similar plot was observed when the solvent system was changed to 7:3 H_2O-MeOH. In this case, the formation of solvolysis product **35** could be detected even at pH = 2 while amide **33** was not observed until using relatively stronger acid (10% H_2SO_4). This is presumably due simply to the fact that MeOH is a much better nucleophile than CH_3CN. The above results show that in acidic medium the

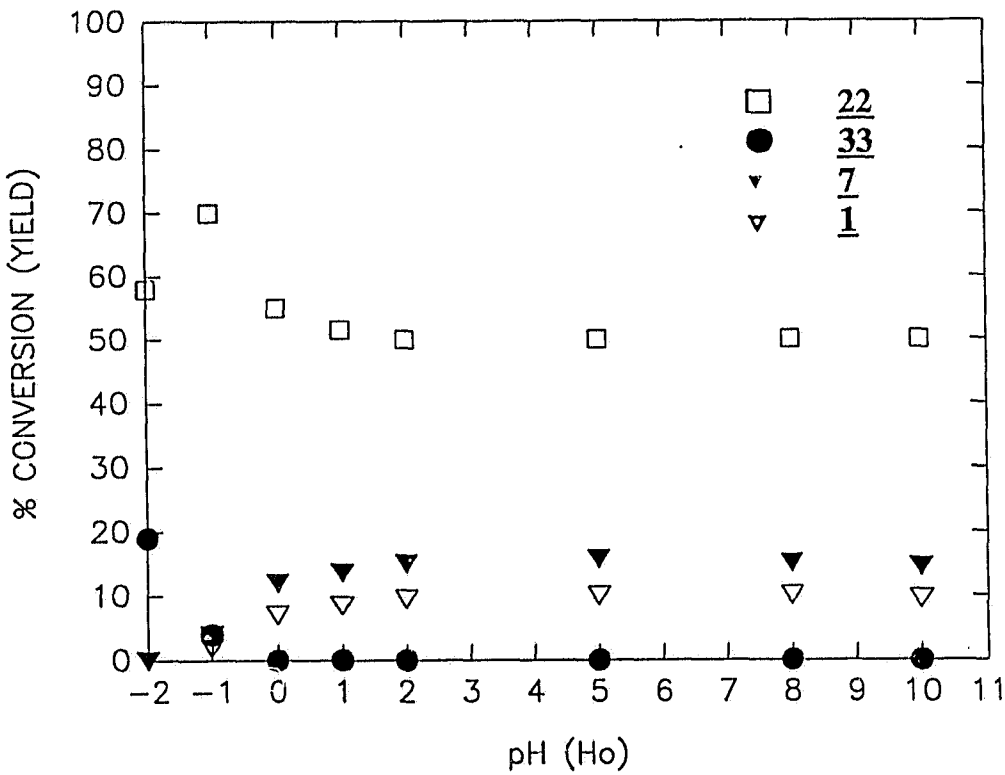

Figure 3.3. Plot of the total loss of **22** and product distributions as a function of pH (H_o) for photolysis of **22** in 7:3 H_2O-CH_3CN. Quoted pH (H_o) is of water portion. A small amount of hydroxybiphenyls (ca. 10%) was not included in the plot. Errors are ± 2-5%.

predominant pathway of benzyl alcohols **22** and **24** is the cleavage of the benzylic

C-OH bond. Homolysis of the aryl-O bond can not compete with this process under these conditions.

^{18}O-Labelling Studies on Photolysis of 1. In order to determine the origin of the oxygen in product **7**, alcohol **22** was irradiated in 1:1 $H_2{}^{18}O$-CH_3CN (H_2O portion was 20% ^{18}O-enriched) and worked-up following the procedure as in normal H_2O-CH_3CN. The product mixture was analyzed by GC/MS which showed that ^{18}O was not incorporated into the pyran product **7**, suggesting the oxygen in **7** is not from the solvent water, and thus it must come from one of the oxygens in substrate **22**. Benzylic ^{18}O-enriched (20%) **22** was prepared by thermal solvolysis of the corresponding bromide in 20% enriched $H_2{}^{18}O$. Photolysis of this ^{18}O-enriched substrate in 1:1 H_2O-CH_3CN resulted in the formation of pyran **7** which had also no enriched ^{18}O content, as analyzed by GC/MS. These results conclusively demonstrate that the oxygen in pyran **7** is derived from the oxygen in the aryl-O ether bond of alcohol **22**.

3.2.2 Quantum Yields and Solvent Effects

Quantum efficiencies for product **7** formation (Φ_p) and loss of substrate **22** (Φ_L) were determined using 280 nm irradiation of degassed ~0.001 **M** solutions taken to low conversion (<20%). Potassium ferrioxalate[97] was used as the chemical actinometer. The conversions and yields of **7** and **22** were determined by GC peak

areas of integrated peaks. Values of Φ_p and Φ_L in aqueous CH_3CN are listed in Table 3.1. Values for the quantum yield of **35** formation (Φ_M) in aqueous MeOH at different pH's are listed in Table 3.2. Table 3.1 demonstrates that the solvent water can considerably enhance the efficiency of product formation and loss of substrate in going from 100% CH_3CN to 6:4 H_2O-CH_3CN (Φ_p, by a factor of ca. 4; and Φ_L, by a factor of ca. 3). From Table 3.2, it is clear that the proton can

Table 3.1. Quantum Efficiencies for Loss of Substrate (Φ_L) and Product 7 Formation (Φ_p) on Photolysis of **22** in H_2O-CH_3CN.[a]

H_2O-CH_3CN ratio[b]	Φ_L[c]	Φ_P[c]
100% CH_3CN	0.0031	0.0015
1:9	0.0038	0.0031
2:8	0.0055	0.0050
3:7	0.0066	0.0058
4.5:5.5	0.0075	0.0063
6:4	0.01	0.0073

[a] Photolysis of **22** also gives **27** and **28**, but these are formed in much lower yields and thus not included.
[b] Neutral water used, ratios are v/v.
[c] Estimated errors are ± 15% of the quoted values.

significantly enhance the photosolvolytic efficiency (Φ_M) of **22**. The photosolvolysis pathway becomes important below pH = 2 and is the predominant

reaction at acidities stronger than H_o = -1, where formation of pyran 7 (via homolysis of the aryl-O bond) is negligible (also see Figure 3.3).

3.2.3 Fluorescence Spectra and Fluorescence Quantum Yields (Φ_f)

Fluorescence studies of **22** give unique insights into the nature of the excited state, which is responsible for the photorearrangement and photosolvolysis reactions of **22**. Steady state fluorescence spectra were recorded on a Perkin-Elmer MPF 66 spectrofluorimeter with a substrate concentration of ~10^{-4} M. Like other diaryl ethers, **22** was weakly fluorescent in organic solvents and in neutral water with λ_{max}=295 nm, as shown in Figure 3.4. The fluorescence emission quantum yields of **22** were determined as Φ_f = 0.038 in CH_3CN and 0.050 in MeOH (bandwidth

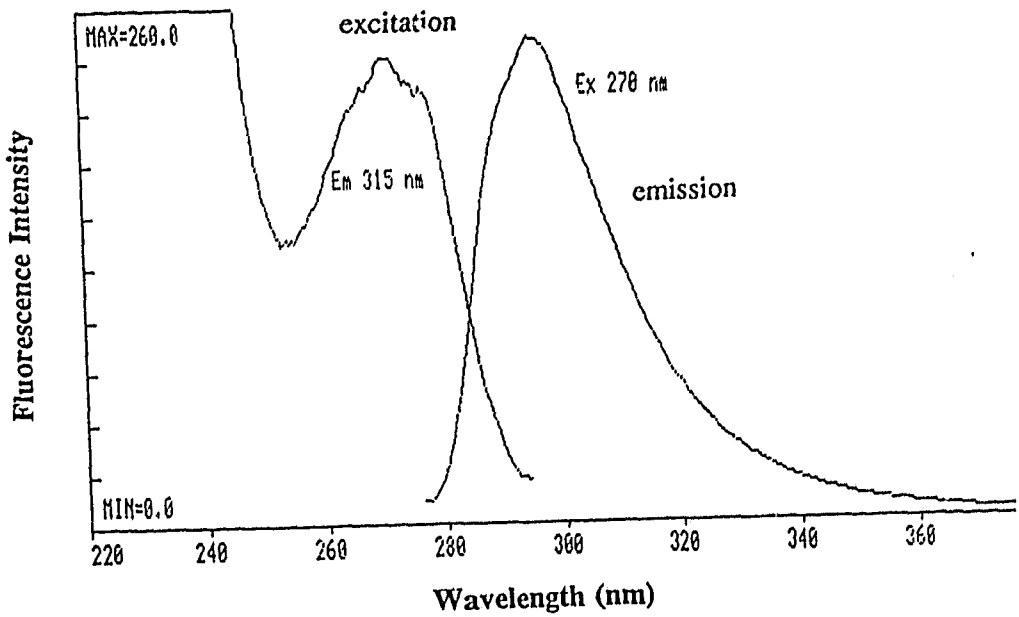

Figure 3.4. Excitation and emission spectra of **22** in 1:1 H_2O-CH_3CN (water portion pH = 7, buffered solution). λ_{ex} = 270 nm, λ_{em} = 315 nm.

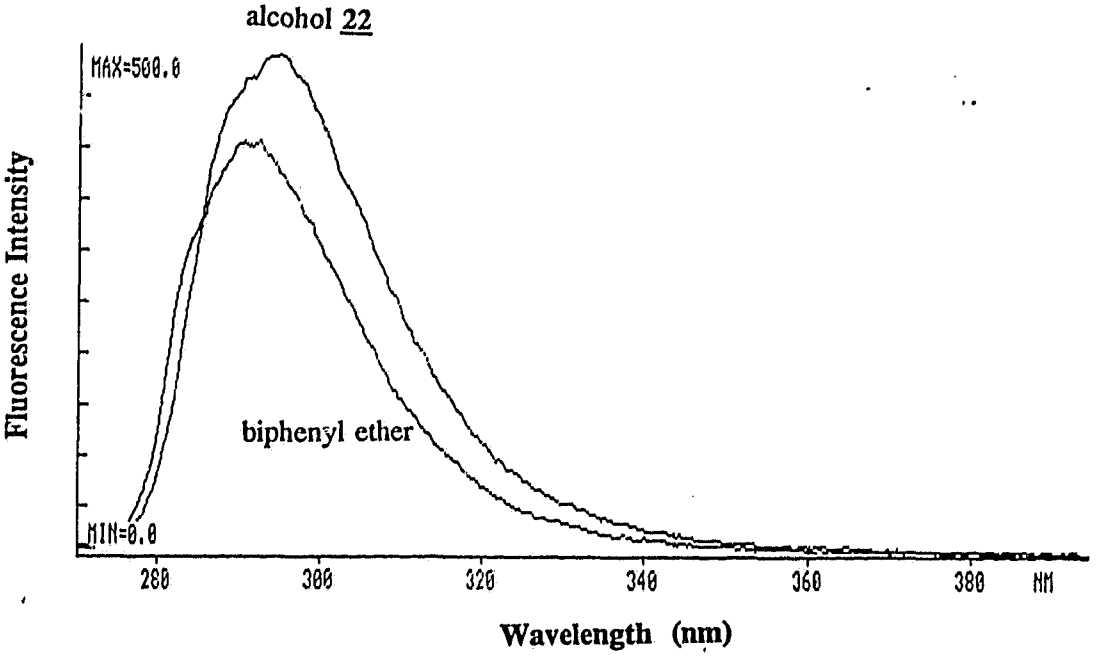

Figure 3.5. A typical fluorescence quantum yield experiment. Shown are the fluorescence emissions of **22** and biphenyl ether in 100% CH_3CN; λ_{ex} = 260 nm. Optical densities were matched at 260 nm prior to measurement.

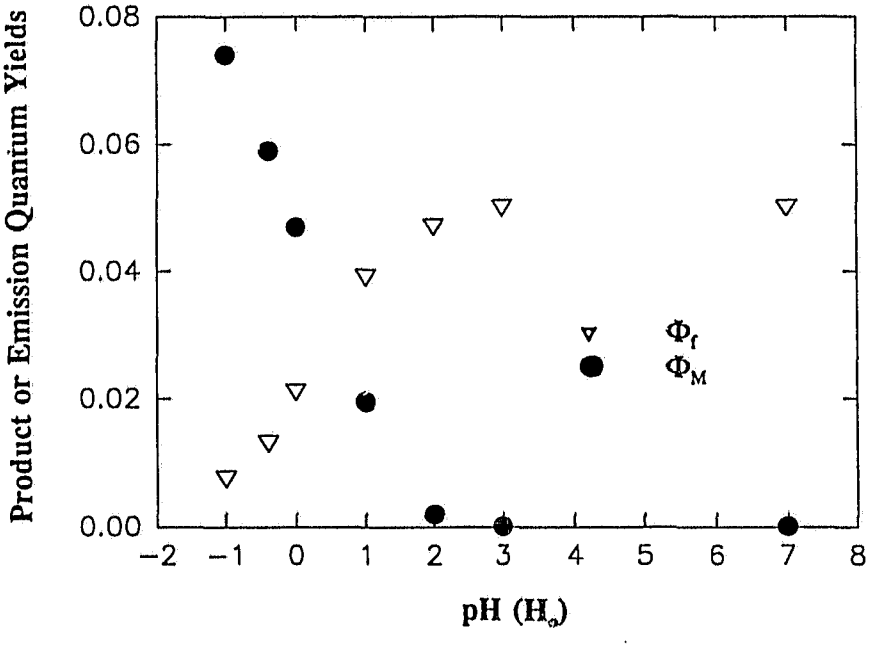

Figure 3.6. Acid-catalyzed photosolvolysis of **22**: The fluorescence quenching (Φ_f) with the concurrent enhancement of the product quantum yield (Φ_m).

270-345 nm), using biphenyl ether as a secondary fluorescence standard[99] as shown in Figure 3.5. The fluorescence emission of **22** was slightly quenched by added water, but dramatically quenched on going to lower pH values, as shown in Table 3.2 and Figure 3.6. Figure 3.6 indicates that the photomethanolysis of **22** was accompanied by a complementary quenching of its fluorescence emission, suggesting that the fluorescence quenching process is due to the acid-catalyzed photodehydroxylation of 22. Such a phenomenon has been observed previously in

Table 3.2. Quantum Efficiencies for Methyl Ether Formation (Φ_M) and Fluorescence Emission Efficiencies (Φ_f) of **22** in 1:1 H_2O-MeOH (v/v) at Various pH (H_o).[a]

pH(H_o)	7	3	2	1	0.0[b]	0.5[b]	-1.0[b]
Φ_M[c]	0.0001	0.0001	0.002	0.019	0.047	0.059	0.074
Φ_f[d]	0.05	0.05	0.047	0.038	0.021	0.013	0.0075

[a] pH quoted is of water portion of solutions.
[b] Value of H_o
[c] Estimated errors are ± 8% of the quoted values.
[d] Measured by using biphenyl ether as the secondary standard (Φ_f = 0.03 in cyclohexane[99]); λ_{ex} = 260 nm, estimated errors are ± 10% of quoted values.

this group for a number of benzyl alcohols.[22,23,29] The fluorescence quenching results have also been used to support a mechanism of reaction via the excited

singlet state.[22] Thus, the acid catalyzed photosolvolysis of **22** most probably is from S_1. This is further confirmed by the following triplet-state sensitization experiment.

2.2.4 Triplet-State Sensitization

The triplet-state sensitization is usually used to probe the multiplicity of reactive states. Apart from other factors controlling the effective energy transfer from the sensitizer to the substrate, the most important criteria for selecting a good triplet sensitizer is that the triplet state energy of the sensitizer must be higher than that of the substrate. The triplet state energy of **22** is estimated to be less than 81 kcal mol^{-1}, based on the fact that E_T for anisole is 80 kcal mol^{-1}.[93a] However, the triplet state energy for most of the water-soluble triplet sensitizers is around 70 kcal $mole^{-1}$. This prevented the use of a variety of triplet sensitizers. In the case of photolysis of **22** in neutral solution, acetone (E_T = 80-82 kcal mol^{-1})[93a] was employed as the triplet sensitizer. Photolysis of **22** in 1:1 H_2O-acetone at 300 nm led to the complete recovery of starting material; no cyclized product **7** was observed. In this experiment, the acetone absorbed most of light at 300 nm (> 95%). In addition, sodium 4-acetylbenzenesulfonate (E_T = 74 kcal mol^{-1})[93a] was also used as a water-soluble triplet sensitizer for photolysis of **22** (at λ_{ex} = 350 nm) in 1:1 20% H_2SO_4-MeOH. Again, this experiment yielded no photoproduct, and the substrate was recovered unchanged. Therefore, the triplet state of **22** is

nonreactive in aqueous CH_3CN and acidic H_2O-MeOH solutions, and it is the S_1 state that is responsible for photorearrangement *and* photosolvolysis. This conclusion is consistent with the fact that only the singlet excited state of **22** (energy of which is estimated to be ca. 100 kcal mol^{-1} on the basis of onset of emission at ~285 nm) has enough energy to break the aryl-O bond, which has a typical bond dissociation energy of 70-80 kcal mol^{-1}.[73]

3.3 Discussion

The above results indicate that *o*-phenoxybenzyl alcohol (**22**) reacts via two different kinds of reactions, depending on the pH (H_o) of the aqueous solution. In neutral solution, photorearrangement (and photocyclization) to **7** is the major pathway. In acidic solution, a photosolvolysis pathway dominates. These mechanisms will be discussed in turn below.

3.3.1 Mechanism of Photocyclization

As mentioned in Chapter One, in general, there are two types of reactions observed in the photochemistry of simple diaryl ether.[63,74,75] (1) Photorearrangement initiated by homolysis of the aryl-O bond to produce a radical pair, which can either escape or recombine to give substituted phenols. (2) Photocyclization to give dibenzofurans (via the 6π electrocyclic reaction), which is much less common and appears to require the presence of a labile substituent

Scheme 3.1

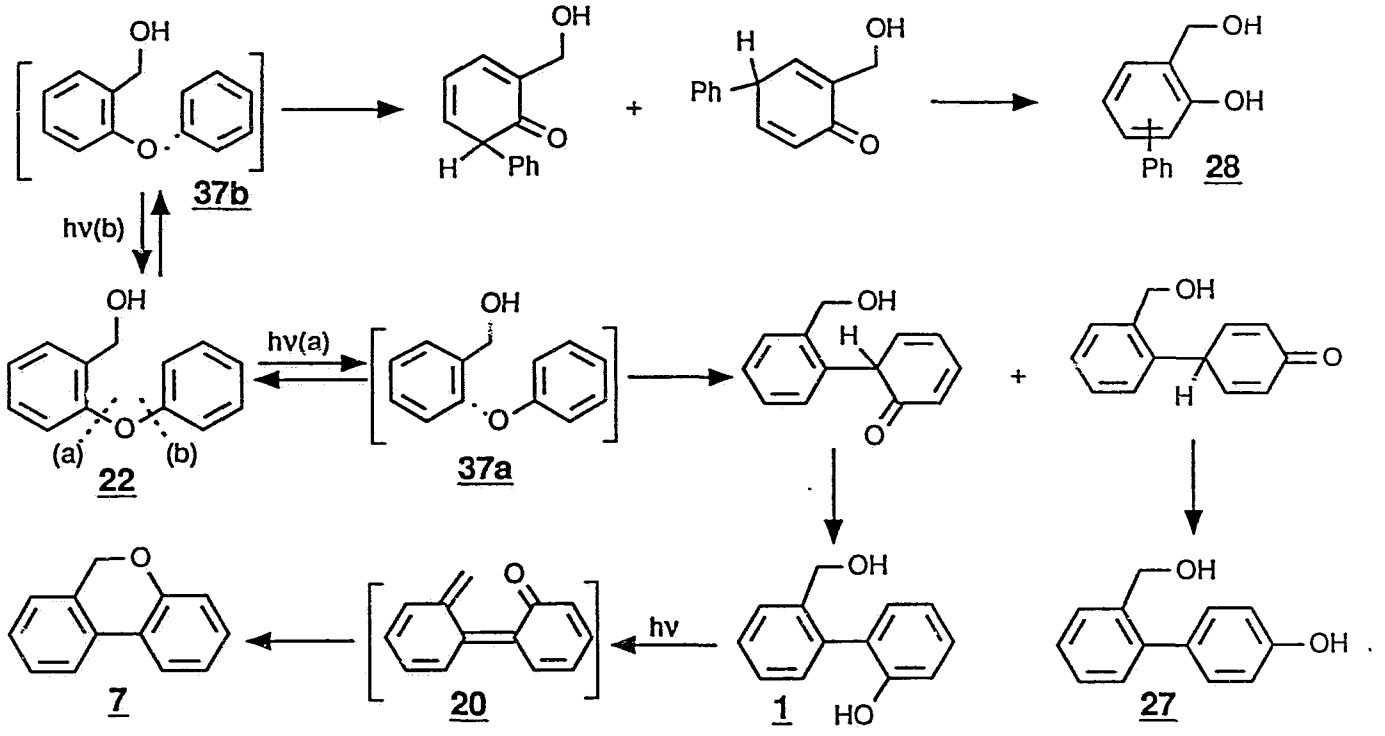

(e.g., halides) *ortho* to the phenoxy.[63]

For alcohol **22** and derivative **23**, there are no labile *ortho* substituents to the phenoxy group apart from the CH_2OH and $CH(CH_3)OH$ substituents which are not sufficiently labile as leaving groups. Therefore, a photoreaction via a 6π electrocyclic ring closure process is unlikely. In fact, the observation of radical rearranged hydroxybiphenyls and escaped benzene derivatives (phenol and benzyl alcohol) is strong evidence in support of the initial homolysis of the aryl-O bond. A mechanistic scheme for photocyclization of **22** in neutral solution is shown in Scheme 3.1, which is consistent with the experimental results. The primary photochemical event is aryl-oxygen bond homolysis from the singlet excited state, to form phenyl/phenoxyl radical pairs **37a,b**. Radical escape to give phenol, benzyl alcohol and *o*-hydroxybenzyl alcohol is a minor route since these products were formed in low yields in aqueous CH_3CN. Aqueous CH_3CN solution is a very polar, but a poor hydrogen-donating solvent system. Thus it is an excellent solvent to enhance *in-cage* recombination, as opposed to radical escape or reduction. Therefore, most of the products (shown in eq. 3.1) are derived from subsequent recombination of **37a,b**, to initially form substituted cyclohexdienones.

There are two different aryl-O bonds in alcohol **22**. Cleavage of bond **b** gives radical pair **37b**, which eventually gives rise to products **28**. Cleavage of bond **a** produces radical pair **37a**. Recombination of radical pair **37a** followed by rearrangement would give hydroxybiphenyls **1** and **27** (*vide infra*) (Scheme 3.1).

Since the yield of **28** was <10% at high conversion, either cleavage of bond **b** is kinetically much slower than cleavage of bond **a**, or **37b** preferentially reverts back to **22** rather than recombine to give cyclohexadienones. The former seems more reasonable. This may be due to the possibility that photogenerated phenyl radical **37a** is perhaps more stable since the *ortho*-alkyl substitution might stabilize it via inductive stabilization or interaction between the radical and the CH_2OH group. Radical pair **37a** recouples to give two possible cyclohexadienones (*via ortho*- and *para*-recombination). It seems that the *ortho*-recoupling process is much faster than the corresponding *para*-recombination since the yield of **7** (via **1**) is much higher than that of **27**. As discussed in Chapter One, this may readily be explained since the *ortho*-recombination might be regarded as a more or less concerted process whereas the *para*-recoupling requires substantial motion of the radical pair in order for the *para* coupling to take place. Enolization of the cyclohexadienones gives phenols **1** and **27** both of which were observed. Both kinetic studies (Figure 3.1) and independent photolysis (*vide supra*) showed that phenol **1** was photochemically transformed with high quantum yield (Φ_f = 0.25 in neutral solution) to pyran **7**, via the proposed *o*-quinonemethide type intermediate **20**, as discussed in detail in Chapter Two.

There is the possibility that a fraction of the *ortho*-substituted cyclohexadienone undergoes an intramolecular cyclization to give **38** (Scheme 3.2). This possibility was ruled out by the ^{18}O-labelling experiment as the photolysis of

^{18}O-labelled **22** gave no ^{18}O-incorporated pyran **7**. *This is inconsistent with the intramolecular cyclization pathway* but consistent with the photocyclization pathway via *o*-quinonemethide **20** (Scheme 3.1) discussed in Chapter Two.

The quantum yields for the formation of **7** and for loss of starting material **22** increase with increasing water content in CH_3CN solution (Table 3.1) by an overall factor of ca. 3 4. Since the quantum yields for photocyclization of **1** to **7** do not show the same sensitivity to water content (only by a factor of ca. 2, see Figure 2.11), a reasonable explanation for above solvent effect is that the recombination of radical pairs **37a,b** to give the corresponding cyclohexadienones

Scheme 3.2

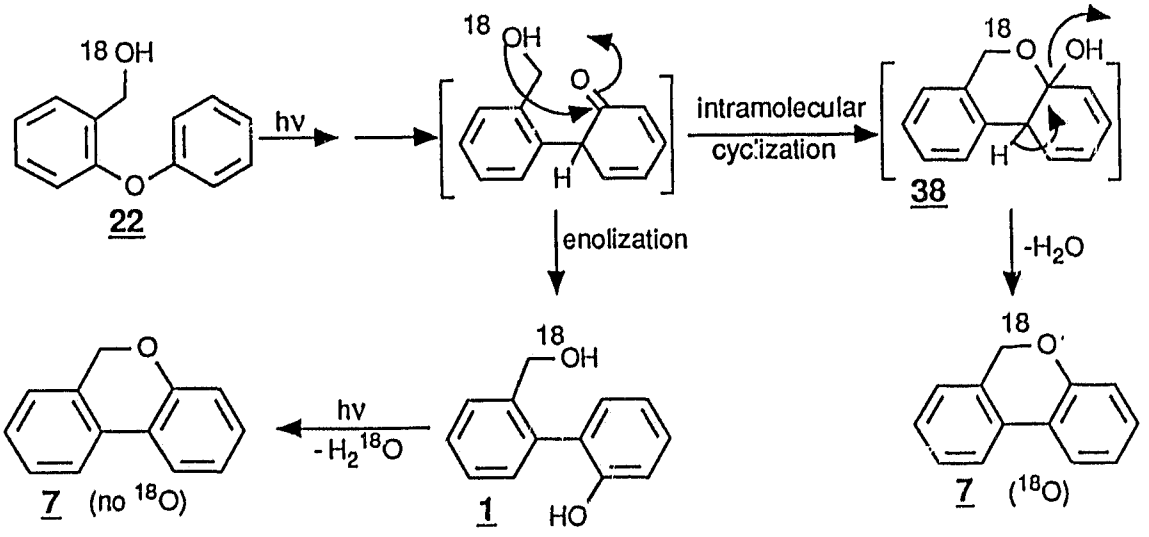

is favoured in hydroxylic solvents. This is not unreasonable since the initial recoupling products are ketone derivatives, possessing much larger dipole moments than the initial radical pairs. Therefore, use of a hydroxylic solvent should favour

this pathway. Ogata and coworkers[74] have offered a similar explanation for the increased yields of phenylphenol recoupling products on photolysis of diphenyl ether as the ethanol-diethylether solvent ratio was increased.

The same mechanism of reaction as discussed above for **22** applies to **23**. However, in this case, the pyran product **29** is *photolabile*, which results in a low overall yield of this product. Although all dibenzo[b,d]pyran derivatives can undergo electrocyclic ring-opening to give *o*-quinonemethide type intermediates, the *o*-quinonemethide **20** returns to pyran **7** predominantly due to the lack of further chemistry. Thus, there is essentially no net photochemistry observed for the parent pyran **7** on photolysis in aqueous CH_3CN. For the substituted *o*-

Scheme 3.3

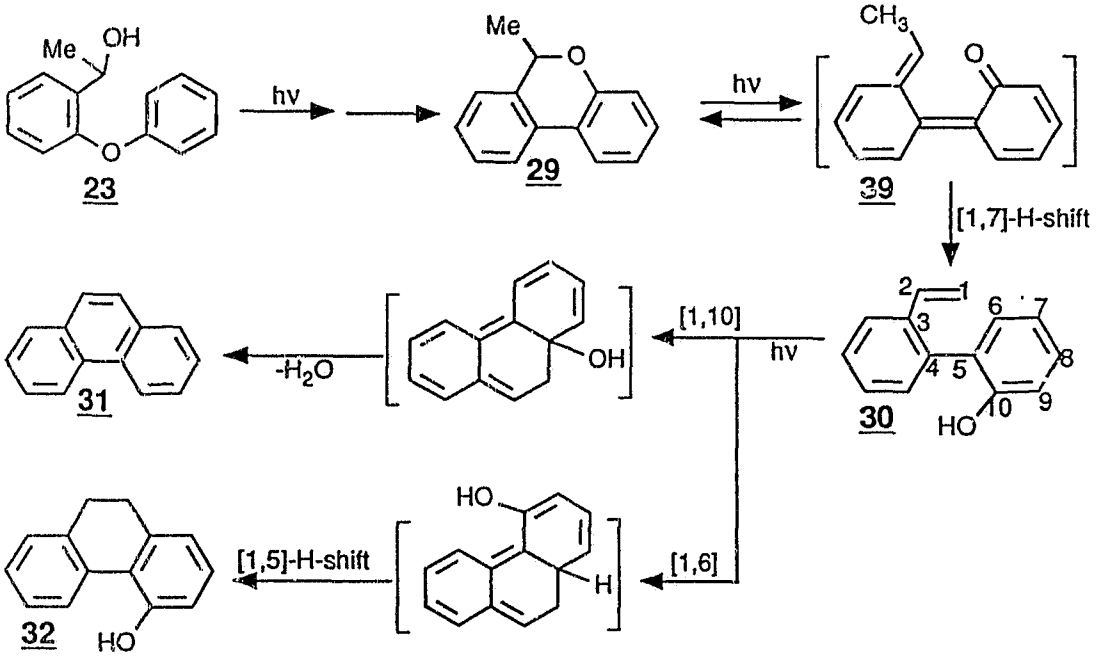

quinonemethide **39** however (Scheme 3.3), a thermal 1,7-hydrogen shift can

compete with the back reaction (i.e., ring closure), resulting in the formation of styryl derivative **30**. Bowd et al.[49] have shown that 6,6'-dimethyl-6*H*-dibenzo[b,d]pyran (**11**) also undergoes the same type of ring-opening photoreaction, as shown in Scheme 1.3 (see Chapter One). 2-Vinyl biphenyls such as **30** are also known to photocyclize efficiently to phenanthrene (**31**) and the dihydrophenanthrene derivative **32** (via initial electrocyclic ring closure followed by hydrogen shift and /or dehydration, Scheme 3.3). Thus, the reaction Scheme 3.3 proposed for the photodecomposition of pyran **29** is consistent with the known photochemistry of related compounds. The initial growth of styrene derivative **30** followed by its gradual decrease to give products **31** and **32** is consistent with this scheme.

The novel photoconversion of **22** to **1** can be ascribed to a unique assembly of *ortho*-phenoxy and CH_2OH functional groups. The *meta* isomer, alcohol **24**, can also undergo aryl-O homolysis upon irradiation but gives only hydroxybiphenyls and escape products since the *meta* orientation of the substituents does not permit a similar kind of chemistry.

3.3.2 Mechanism of Photosolvolysis

The results indicate that irradiation of alcohols **22-24** in moderately strong acid promotes a photosolvolysis pathway. The mechanistic scheme of acid-catalyzed photosolvolysis is shown in Scheme 3.4, using alcohol **22** as the model

Scheme 3.4

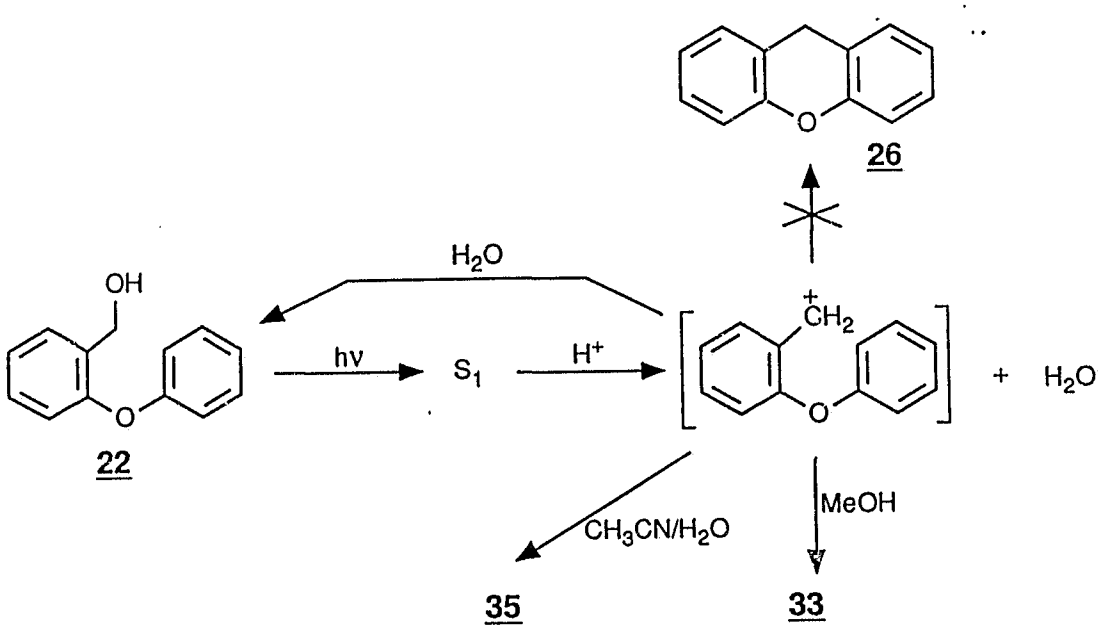

compound. Thus, in acid, the primary photochemical step is heterolytic cleavage of the benzylic C-OH bond, assisted by hydronium ion while the homolysis of the aryl-O bond process is negligible. In addition, a better leaving group such as -OAc also induces photosolvolysis in neutral aqueous solution, as observed for photolysis of **25**. It is clear that the photogenerated carbocation does not undergo the Friedel-Crafts alkylation reaction with the adjacent benzene ring. The phenoxy ring apparently is not electron rich enough (ground state σ(para) = -0.02)[17] to attack what should be a very short lived carbocation, since according to Barti and coworkers,[101] even diphenylmethyl cation has a very short lifetime (0.4 μs) in 100% CH_3CN, which is essentially not a nucleophilic solvent. The estimated rate of nucleophilic attack by water in CH_3CN on diarylmethyl carbocations is $\approx 1 \times 10^8$

M^{-1} s^{-1}.[101] Therefore, photogenerated primary benzylic carbocations would be expected to be very short lived since they will be even more rapidly quenched by solvent water. The adjacent phenoxy ring capture cannot compete with the solvent trapping process and thus no Friedel-Craft product xanthene **26** was observed (Scheme 3.4).

3.4 Conclusions

A novel photocyclization reaction of 2-phenoxybenzyl alcohols **22** and **23** to dibenzo[b,d]pyrans **7** and **29**, respectively, has been demonstrated (with 75% yield for **7** from **22**). The reaction was found to proceed via the excited singlet state. Use of the solvent water can considerably enhance the relative product quantum efficiency of the photocyclization reaction. In neutral solution, aryl-O bond homolysis is the predominant event to give a radical pair, which largely leads to *ortho*-substituted cyclohexadienones. These dienones suffer rapid enolization, to afford alcohols **1** and **27**. Subsequent absorption of a second photon in **1** results in pyran **7**. In acidic solution, proton-assisted photosolvolysis of the benzylic C-OH bond occurs overridingly, to give an initial carbocation intermediate, which is trapped by solvent water, MeOH or CH_3CN. The photocyclization reaction appears to be general for 2-phenoxybenzyl alcohol systems, in which an appropriate assembly of phenoxy and hydroxymethyl (CH_2OH) functional groups is a necessary requirement for the reaction.

3.5 Experimental

A general description of various instruments, techniques and procedures used in these studies has already been discussed in Chapter Two.

3.5.1 General

3.5.2 Materials

o-Phenoxybenzoic acid, *m*-phenoxybenzyl alcohol, 4-bromoanisole, $Pd(PPh_3)_4$ and trimethyl borate were purchased from Aldrich and used as received. All compounds were checked for purity by GC and ^1H NMR prior to photochemical study.

2-Phenoxybenzyl alcohol (22). To 7.1 g (33.2 mmol) of 2-phenoxybenzoic acid (Aldrich) dissolved in 200 mL dry THF cooled by an ice-bath was carefully added 50 mL (1.5 equiv.) of 1 M BH_3-THF solution. After addition, the reaction mixture was warmed to 40-50°C and stirred for 3 h. The reaction solution was quenched with 100 mL distilled water and then extracted with 3 x 100 mL CH_2Cl_2. The combined organic layers were washed with 1 M NaOH (100 mL), dried over $MgSO_4$, and evaporated to yield a colourless oil which was purified by bulb-to-bulb distillation and shown to be analytically pure **22** by GC. Yield 5.2 g (73 %); ^1H NMR δ 7.4-6.8 (m, 9H, Ar-H), 4.70 (s, 2H, $-CH_2O$), 2.1 (br, 1H, exchangeable with D_2O, -OH); MS (EI) m/z (rel int) 200 (M^+) (15), 182 (M^+-H_2O) (42), 181 (M^+-

OH) (100), 170 (70), 152 (19), 149 (21), 115 (28); IR (cm^{-1}) (neat) 3300 (broad, s), 3025 (m), 1600 (s), 1590 (m), 1500 (m), 1480 (s). These data are identical to those of an authentic sample.

***o*-Phenoxylbenzyl alcohol-^{18}O (22).** To a solution of 1 mL H_2O (20% ^{18}O-enriched water) and 1 mL CH_3CN was added 200 mg (0.72 mmole) of 2-phenoxylbenzyl bromide (made from **22** on reaction with HBr/LiBr).[82] The solution was refluxed overnight at 80°C and then cooled to room temperature. The conversion of the reaction was monitored by TLC (silica gel; CH_2Cl_2) and estimated as 60%. The solution was then treated with 3 mL distilled water, saturated with NaCl and extracted with 3 x 5 mL dichloromethane. The combined organic layers were dried over $MgSO_4$ and evaporated at reduced pressure to give an oily residual. The crude alcohol was purified by preparative TLC (silica gel; CH_2Cl_2) and characterized by MS and ^{1}H NMR. MS (CI) m/z (rel int) 203 (M^++1, ^{18}O) (8), 201 (M^++1, ^{16}O) (40). ^{1}H NMR data of ^{18}O-labelled **1** are the same as those of ^{16}O alcohol **22**.

2-Phenoxy-α-methylbenzyl alcohol (23). To a magnetically stirred solution of 16 g (75 mmol, 1.5 equiv.) of pyridinium chlorochromate complex (PCC) in 200 mL CH_2Cl_2 was added, in one portion, 10 g (50 mmol) of alcohol **22** in 20 mL CH_2Cl_2. After 1.5 h, 200 mL of dry ether was added and the supernatant decanted

from the black gum. The organic solution was passed through a short pad of Florisil, and the solvents were evaporated to yield a colourless oil which was identified as the corresponding aldehyde by ^{1}H NMR. To 8.0 g (40 mmol) of the crude aldehyde dissolved in 200 mL anhydrous ether was added dropwise 50 mL (50 mmol) of 1 M Grignard reagent CH_3MgBr in 20 mL dry ether at -5°C. After addition, the solution was warmed up to room temperature and refluxed for 30 min. The solution was quenched with 200 g of ice and acidified with 10 % sulfuric acid. The organic layer was separated and evaporated to give an oil, which was purified by bulb-to-bulb distillation, to give analytically pure **23** (by GC). Yield 6.5 g (60%). ^{1}H NMR δ 7.62-6.90 (m, 9H, Ar-H), 5.25 (q, J = 7.5 Hz, 1H, ArCH), 2.38 (s, broad, exchangeable with D_2O, 1H, -OH), 1.55 (d, J = 7.5 Hz, 3H, $-CH_3$); MS (EI) m/z (rel int) 214 (M^+) (10), 197 (20), 182 (50), 122 (40), 118 (100); IR (cm^{-1}) (neat) 3350 (broad, s), 3058 (m), 1600 (s), 1490 (s).

2-Phenoxybenzyl acetate (25). To 3 g (15 mmol) of alcohol **22** dissolved in 250 mL CH_2Cl_2 was added dropwise 10 mL acetyl chloride. The solution was stirred overnight and washed with 2 x 150 mL saturated $NaHCO_3$ solution and then dried over $MgSO_4$. Evaporation of the solvent gave a clear liquid which was purified by bulb-to-bulb distillation, to give analytically pure **25** (by GC). Yield 2.5 g (80%). ^{1}H NMR δ 7.40-6.90 (m, 9H, Ar-H), 5.20 (s, 2H, $-CH_2O$), 1.96 (s, 3H, $-COCH_3$); MS (EI) m/z (rel int) 242 (M^+) (25), 200 (6), 199 (15), 181 (100),

183 (7); IR (cm^{-1}) (neat) 3050 (m), 1725 (s), 1600 (m), 1480 (m).

4'-Methoxy-2-methylbiphenyl (27a). The synthesis of **27a** was carried out according to a procedure described by Thompson et. al.[102,103] In a typical experiment, to a stirred solution of the 4-bromoanisole (4.45 g, 24 mmole) and $Pd(PPh_3)$ (0.87 g, 0.8 mmole) in 40 mL of toluene under a nitrogen atmosphere was added 40 mL of 2 **M** aqueous Na_2CO_3 and 3.4 g (25 mmole) of 2-methylbenzene boronic acid (made from the reaction of 2-methylbenzene magnesium bromide with trimethyl borate) in 15 mL of 95% EtOH. The vigorously stirred mixture was warmed to 80°C and kept for 15 h, then cooled, and partitioned between CH_2Cl_2 (3 x 150 mL) and 2 **M** aqueous Na_2CO_3 (80 mL) containing 10 mL of concentrated NH_3. The organic layer was dried ($MgSO_4$), and then concentrated to dryness at reduced pressure. Flash chromatography on silica gel afforded the pure **27a**. Yield 4.5 g (94%). ^1H NMR δ 7.32 (dd, J = 2 and 8 Hz, 2H, Ar-H), 7.21 (m, 4H, Ar-H), 6.92 (dd, J = 2 Hz, 2H, Ar-H), 2.21 (s, 3H, $-CH_3$); MS (EI) m/z (rel int) 198 (M^+) (100), 197 (9), 183 (21), 167 (19), 155 (31), 55 (17).

2-(4'-Methoxyphenyl)benzyl bromide (27b). To a stirred solution of **27a** (4.5 g, 22.7 mmole) in 150 mL CCl_4 was added 7.2 g (40 mmole) of *N*-bromosuccinimide (NBS) and 0.1 g benzoyl peroxide. The reaction mixture was

heated under reflux for 36 h, cooled and filtered. The solvent CCl_4 was removed at reduced pressure to give a crude product which was purified by column chromatography (silica, CH_2Cl_2) to give 5.4 g (85%) of **27b**. ^{1}H NMR δ 7.45-7.15 (m, 6H, Ar-H), 6.97 (dd, J = 2 and 8 Hz, 2H, Ar-H), 4.42 (s, 2H, -CH_2Br), 3.80 (s, 3H, -OCH_3); MS (EI) m/z (rel int), 278 (7), 277 (5), 276 (M^+) (8), 197 (100), 182 (30), 165 (91), 152 (76).

2-(4'-Methoxyphenyl)benzyl alcohol (27c). The compound **27c** was made by following the method described by Iihaman.[104] A solution of **27b** (6.3 g, 24 mmole) and KOAc (4.68 g, 47.8 mmole) in HOAc (100 mL) was refluxed for 5 h. The mixture was extracted with CH_2Cl_2 (3 x 100 mL), and the organic layer was successively washed with water (2 x 100 mL) and aqueous $NaHCO_3$ (100 mL), dried over $MgSO_4$, and evaporated to dryness at reduced pressure, to give crude 2-acetoxymethyl-4'-methoxy-1,1'-biphenyl. The crude acetate was dissolved in EtOH-THF (1:3, 160 mL) and 1 N aqueous NaOH (38 mL) and the mixture stirred at room temperature for 12 h. The solution was extracted with 3 x 300 mL CH_2Cl_2 and organic layer was dried ($MgSO_4$) and evaporated to dryness to give crude **27c**, which was recrystallized from toluene, to afford white needles. Yield 4.1 g (80%). ^{1}H NMR δ 7.60 (m, 4H, Ar-H), 7.26 (dd, J = 2 and 8 Hz, 2H, Ar-H), 6.95 (dd, J = 2 and 8 Hz, 2H, Ar-H), 4.56 (s, 2H, -CH_2O), 3.80 (s, 3H, -OCH_3); MS (EI) m/z (rel int) 214 (M^+) (100), 212 (6), 199 (12), 196 (14), 181 (22), 153 (11).

2-(4'-Hydroxyphenyl)benzyl alcohol [4'-hydroxyl-(1,1'-biphenyl)-2-methanol] (27). The synthesis of **27** from **27c** followed a known procedure.[105] To a stirring solution of 0.2 g (0.93 mmole) of **27c** in 20 mL CH_2Cl_2 cooled to -80°C under nitrogen was added dropwise 0.5 mL of 1 M boron tribromide in CH_2Cl_2. The solution was warmed to room temperature and stirred overnight. The reaction was quenched by adding 50 mL water and then treated with 150 mL of 2 N NaOH. The aqueous phase was then acidified with 5% HCl and extracted with 3 x 50 mL ether. The ether was dried over $MgSO_4$ and evaporated to dryness to give crude **27**, which was purified by preparative TLC (silica, 3:97 MeOH-CH_2Cl_2). Yield 0.08 g (43%). mp 113-114°C. ^{1}H NMR δ 7.45-7.26 (m, 4H, Ar-H), 7.23 (d, J = 8 Hz, 2H, Ar-H), 6.84 (d, J = 8 Hz, 2H, Ar-H), 4.58 (s, 2H, -CH_2O); MS (EI) m/z (rel int) 200 (M^+) (100), 183 (13), 182 (41), 181 (60), 153 (38), 77 (14); IR (cm^{-1}) (mineral oil) 3400 (broad, s), 3050 (m), 1600 (m), 1590 (m), 1505 (m), 1250 (m), 1225 (s). Anal. calc. for $C_{13}H_{12}O_2$: C, 77.98; H, 6.04. Found: C, 77.51; H, 6.05.

3.5.3 Product Studies

General procedures for preparative and analytical photolysis and dark control runs have already been described in Chapter Two.

Photolysis of **22** *in 1:1 or 6:4 H_2O-CH_3CN.* In a typical preparative study, 200 mg of substrate **22** was dissolved in CH_3CN and then diluted with H_2O. The

solution was then transferred to a quartz tube and irradiated at 254 nm for 2h. After photolysis, the solution was worked up by saturating it with NaCl, followed by extraction with 3 x 100 mL of CH_2Cl_2. The organic layer was washed with 3 x 100 mL of 1 N NaOH solution, dried over $MgSO_4$ and evaporated to dryness to afford crude **7**, which was purified by preparative TLC (silica gel plates, developed with CH_2Cl_2). Its MS and ^1H NMR data were consistent with those of authentic sample obtained by synthesis. GC retention time of **7** at 180°C was 4.53 min.

The combined aqueous NaOH solution was acidified by 1 M HCl and then extracted with 3 x 100 mL of CH_2Cl_2. The organic layer was again dried and evaporated to give hydroxybiphenyls **1, 27-28.** Products **1, 27** were isolated by preparative TLC (silica, 3:97 MeOH-CH_2Cl_2) and characterized by ^1H NMR and GC/MS and by comparison to authentic samples. GC retention times at 180°C: **1** (5.52), **27** (9.16), **28** (5.21 and 7.20).

In an analytical scale experiment, a solution of 20 mg **22** in 1:1 aqueous CH_3CN (100 mL) in a 100 mL quartz tube was irradiated. 1 mL portions of the photolyzed solution were removed at intervals and then treated with 2 mL of distilled water, 1 mL of stock solution of xanthene (**26**) in CH_2Cl_2 and then saturated with NaCl. The mixture was then extracted with CH_2Cl_2 (3 x 1 mL) and the organic layer was separated and dried over $MgSO_4$. The condensed solution (~0.2 mL) was subjected to the GC analysis at 180°C. The conversion and yields were calculated on the basis of the integrated areas of GC peaks. Photoproducts

1, **7** and **27** were identified by comparing their retention times with those of authentic samples.

Photolysis of 22 in 1:1 MeOH-20% H_2SO_4. In a typical preparative photolysis, a solution of 200 mg (1 mmole) of **22** in 100 mL of MeOH and 100 mL of 20% H_2SO_4 was irradiated at 254 nm for 2h. The solution was neutralized by adding 2 N aqueous NaOH, saturated with NaCl and extracted with 3 x 100 mL CH_2Cl_2. The combined organic layers were dried over $MgSO_4$ and evaporated to dryness to afford an oil residue. The product **35** was then isolated by preparative TLC (silica, CH_2Cl_2) and identified by MS and ^{1}H NMR. Yield 55 mg (25%). MS (EI) m/z (rel int) 214 (M^+) (23), 163 (23), 182 (47), 181 (100), 121 (19), 77(32), 39 (20); ^{1}H NMR δ 7.51 (m, 9H, Ar-H), 4.40 (s, 2H, -CH_2O), 3.34 (s, 3H, -OMe). These spectroscopic data were identical to those of an authentic sample made by a thermal method (refluxing **22** in 1:9 conc.H_2SO_4-MeOH).

Photolysis of 22 in 1:1 CH_3CN-20% H_2SO_4. In a typical experiment, a solution of 200 mg (1 mmole) of substrate **22** in 100 mL of CH_3CN and 100 mL of 20%H_2SO_4 was photolyzed at 254 nm for 3 h. After irradiation, the solution was neutralized and worked up by the standard procedure. The product **33** was isolated by preparative TLC (silica, 3:97 MeOH-CH_2Cl_2) and then characterized by MS and ^{1}H NMR. Yield 40 mg (17%, colourless oil). ^{1}H-NMR δ 7.42 (m, 9H, Ar-H), 4.48, 4.42 (s, 2H, -CH_2, *cis* and *trans* rotamers), 1.89 (s, 3H, -$COCH_3$); MS (EI) m/z (rel int), 241 (M^+) (10), 182 (36), 181 (100), 77 (5). IR (cm^{-1}) (mineral

oil) 3260 (s), 3080 (m), 1652 (s), 1635 (s), 1600 (m), 1580 (m), 1550 (m), 1480 (s). The ^{1}H NMR, MS and IR data are identical to those of an authentic sample made by a thermal method (refluxing **22** in 1:1 CH_3CN-50%H_2SO_4).

*Photolysis of **23** in H_2O-CH_3CN.* In a typical preparative photolysis, a solution of 200 mg (1 mmole) of **23** in aqueous CH_3CN (1:1 or 2:1, v/v, 200 mL) was irradiated at 254 nm for 30 min. After photolysis and normal work up, the product **29** was isolated by preparative TLC (silica, 1:1 hexanes-CH_2Cl_2) and characterized by MS and ^{1}H NMR. Yield 15 mg (7%, a colourless oil). ^{1}H NMR δ 7.75 (m, 2H, Ar-H), 7.41-6.95 (m, 6H, Ar-H), 5.28 (q, J = 8.0 Hz, 1H, -CHO), 1.59 (d, 3H, J = 8.0 Hz, -CH_3); MS (EI) m/z (rel int) 196 (M^+) (26), 182 (14), 181 (100), 165 (5), 152 (17), 90 (7). The GC retention time at 180°C was 5.53 min.

A solution of 15 mg **29** in 6:4 aqueous CH_3CN (50 mL) was photolyzed for 2 h. After the normal work-up, the product mixture was subjected to ^{1}H NMR (360 MHz) and GC/MS analysis. The photoproducts **30-32** were identified. **30**: partial ^{1}H NMR δ 6.80 (dd, J_1 = 14 Hz, J_2 = 7.5 Hz, Ar-CH=), 5.22 (dd, J_1 = 14 Hz, J_2 = 7.5 Hz, =CH_2); MS (CI) m/z (rel int) 196 (M^+ + 1) (100). **31** was identified by GC/MS (CI) m/z (rel int) 179 (M^+ + 1) (100) and by comparison of GC/MS data to an authentic sample. **32**: partial ^{1}H NMR δ 2.70 (m, CH_2CH_2); MS (CI) m/z (rel int) 196 (M^++1) (100). GC retention times at 180 °C: **29** (5.52), **30** (4.34), **31** (4.98), **32** (7.3).

*Photolysis of **24** in 6:4 H_2O-CH_3CN.* A solution of 100 mg of **24** in 6:4

aqueous CH_3CN (200 mL) was photolysed for 2 h. After the normal work up, the product mixture was analyzed by ^1H NMR and GC/MS. The ^1H NMR indicated there were four singlet signals at around δ 4.5 ppm, indicative of isomeric benzyl alcohols. MS (CI) m/z (rel int) 201 ($M^+ + 1$) (100) for all four hydroxybiphenyls. Although these hydroxybiphenyls were only tentatively identified no simple cyclization product **7** was observed.

Photolysis of 24 in 1:1 MeOH-20% H_2SO_4. In a typical experiment, a solution of 200 mg of substrate **24** in 100 mL MeOH and 100 mL of 20%H_2SO_4 was photolyzed at 254 nm for 2 h. The solution was neutralized and worked up in a normal manner to afford a crude residue. The product methyl ether **36** was isolated by preparative TLC (silica gel, CH_2Cl_2) and characterized by MS and ^1H NMR. Yield 50 mg (23%, a colourless oil). ^1H NMR δ 7.40-6.90 (m, 9H, Ar-H), 4.47 (s, 2H, -CH_2O), 3.31 (s, 3H, -OMe); MS (EI) m/z (rel int) 214 (M^+) (100), 183 (46), 181 (24), 121, 41), 91 (37), 78 (41), 77 (71), 51 (69), 39 (48). These data are identical to those of an authentic sample made by a thermal method (refluxing **24** in 1:9 concH_2SO_4-MeOH).

Photolysis of 24 in 1:1 CH_3CN-20% H_2SO_4. In a typical procedure, a solution of 200 mg **24** in 1:1 CH_3CN-20% H_2SO_4 (200 mL) was irradiated at 254 nm for 3 h. After photolysis, the solution was neutralized and worked up to give a crude mixture. The product amide **34** was isolated by preparative TLC (silica gel, 3:97 MeOH-CH_2Cl_2) and characterized by MS and ^1H NMR. Yield 40 mg

(17%, a colourless oil)). MS (EI) m/z (rel int) 241 (M^+) (100), 198 (93), 181 (32), 106 (87), 77 (68), 51 (37), 43 (89); ^{1}H NMR δ 7.35-6.85 (m, 9H, Ar-H), 4.35, 4.28 (s, 2H, -CH_2-, *cis* and *trans* rotamers), 1.89 (s, 3H, $COCH_3$). IR (cm^{-1}) (neat) 3290 (s), 3060 (m), 1650 (s), 1575 (s), 1540 (s), 1480 (s), 1250 (s). The ^{1}H NMR, MS and IR data are identical to those of an authentic sample made by a thermal method (refluxing **22** in 1:1 CH_3CN-50%H_2SO_4).

*Photolysis of **25** in 1:1 H_2O-CH_3CN.* A number of solutions containing 100 mg of **25** in 1:1 aqueous CH_3CN (100 mL) was irradiated, respectively, as a function of time. After the normal work-up of each photolyzed solution, the product mixture was analyzed by GC and ^{1}H NMR. Conversions and yields were determined on the basis of the integrated areas of GC or ^{1}H NMR (using -CH_2- signal) peaks. The average results of both methods were used.

3.5.4 Quantum Yield Measurements

Quantum yields were measured using 280 nm excitation from the output of an Oriel 200 W Hg lamp filtered through an Applied Photophysics monochromator and a 254-400 bandpass filter. Solutions (10^{-3} M) were prepared in 3 mL quartz cuvettes and purged with a stream of argon prior to photolysis. Potassium ferrioxalate was used for chemical actinometry.[97] The details of this technique are described in Appendix C. After photolysis, the sample was saturated with NaCl

and then extracted several times with CH_2Cl_2. The conversion and yields were based on the calculation of integrated areas of GC and ^1H NMR. Excellent material balances were observed, as determined by xanthene (**26**) internal standard. GC responses were essentially identical for starting material and all of the photoproducts.

3.5.5 Fluorescence Measurements

Fluorescence emission spectra (uncorrected) were taken in 3.0 mL quartz cuvettes at about 10^{-4} M using a Perkin-Elmer MPF 66 spectrophotometer at ambient temperature. Standardized HCl or H_2SO_4 solutions were used for acid quenching experiments. The fluorescence quantum yield of **22** in neutral 1:1 H_2O-CH_3CN was measured relative to diphenyl ether (Φ_f = 0.03 in cyclohexane[99]) as secondary fluorescence standard. Optical densities at λ_{ex} = 260 nm were matched prior to measurement.

3.5.6 Triplet State Sensitization

For a typical experiment in neutral solution, a solution of 2 mg **22** in 1:1 acetone-H_2O (150 mL) was irradiated at 300 nm for 2 h with argon purging. At 300 nm, the sensitizer acetone absorbed over 95% of the irradiation. After photolysis, the solution was condensed, saturated with NaCl (2 g) and then extracted with CH_2Cl_2 (3 x 100 mL). The combined organic layers were

evaporated and the residue analyzed by GC and ^{1}H NMR. In all runs, no photoproducts were formed and the starting materials recovered completely unchanged. For a typical experiment in acidic solution, a solution of 20 mg of **22** and 2 g of sodium 4-acetylbenzenesulfonate in 1:1 H_2SO_4-MeOH (v/v) was irradiated at 350 nm for 1 h with argon purge. After normal work up, the product mixture was analyzed by GC and ^{1}H NMR. No solvolytic products were obtained and starting materials were recovered unchanged.

CHAPTER FOUR: Photoisomerization and Related Reactions of Xanthene (26) and Derivatives 42 and 44

4.1 Introduction

As discussed in Chapter Three, the photoinduced homolysis of the aryl-O bond in diaryl ethers gives rise to phenyl/phenoxy radical pairs. The subsequent reaction of radical pairs can give either escaped or rearranged products. The ratio of their yields depend upon the nature of the reaction medium. Polar and sluggish hydrogen-donating solvents (e.g., H_2O-CH_3CN) diminish the yield of escaped products and enhance the yield of rearranged products. In order to minimize the number of photoproducts, one approach is to generate phenyl/phenoxy biradical in aqueous CH_3CN. Limiting the number of reaction pathways available for such biradical should result in a clean photoreaction on irradiation of such types of diaryl ethers. Xanthene derivatives are ideal candidates in this regard since they generate biradicals, instead of radical pairs. Studies of intramolecular reactivity of phenyl/phenoxy biradicals have not been reported so far. The present chapter will report on the development of a photoisomerization reaction of xanthene (**26**) and derivative **42** as well as the interpretation of its reaction mechanism. In addition, the related phototransformation of dibenzo-p-dioxin (**44**), a xanthene derivative, will also be examined. Its photochemistry provides further insights into the reactivity of photogenerated intramolecular biradicals. Our results reveal that photogenerated

phenyl/phenoxy biradicals can undergo a radical *ipso*-attack on the adjacent phenyl ring and induce a novel rearrangement. Such a pathway is shown to be more efficient in aqueous solutions.

4.2 Results

4.2.1 Product Studies

Photolysis of 26 in Aqueous CH_3CN. Photolysis of 10^{-3} M solution of **26** in 1:1 or 7:3 H_2O-CH_3CN (254 nm; solution was vigorously purged with argon and cooled; 1-2 h) gave 6*H*-dibenzo[b,d]pyran (**7**, 70%) as the major product, along with some minor products, namely phenols **1** (2%), **40** (15%) and 9,9'-bixanthyl

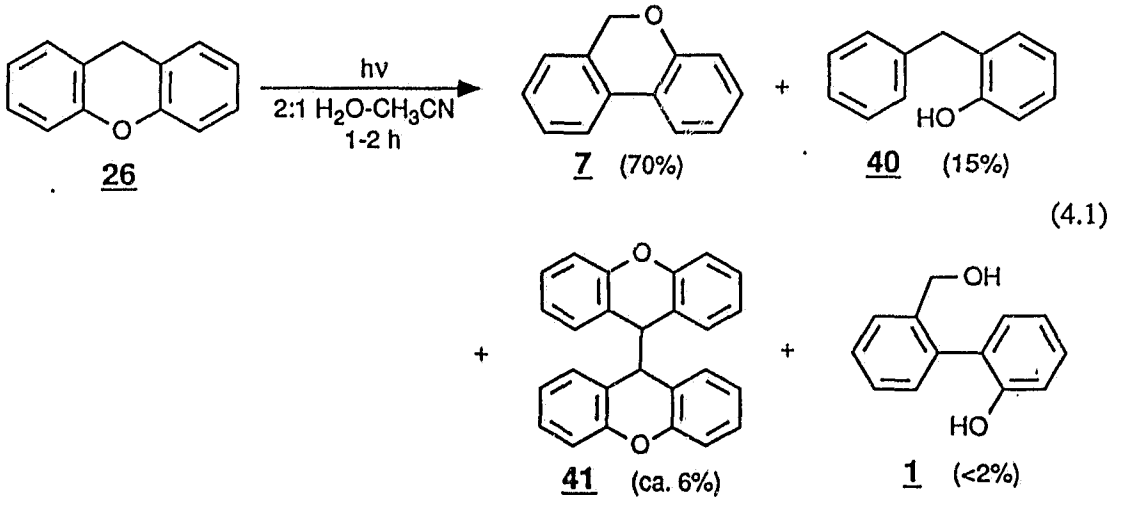

26 → 7 (70%) + 40 (15%) + 41 (ca. 6%) + 1 (<2%) (4.1)

41 (ca. 6%) (eq.4.1). Photoproducts **7**, **40** and **41** were isolated by prep TLC and identified by ^{1}H NMR, MS and by comparison with authentic samples. 9,9'-Bixanthyl (**41**) was further unambiguously characterized by X-ray crystallography. The crystallographic data and ORTEP view of **41** are shown in Table 4.1 and

Figure 4.1, respectively. Note that the crystal structure is completely *anti*. Selected bond lengths and angles for **41** are given in Appendix B. Only a trace amount of phenol **1** (2%) was detected even after exhaustive photolysis. The presence of this compound was confirmed by co-injection into the GC with an authentic sample.

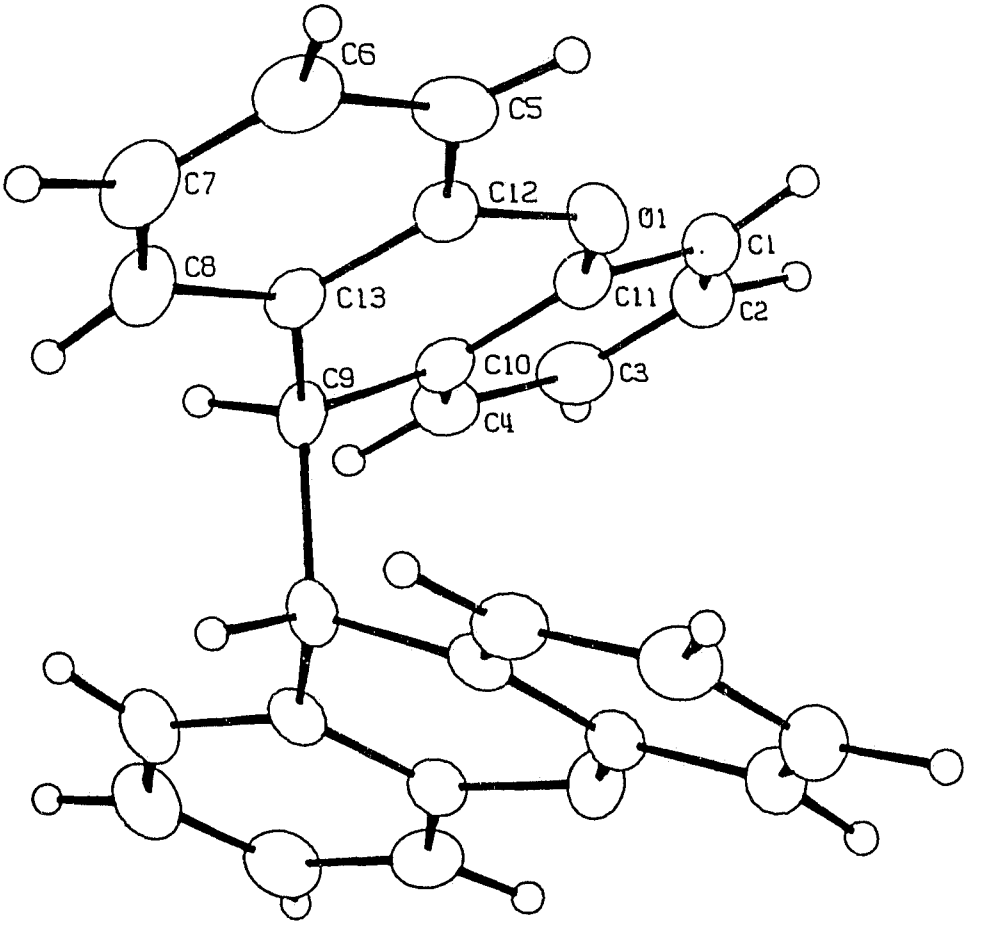

Figure 4.1. ORTEP drawing of 9,9'-bixanthyl (**41**).

Table 4.1. Summary of Crystallographic Data for 9,9'-Bixanthyl (**41**).

formula	$C_{26}H_{18}O_2$
mol wt	362
crystal system	orthorhombic
space group	p2,2,2
cell dimensions	
a, Å	12.493(92)
b, Å	10.752(2)
c, Å	6.876(1)
α, deg	90
β, deg	90
γ,deg	90
V, Å^3	923.6
Z	4
T	20°C
λ	Mo Ka (0.71069)
ρ_{obsd}, g cm^{-1}	1.2945
ρ_{cald}, g cm^{-1}	1.301
μ, cm^{-1}	0.44
$R(F_o)$	0.0638
$R_w(F_o)$	0.0563

Control experiments showed that no reaction was observed in the absence of light and that irradiation of authentic samples of **40** or **41** did not give pyran **7**. However, photolysis of biphenyl alcohol **1** gave **7** with high chemical (>90%) and quantum yields ($\Phi = 0.25$), as discussed in detail in Chapter Two. This raises the possibility that pyran **7** is a photoproduct from secondary photolysis of the initially formed alcohol **1**. The very low yields observed for **1** would be consistent with this pathway. In addition, pyran **7** was also found to be photolabile and gave rise

to alcohol **1** in low yield (2%) on extended photolysis. The additional possibility that alcohol **1** is from the secondary photolysis of pyran **7** cannot be ruled out. Nevertheless, this issue will be readily resolved by the kinetic photolysis of **26** in 100% MeOH, which provides an unequivocal argument that alcohol **1** is the primary photochemical product of **26** (*vide infra*).

The kinetic photolysis of **26** in 7:3 H_2O-CH_3CN is shown in Figure 4.2. This plot shows that pyran **7** is the major product at all conversions. The yield of 9,9'-bixanthyl (**41**) decreases on prolonged irradiation time presumably due to

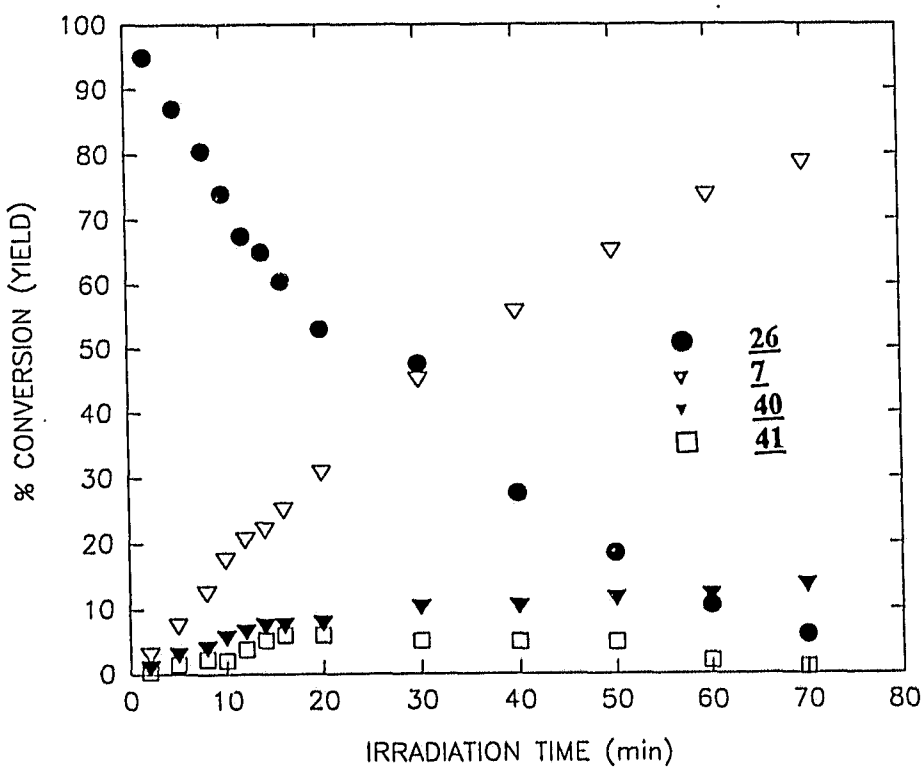

Figure 4.2. Plot of product yields as a function of photolysis time on irradiation of **26** in 7:3 H_2O-CH_3CN (v/v).

photochemistry which is not unexpected. Independent photolysis of **41** under the same condition as for **26** resulted in facile decomposition to a number of products which was not identified. The points for alcohol **1** are not shown in Figure 4.2 for clarity since only trace amounts (<2%) were observed at all photolysis times.

Table 4.2. Product Ratios as a Function of Water Content in CH_3CN in the Photolysis of **26** as Determined by GC.[a]

H_2O-CH_3CN ratio	%		
	7	**40**	**41**
100% CH_3CN[b]	10 ± 2	6 ± 2	2 ± 1
1:9	15	3 ± 1	1
3:7	26	4	2
1:1	29	6	3
7:3	35	12	6

[a] % given are mole ratios, after correction for GC response, where required.
[b] Ratios are v/v. All samples were irradiated for the same time.

When irradiated in 100% CH_3CN, **26** gave the same product mixture as observed in aqueous solution (except no alcohol **1** was detected), but with considerably lower yields (by a factor of ca. 2.5) after the same photolysis time.

Relative yields of products on photolysis **26** in varying H_2O-CH_3CN (v/v) mixtures as determined by GC are shown in Table 4.2. It is clear that solvent water has an enhancing effect on the yields of **7** and **41**. For the phenol **40**, its yield varies in a more complicated way. This can be readily explained as follows. The solvent CH_3CN is a better hydrogen-donor than the solvent water. Its presence will enhance the yield of phenol **40**. However, a more polar solvent such as water can enhance the efficiency of the aryl-O bond cleavage step (vide infra), which is overall product-determining. Thus, the combined contributions from these two contrasting effects account for the observed behavior of the yield of **40**.

Photolysis of 26 in 2-PrOH. The above results indicate that use of a better hydrogen-donating solvent can enhance the yield of the phenol **40**. Photolysis of **26** in 100% 2-PrOH, an excellent hydrogen-donor, gave almost exclusively phenol **40** (>90%) at all conversions, with only a trace amount of **7** and several very minor products (2%) which were not identified (eq. 4.2). In this photolysis, 9,9'-bixanthyl (**41**) was not observed. With respect to relative reaction efficiency, the conversion in 100% 2-PrOH was 32 ± 5% as opposed to 40 ± 5% when irradiated in 1:1 H_2O-CH_3CN under otherwise identical conditions. The very similar overall conversions observed in these two solvent systems indicate that photolysis of **26** initially generates a phenyl/phenoxy biradical intermediate, which abstracts hydrogen from the solvent 2-PrOH, to give rise to the phenol **40**, or otherwise reacts via *a new rearrangement pathway*, which ultimately results in the formation

of pyran 7. In other words, formation of 7 and **40** is from a competing reaction of the initially generated biradical.

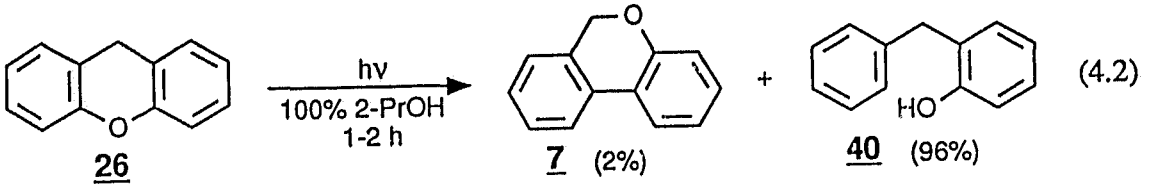

(4.2)

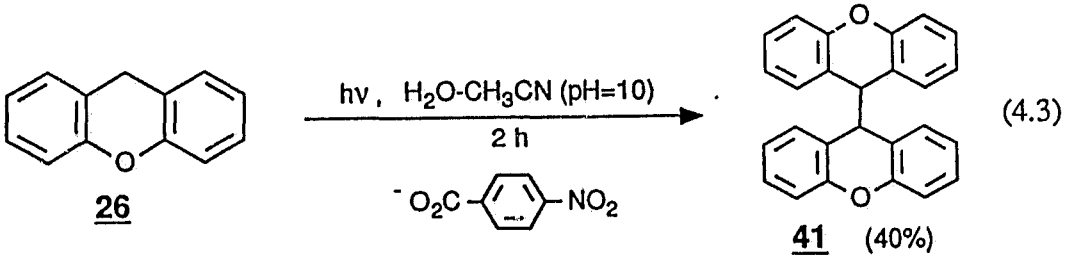

(4.3)

Photolysis of 26 in the Presence of Para-nitrobenzoic acid (PNBA). The formation of bixanthyl **41** in photolysis of **26** appears to be via a different reaction pathway from the one discussed above for 7 and **40**. We found that by adding 10^{-2} **M** *para*-nitro-benzoic acid (PNBA), a good electron acceptor,[106] irradiation of **26** in basic solution (pH > 9, 1:1 H_2O-CH_3CN) at 350 nm resulted in an exclusive formation of the dimer **41** (eq. 4.3), suggesting that formation of **41** from **26** involves an initial electron transfer (ET) process. A similar type of photodimerization reaction in *N*-methylacridan has been reported recently (eq. 4.4).[107]

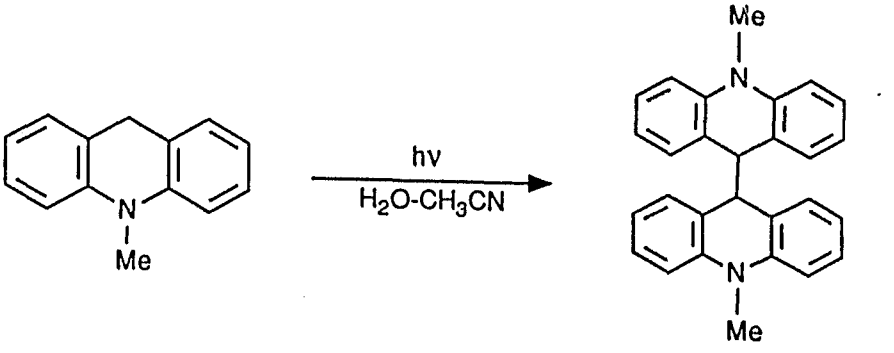

(4.4)

Photolysis of ***26*** *in 100% MeOH.* Results from the photolysis of xanthene (**26**) in MeOH provides important new insights into the mechanism of the photoisomerization reaction. Irradiation of **26** (3 h) in 100% MeOH gave 2-(2'-hydroxyphenyl)benzyl methyl ether (**5**) as well as products **7** and **40** in the quoted yields (eq. 4.5). Since methyl ether **5** could be a secondary photoproduct of pyran **7** (see eq. 2.4), a kinetic photolysis of **26** in 100% MeOH was then undertaken to

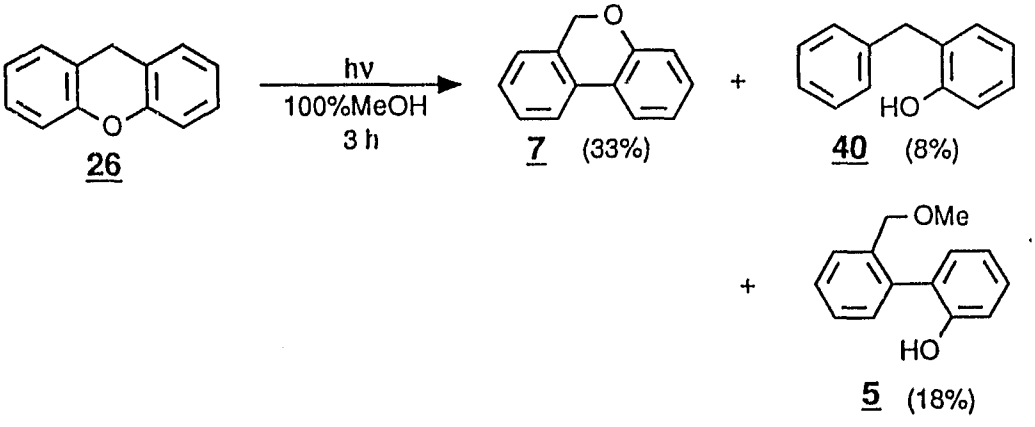

(4.5)

delineate the pathway for its formation. The results are shown in Figure 4.3. This plot indicates that, at low conversion (<10%), the yield of pyran **7** was also low (~4%). However, methyl ether **5** was already detectable (~1%). At this low

conversion, the starting material 26 absorbed most of the light and thus secondary photolysis of pyran **7** would not be important at this initial stage. On further photolysis, the rate of growth of **5** increases as expected since **7** will begin to absorb light, which will lead to **5**. This is manifested by the "crossing" observed at ~150 min for curves for **40** and **5**. These results demonstrate that **5** is probably a primary photoproduct of substrate **26**. That is, the photogenerated phenyl/phenoxy biradical from **26** can undergo a rearrangement to give the *o*-

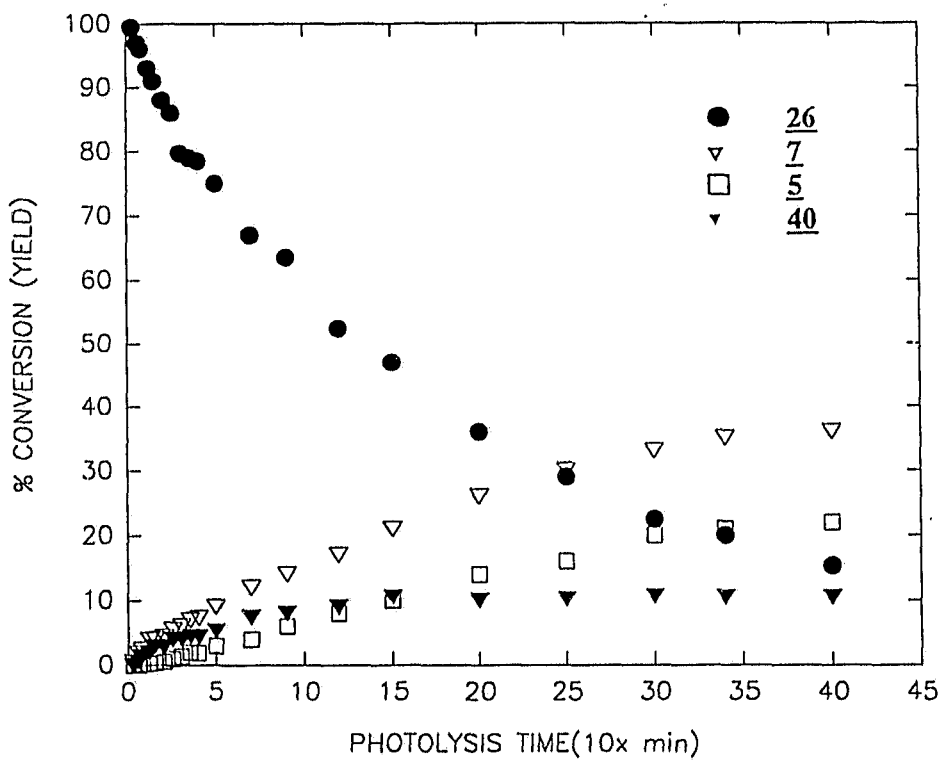

Figure 4.3. Plot of product yields as a function of photolysis time on irradiation of **26** in 100% MeOH.

quinonemethide intermediate **20**, which can be trapped by external nucleophilic solvents such as H_2O and MeOH to give alcohol **1** and ether **5**; respectively, or cyclize to **7**.

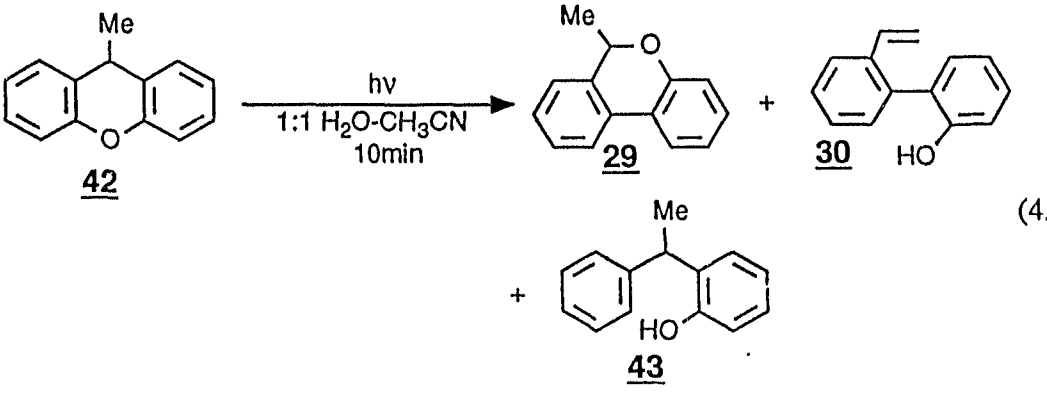

(4.6a)

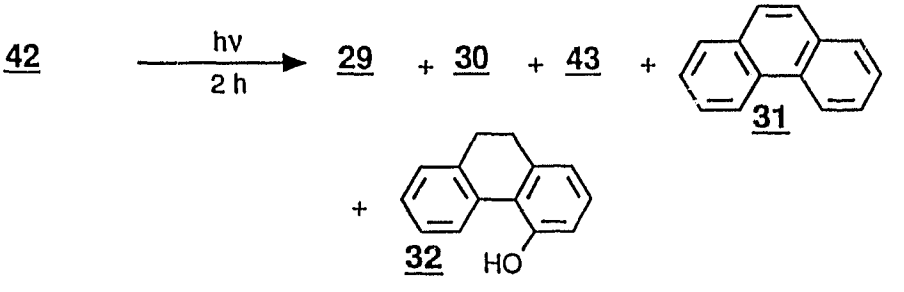

(4.6b)

Photolysis of 42. The reaction observed for xanthene (**26**) appears to be general for other xanthene derivatives. Results from studies of 9-methylxanthene (**42**) provided additional insights into the mechanism of this photoisomerization. Irradiation of **42** in 1:1 H_2O-CH_3CN for 15-20 min produced the pyran **29** as the major product (~15%), along with a small amount of styryl derivative **30** and phenol **43** (eq. 4.6a). On prolonged photolysis (2 h), the yield of pyran **29**

decreased with concurrent formation of two more compounds **31** and **32** (eq. 4.6b). Product **29** was isolated and photolyzed under the same condition as for **29** to give products **30-32**. Thus, products **30-32** are probably secondary photoproducts from pyran **29**. As discussed in Chapter Three, pyran **29** is photolabile, which again accounts for its overall low yield in this reaction. A kinetic study of **42** in 1:1 H_2O-CH_3CN is shown in Figure 4.4. It is clear that both pyran **29** and styryl derivative **30** are formed as primary photochemical products from **42**. The relatively efficient formation of styryl **30** at initial stages of the reaction further

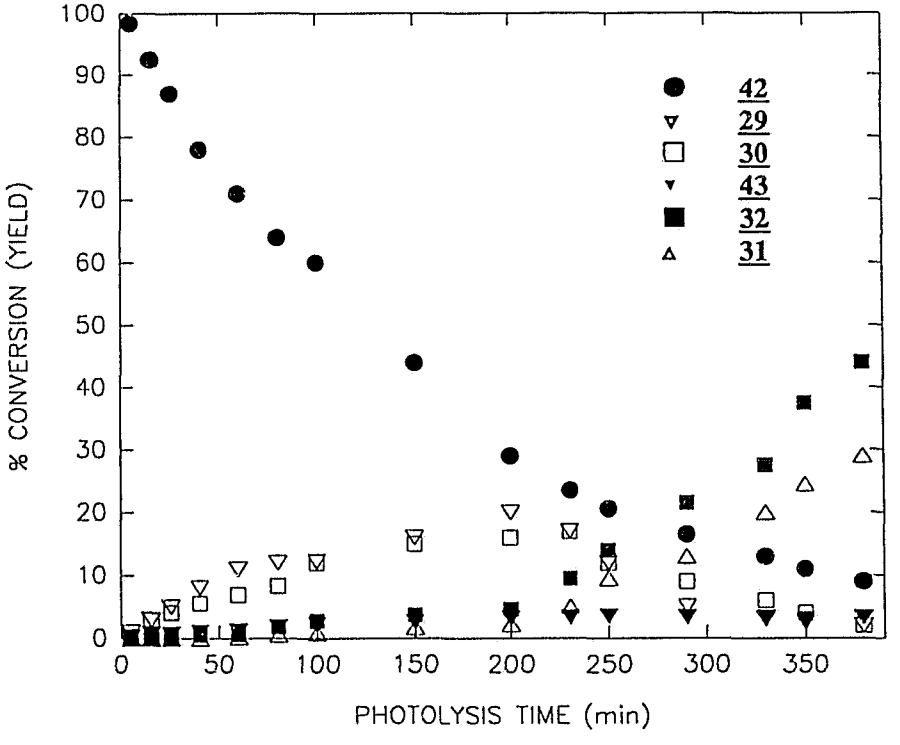

Figure 4.4. Product distributions vs the photolysis time on irradiation of **42** in 1:1 H_2O-CH_3CN. Several unidentified photoproducts were not shown here, which account for a total of 10-15% yield.

suggests that this is the first formed secondary photoproduct, which on further photolysis leads to **31** and **32**. Unlike the parent xanthene (**26**), compound **42** did not give a bixanthyl product upon irradiation. The corresponding bixanthyl product from **42** would be sterically crowded at the 9,9'-positions due to the extra methyl groups, which probably prevented its formation. Photolysis of **42** in 100% 2-PrOH afforded almost exclusively phenol **43**, via a photoreduction process (of the initially formed biradical).

Photolysis of 26 in $H_2{}^{18}O$-CH_3CN. In order to determine where oxygen in product **7** comes from, xanthene (**26**) was irradiated in 2:1 $H_2{}^{18}O$-CH_3CN (water portion was 20% ^{18}O-enriched). The photoproducts analyzed by GC/MS showed that ^{18}O was not incorporated into the product **7**. By default the oxygen in **7** must come from the oxygen of substrate **26**.

Photolysis of 9,9'-Dideuterioxanthene (26). Formation of **40** suggests that the initially photogenerated phenyl/phenoxy biradical can abstract hydrogen from the solvent. However, there is the possibility that the biradical abstracted hydrogen from substrate itself, giving rise to a portion of **40** observed. Xanthene (**26**) has been widely employed as a hydrogen donor since its benzylic hydrogens are abstracted by reactive radicals.[105a-c] To examine this possible pathway, photolysis of a 1:1 mixture of **26** and 9,9'-dideuterioxanthene (**26a**) was carried out. The results show that deuterium was not incorporated into phenol **40**, showing that the additional hydrogens in phenol **40** comes exclusively from the solvent.

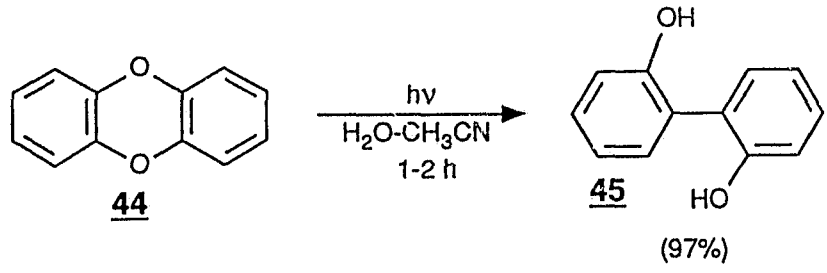

(4.7)

Photolysis of Dibenzo-p-dioxin (44). In order to extend the above results to structurally related xanthene derivative, dibenzo-p-dioxin (DBD, **44**) was studied. Derivatives of this compound (e.g., tetrachlorodibenzo-p-dioxin) are well-known in the *public eye* due to their often quoted toxicity. Studies of its photodecomposition mechanism, particularly in aqueous solution, may prove relevant to disposal of such derivatives. Photolysis of 10^{-3} M aqueous CH_3CN solutions (typically 1:1 H_2O/CH_3CN) of **44** (254 nm lamps; 1-2h; the solution was cooled and argon purged) gave > 50% yield of 2,2'-biphenylphenol (**45**) (ca. Φ_p = 0.01) as the major product (~97%) (eq. 4.7). The photoproduct **45** was isolated by preparative TLC and characterized by GC, MS and ^1H NMR and comparison to an authentic sample. When irradiated in 100% CH_3CN, MeOH and 2-PrOH, **44** again gave **45** as the major product. For comparable runs under otherwise identical conditions, the yield of **45** in 2-PrOH was considerable higher than in CH_3CN, suggesting that use of a better hydrogen-donating solvent can enhance the yield of the product **45**. Interestingly, even use of the solvent water can significantly enhance the quantum efficiency of product **45** formation. For instance, on parallel

photolysis of **44** in 100% MeOH and in 1:1 H_2O-MeOH, the product yields of **45** were 20% and 30%, respectively. The relative product quantum yields for photolysis of **44** as a function of water content in CH_3CN solutions are shown in Figure 4.5. It is clear that solvent water can dramatically increase the efficiency

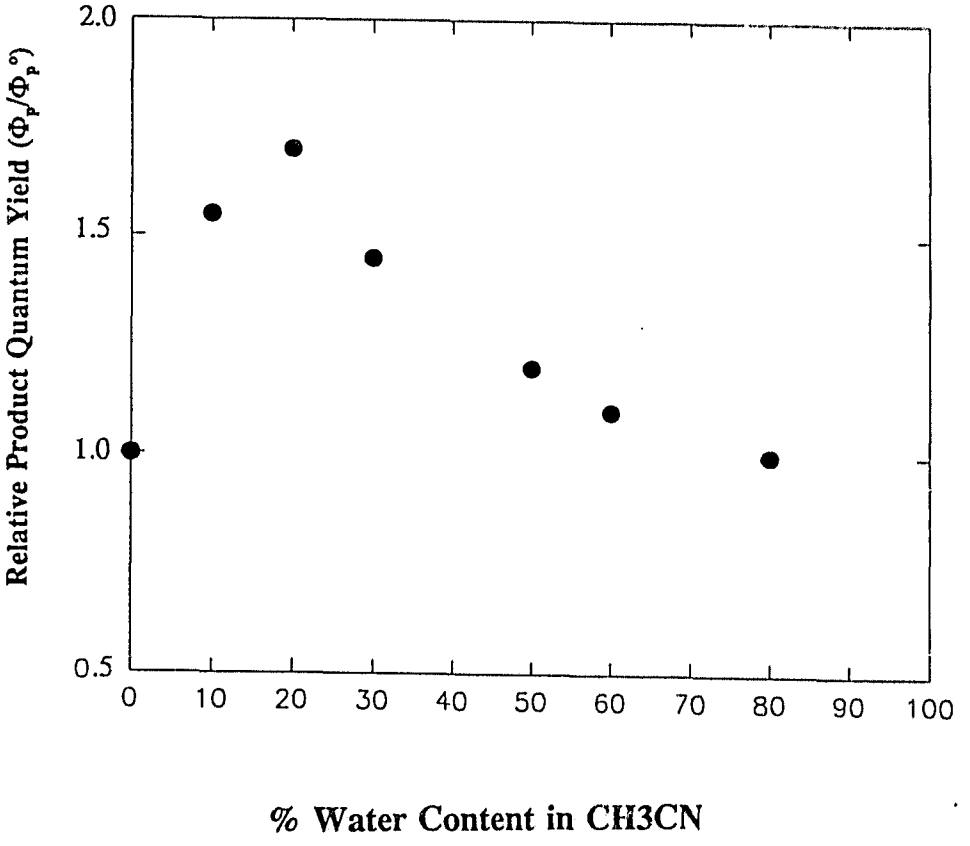

Figure 4.5. Relative Quantum Yields vs % (v/v) Water Content in CH_3CN on Irradiation of **44** (Φ_p° is defined as the yield in 100% CH_3CN).

of the reaction even at low concentration of water. However, on further increasing the water content in solutions, Φ_p/Φ_p° begins to decrease. The decline in Φ_p/Φ_p° at higher water content indicates that the formation of product **45** requires a

hydrogen-donating source from the solution. As CH_3CN is depleted, a viable hydrogen donor is removed. The initial enhancement in quantum yield by added water is probably due to a simple solvent polarity effect. That is, aryl-O bond homolysis is polarized in the transition state and a more polar solvent in H_2O helps this initial step.

In order to investigate the possibility that a reactive intermediate might be formed with a significantly long lifetime, two work-up procedures were employed on photolysis of **44** in aqueous CH_3CN. That is, two identical irradiated solution were worked up after 2 min and after 2 h, respectively. It was found that the yields of photoproduct **45** were 9 ± 2% and 25 ± 3%, respectively. Thus, the yield of **45** was higher when the irradiated solution was left standing for a longer period of time, suggesting that a reactive intermediate is formed which is reasonably long-lived, and which transfers to **45** over a period of time. When a similar run was carried out in which $NaBH_4$ was added after photolysis, the yield of **45** was 23 ± 3%. This observation shows that the intermediate is reducible with $NaBH_4$, giving rise to **45**. Moreover, on irradiation of **44**, a deep red-orange colour develops which slowly faded into a yellowish colour on standing over several hours. These results promoted us to make an attempt to detect the transient absorption spectrum of a possible reactive intermediate which leads to the final product **45** via reduction pathway.

Fortunately, this was readily accomplished by UV-Vis. Shown in Figure 4.6

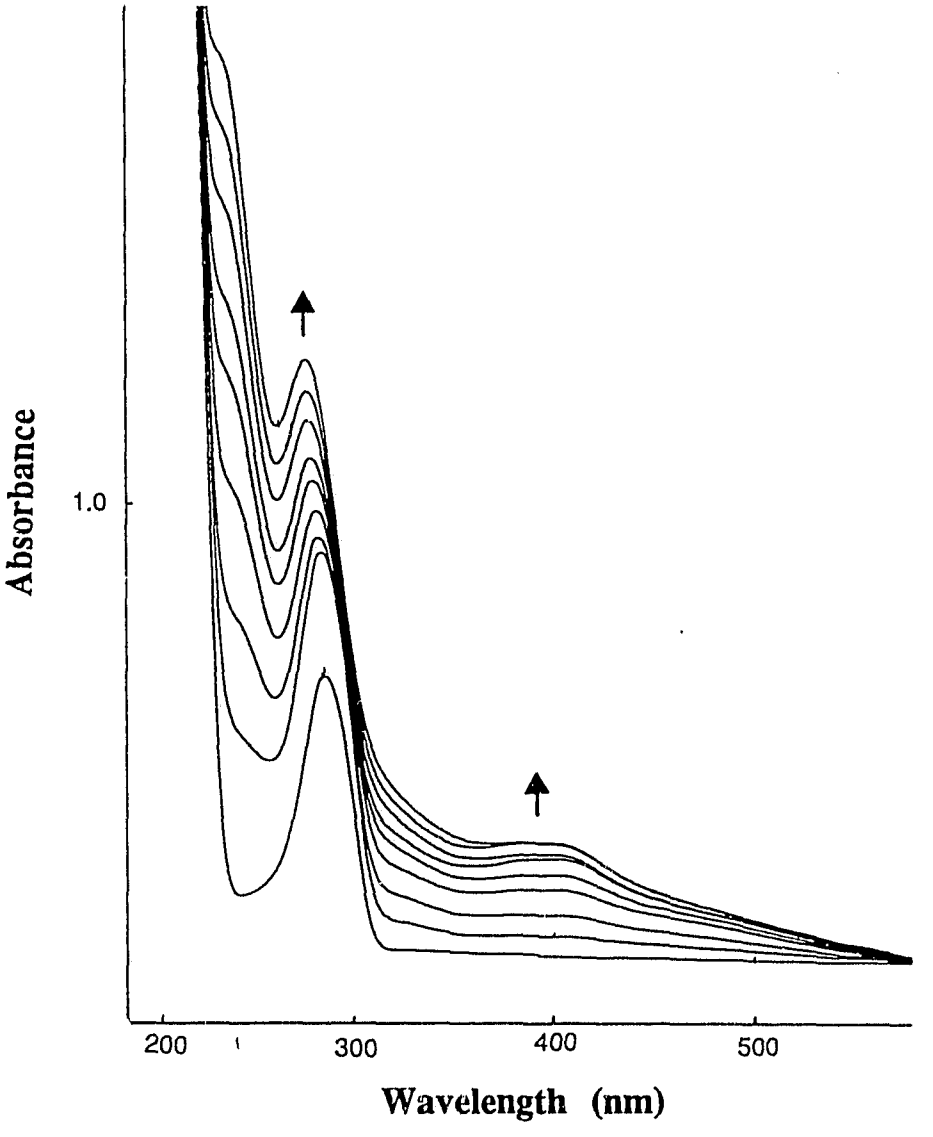

Figure 4.6. Time dependent UV-Vis absorption change studies on photolysis of **44** in 2:1 H_2O-CH_3CN. Photolysis time was 2 min for each trace.

is the time-dependent UV-Vis absorption change study on irradiation of **44** in 7:3 H_2O-CH_3CN. A broad band with λ_{max} = 405 nm gradually builds up as the starting

material was lost on photolysis. At the same time, the absorbance at 240-290 nm region dramatically increased due to the formation of product **45** which has a maximum at 280 nm in aqueous CH_3CN. This observation led us to study the

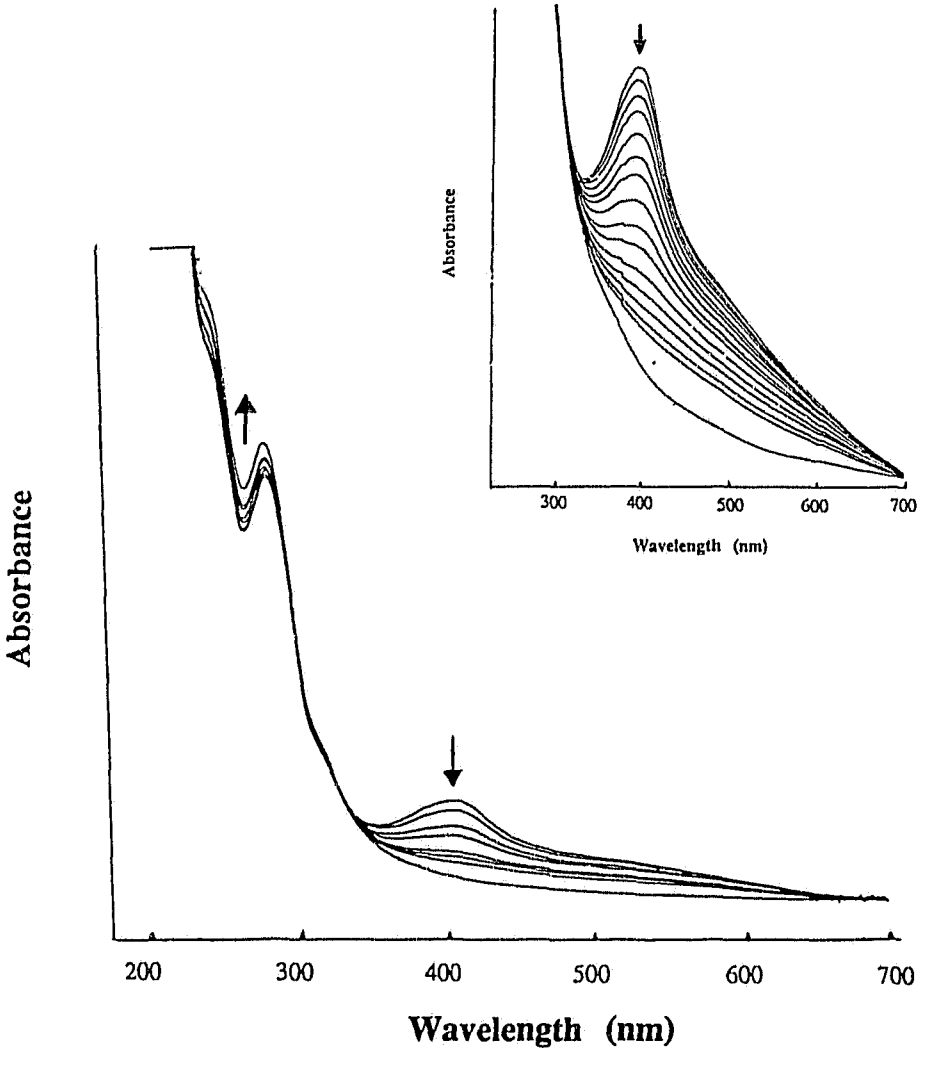

Figure 4.7. UV-Vis spectrum of decay of the transient with λ_{max} = 405 nm with concomitant increase at 240-290 nm in 7:3 H_2O-CH_3CN. The inset is the decay of an enlarged absorption spectrum of the transient at 405 nm.

kinetic behaviour of the reactive intermediate with a transient at 405 nm in various solvents. It was found that the decay of the transient at 405 nm (see Figure 4.17 and inset) was concurrent with increasing formation of product **45** (increasing the absorbance at 240-290 nm region, as shown in Figure 4.7). The half-life of the intermediate was estimated as 100 min in 7:3 H_2O-CH_3CN, and 60 min in 7:3 H_2O/2-PrOH and 70 min in 100% CH_3CN, respectively. If $NaBH_4$ was present in the solution on photolysis, the transient at 405 nm was not detected. In addition, when a small amount of $NaBH_4$ was added after photolysis, the 405 nm transient vanished in less than 1 min. Irradiation of product **45** under the same conditions as for **44** did not produce the band at 405 nm. Therefore, the transient at 405 nm is probably due to a reactive intermediate which is the precursor to **45**. Based on xanthene (**26**) photoisomerization discussed above, a reasonable intermediate is *o*-biphenylquinone (**46**). Several 2,2'-biphenyl quinone derivatives such as **53** and **54** (see discussion section) are known to be stable in air for a few hours, their lifetimes being dependent on the nature of the substituents on the phenyl rings (*vide infra*).[109-113]

4.2.2 Quantum Yields and Solvent Effects

Quantum efficiencies for formation of products **7** and **40** were determined using 280 nm irradiation of degassed 0.001 **M** solutions of **26** (the substrate absorbed >99% of light at 280 nm). Conversions were kept low (<20%) and

product analyzed by GC, using potassium ferrioxalate[97] as chemical actinometry. Product **7** quantum yields on photolysis of **26** in various H_2O-CH_3CN mixtures are listed in Table 4.3. The higher water content in CH_3CN considerably enhances the quantum yield of product **7**. The value for the formation of product **40** in 100%

Table 4.3. Quantum Efficiencies for Product **7** Formation on Photolysis of **26** as a Function of Water Content in CH_3CN[a].

H_2O-CH_3CN ratio[a]	Φ[b]
100% CH_3CN	0.0014 ± 0.0002
1:9	0.0015
2:8	0.0019
3:7	0.0024
1:1	0.0031
7:3	0.0035 ± 0.0004

[a] v/v

[b] Quantum yields for appearance of photoproduct **7**. Quantum yields for loss of substrate **26** are 10-15% higher, as expected due to formation of side products (see eq. 4.1).

2-PrOH was found to be 0.0028. The quantum yield for the formation of product **45** on irradiation of **44** in 7:3 H_2O-CH_3CN was estimated to be 0.01, using

xanthene **26** as secondary standard. The irradiated solution in this case was worked up immediately.

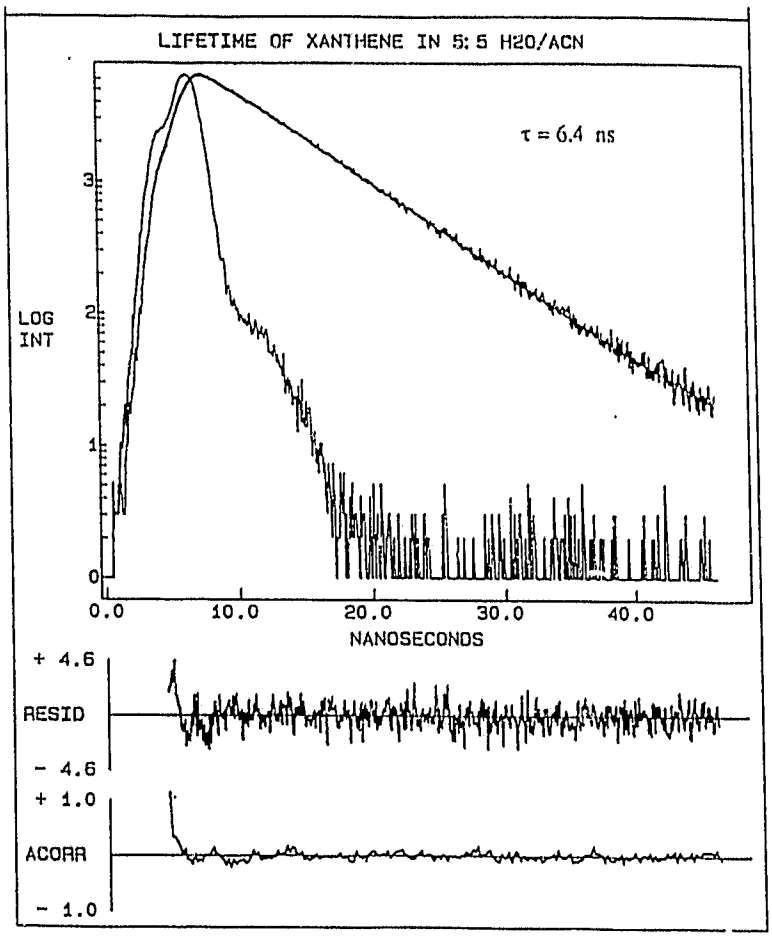

Figure 4.8. A typical fluorescence decay curve generated by single photon counting: fluorescence lifetime of xanthene **26** in 1:1 H_2O-CH_3CN (τ = 6.4 ns).

4.2.3 Steady State and Transient Fluorescence Measurements

Steady state fluorescence spectra were recorded on a Perkin-Elmer MPF 66

spectrofluorimeter with a substrate concentration of ~10^{-4} **M**. Xanthene (**26**) was weakly fluorescent in organic and aqueous solvents (λ_{max} = 305 nm) with a fluorescence quantum yield of Φ_f = 0.054 (bandwidth 280 - 350 nm) in CH_3CN,

Table 4.4. Fluorescence Lifetimes of **26** as Measured by Single Photon Counting.

solvent	lifetime (ns)[a]
100% CH_3CN	7.4 ± 0.2
1:9 H_2O-CH_3CN[b]	6.9
4:6 H_2O-CH_3CN	6.6
5:5 H_2O-CH_3CN	6.4
9:1 H_2O-CH_3CN	3.5
100% H_2O	2.7
100% MeOH	7.5
100% 2-PrOH	7.5
100% n-hexane	8.3

[a] All decays were fitted to a single exponential decay with the fitting parameter χ^2 < 1.4. Measured with the assistance of Mr. D. Shukla of this group.
[b] v/v

determined using biphenyl ether as fluorescence reference standard.[99] Fluorescence lifetimes of **26** were measured in a number of organic solvents and H_2O-CH_3CN solutions and are listed in Table 4.4. Shown in Figure 4.8 is a typical fluorescence decay as measured by the single photon counting instrument. The lifetime of **26** was found to decrease slightly with increasing water content. In addition, the steady-state fluorescence intensity was considerably quenched by added water in CH_3CN. The concomitant decrease in fluorescence intensity and lifetime with increasing product quantum efficiency for photoproduct **7** suggests that the photoisomerization of **26** is via the singlet excited state S_1.

4.2.4 Triplet-State Sensitization

As discussed in Chapter Three, the triplet state energy of diaryl ethers, e.g. **26**, could be over 80 kcal mol^{-1}.[99] However, the triplet state energy for most of the known water-soluble triplet sensitizers is about 70 kcal mol^{-1}. Therefore, like in the case of diaryl ether **22**, acetone (E_T = 82 kcal mol^{-1}) was used as a triplet sensitizer for xanthene (**26**). Photolysis of **26** in 1:1 H_2O-acetone at 300 nm led to the complete recovery of starting material, where the acetone absorbed most of light at 300 nm (>90%). Therefore the triplet state of **26** is probably nonreactive in aqueous CH_3CN and it is the S_1 that is responsible for photoisomerization. This is consistent with the fact that the dissociation energy of aryl-O bond is estimated to be 70-80 kcal mol^{-1}, and thus only the singlet state of **26** (E_S = 95 kcal mol^{-1} on

the basis of the onset of emission at 290 nm) has enough energy to break this aryl-O bond.

4.3 Discussion

The above results demonstrate that there are two different primary photochemical pathways available for xanthene (**26**) in S_1. These two reaction pathways are responsible for the "photodimerization" (to give **41**) and photoisomerization, respectively, the details of which are discussed below. In addition, the mechanism of reaction of **44** will also be discussed.

4.3.1 Mechanism of 9,9'-Bixanthyl (41) Formation

The formation of 9,9'-Bixanthyl (**41**) from xanthene **26** is apparently due to initial photogeneration of a xanthyl radical, which recombines to afford its dimer **41**. The proposed mechanism of this photoreaction is shown in Scheme 4.1. The primary photochemical event is proposed to proceed via an electron ejection step (photoionization) into the solution, to give xanthyl radical cation **47**. Evidence in support of this electron transfer process is that when there was a good electron acceptor in solvent system (PNBA), the efficiency for formation of **41** was greatly enhanced; **41** was formed as the only photoproduct. In addition, direct single step homolysis of the benzylic C-H bond to generate a xanthyl/hydrogen radical pair would be an unfavourable process since the dissociation energy of such a C-H bond

Scheme 4.1

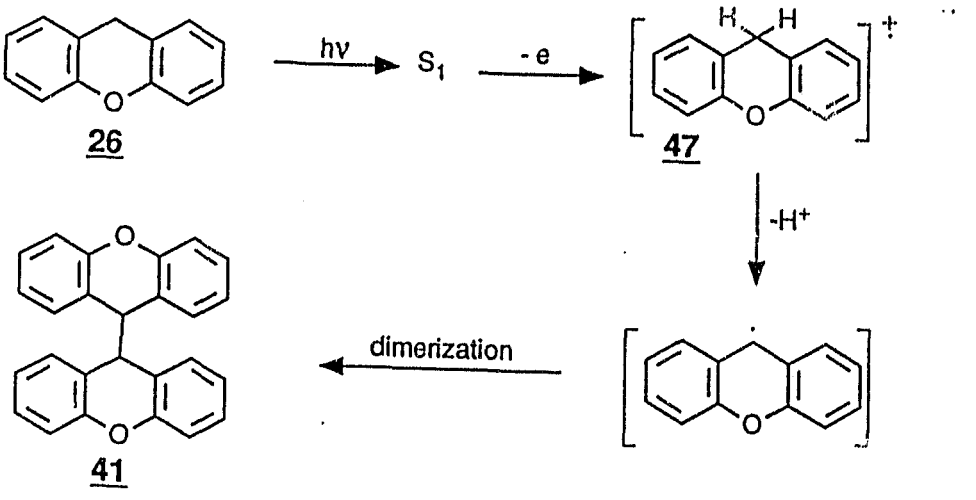

is high (~90-98 kcal mol^{-1}) (please recall that the photogenerated phenoxy/phenyl radical pair does not abstract hydrogen atom from the substrate **26**, see page 153). Radical cations of the type **47** are very acidic at benzylic position (pK_a = -2 for C-H ionization) and readily undergo an C-H ionization to generate the xanthyl radical with loss of a proton. That a polar solvent such as water can enhance the formation of **41** (Table 4.2) is consistent with this pathway, since ion **47** would be well-solvated by water. The recoupling of xanthyl radical gives rise to the dimer **41**. There have been several reports of photoionization of organic substrates via a mono-photonic process,[114-116] although in general, it is rarely observed. For example, *N*-methylacridan efficiently undergoes a similar type of photoionization via a one-photon process, to yield the dimer in deaerated aqueous solution (eq. 4.4).[107] Although *N*-methylacridan is clearly much more electron rich than xanthene **26**, the same photoionization process of **26** apparently also takes place but

in much lower yield.

4.3.2 Mechanism of Photoisomerization

Xanthene derivatives can be regarded as formal diphenyl ethers with a methylene chain connecting the two phenyl rings. As discussed in Chapter Three, the photoinduced homolysis of the aryl-O bond is one of two primary photochemical processes available for diaryl ethers. All results indicate that the photoisomerization of **26** to pyran **7** is initiated by homolysis of the aryl-O ether

Scheme 4.2

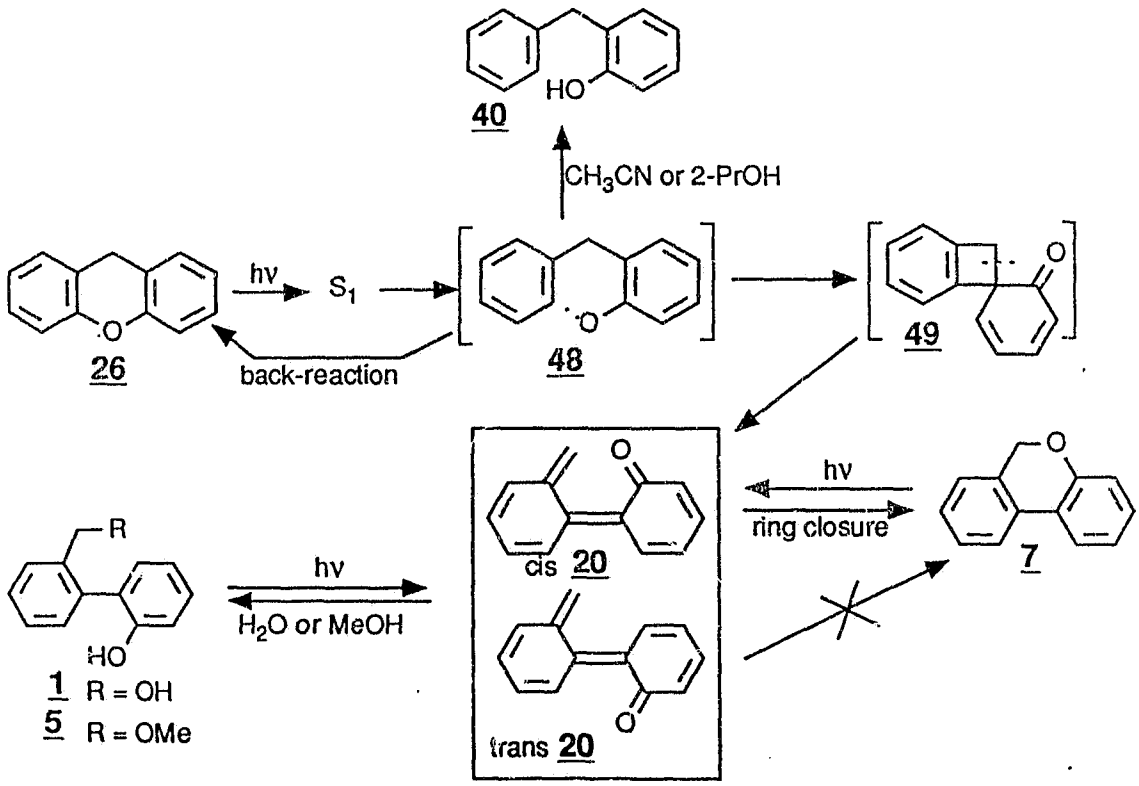

bond. However, unlike diaryl ether **22**, which produces a phenoxy/phenyl radical pair, xanthene (**26**) generates a *singlet biradical* **48** (Scheme 4.2). There are three chemical deactivation pathways available for this biradical. Apart from recombining to give back starting material, the biradical **48** can either abstract hydrogen from solvent to give phenol **40**, or undergo a radical *ipso*-attack on the adjacent phenyl ring, to yield the spiro ketone intermediate **49**. The quantum efficiency for homolysis of the aryl-O bond is probably much higher than the total quantum yields for formation of **7** and **40** from **26** due to the back reaction. Since a polar solvent can stabilize the ketone intermediate **49** the presence of H_2O in solution would enhance its formation from **48**, vs simple recombination to give back **26** or hydrogen abstraction from the solvent. The spiro ketone **49** is a highly strained and thus unstable intermediate. Subsequent homolysis of the benzylic C-C bond in **49** gives the *o*-quinonemethide **20**, the *cis*-isomer of which is expected to undergo electrocyclic ring closure to give observed pyran **7**. Either *cis* or *trans* forms may be trapped by H_2O (MeOH) to give **1** (**5**), which are observed. Although photolysis of **1** or **5** also gives **7**, as discussed in Chapter Two, the ether **5** was found to be a *primary* photochemical product from **26**, as shown in Figure 4.3. The formation of **5** as primary photochemical product on irradiation of **26** in MeOH is consistent with the above proposed reaction pathway. Therefore, the *o*-quinonemethide **20** must be directly generated from the starting material **26**.

There have been several reports mentioned where use of polar solvents,

particularly hydroxylic solvents, can increases the yields of recombination products (biphenyl phenols) from photolysis of diaryl ethers.[63] As discussed in Chapter One, Ogata et al.[74] proposed that the transition state for the aryl-O homolysis is polarized (towards oxygen) and that hydroxylic solvents are able to stabilize this transition state by forming a hydrogen bond. Since biradical **48** cannot give escaped products, there is overall simplicity in the observed photochemistry of xanthene derivatives.

Scheme 4.3

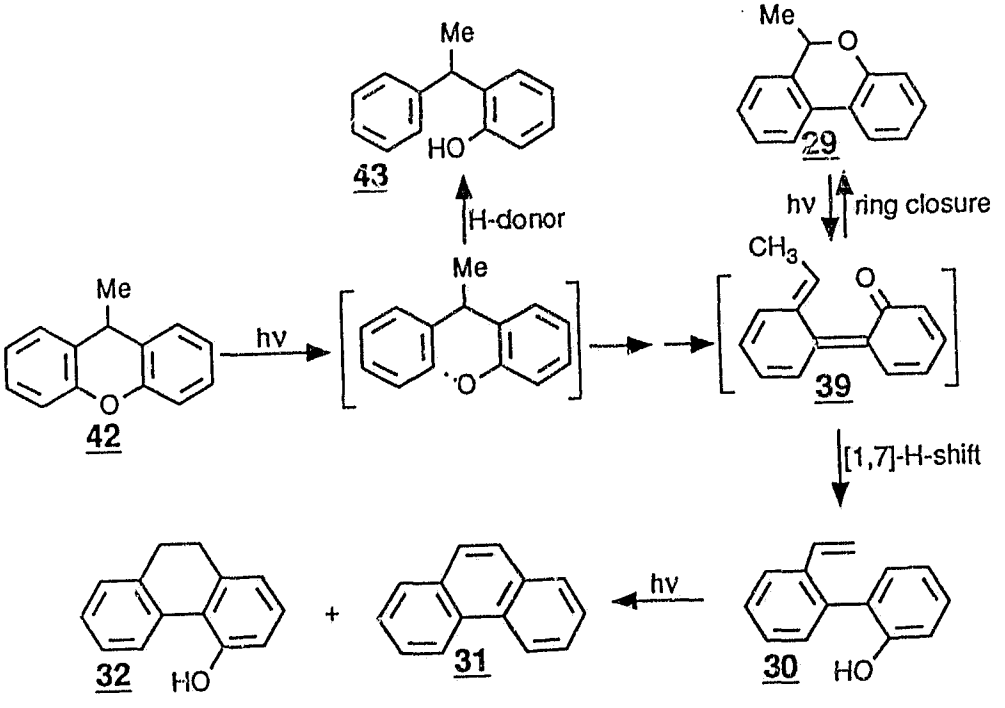

According to the above proposed mechanism for photoisomerization of **26**, photolysis of 9-methylxanthene (**42**) would lead to the corresponding *o*-quinonemethide intermediate **39** (Scheme 4.3). Electrocyclic ring closure of **39**

would give pyran **29**, which was found to be photochemically unstable. The details of this have been discussed in Chapter Three. Unlike *o*-quinonemethide **20**, the 6-methyl substituted *o*-quinonemethide **39** could undergo a sigmatropic 1,7-hydrogen shift from the methyl group to the phenol oxygen to give styryl derivative **30**. Therefore, like pyran **29** and phenol **43**, styryl derivative **30** should also be the primary photochemical product from xanthene derivative **42**. The kinetic photolysis of **42** does show (see Figure 4.3) that at early photolysis times, both of

Scheme 4.4

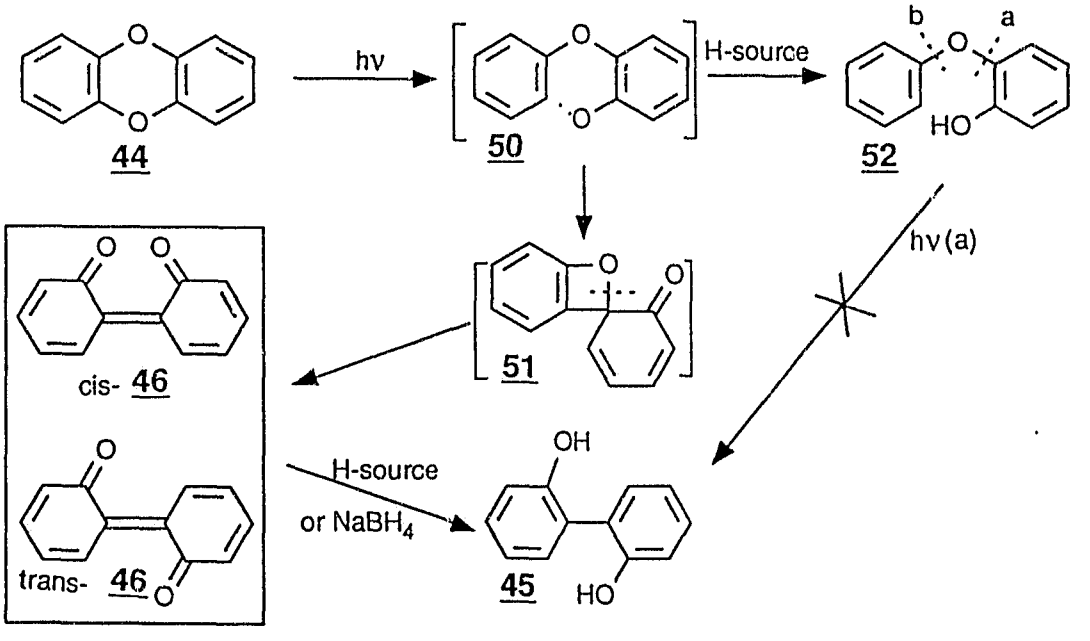

29 and **30** are formed at about same rate, with **30** becoming more dominant at much longer photolysis times, due to eventual secondary photolysis of **29** as already discussed in Chapter Three.

The phototransformation pathway of **44** to **45** is similar to that shown in Scheme 4.2 for the photoisomerization of xanthene (**26**). As shown in Scheme 4.4, the primary photochemical event is again believed to proceed via homolysis of the aryl-O ether bond, to give a singlet phenoxy/phenyl biradical **50**. This biradical can either recombine to give back starting material or undergo a subsequent radical *ipso*-attack on the adjacent phenyl ring, to afford a spiro ketone intermediate **51**. In principle, biradical **50**, like biradical **48**, could also abstract hydrogens from solvents, to give the corresponding phenol **52**. However, phenol **52** was not detected at all conversions. This suggests that the rate of the radical *ipso*-attack process is probably much faster than that of hydrogen abstraction for biradical **50**, whereas these two process are competitive for biradical **48**. The ketone **51** has been claimed as an isolable species,[112] but its isolation was not attempted in this study. Homolysis of the benzylic C-O bond in ketone **51** gives rise to 2,2,-biphenyl-quinone **46**, which can be reduced into 2,2'-biphenylphenol (**45**) by hydrogen abstraction from organic solvents or by $NaBH_4$. The thermal generation of reactive quinone **46** has been reported, but it has never been isolated as a stable compound.[110] However, as discussed in Chapter One, derivatives such as **53** and **54** have been isolated and found to be stable in air for a few hours.[112,113] The UV-Vis spectra of **53** has two absorbance bands at 380 nm and 550 nm.[112] Similarly, the UV-Vis spectrum of quinone **46** shows two maxima, a band at 405 nm and a shoulder at 550 nm. Direct observation of **46** by UV-Vis provides strong evidence

in support of the phototransformation mechanism of **44**.

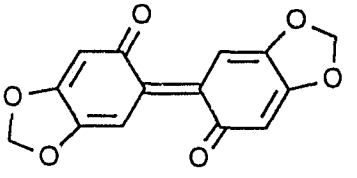

53

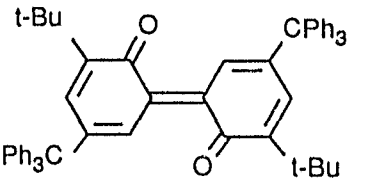

54

The photochemistry of **44** in organic solvents has been studied recently by Masse and Pelletier.[117] They found that photolysis of **44** in aerated solutions led to the formation of 2,2'-biphenylphenol (**45**) along with several highly oxidized hydroxybiphenyls. They proposed that **45** was the secondary photoproduct of an intermediate, namely 2-phenoxyphenol (**52**) (Scheme 4.4). However, Joschek and coworkers[73] have reported that photolysis of **52** under the same conditions as for **44** did not give biphenyl phenol **45** (derived from cleavage of bond *a*), but instead produced several phenols derived from a regio-specific cleavage of the aryl-O bond *b*, as discussed in Chapter One (see eq. 1.26 and 1.27). The Joschek et al.'s results are consistent with other observations from studies of similar diaryl ether systems. In Masse and Pelletier's study, only a trace amount of 2-phenoxyphenol (**52**) (~2%) was detected, and thus **45** could not be wholly derived from **52**. This implies that there is an additional reaction pathway available for biradical **50**. This new pathway we believe is the radical *ipso*-attack and subsequent rearrangement to give **51** (Scheme 4.4).

4.4 Conclusions

A new photoreaction, the photoisomerization of xanthene (**26**) and derivative **42** to dibenzo[b,d]pyrans **7** and **29**, has been documented. The photoreaction is most favourable in aqueous solution. The primary photochemical event is homolysis of the aryl-O bond, to give a singlet phenyl/phenoxy biradical, which undergoes an intramolecular radical *ipso*-attack on the adjacent phenyl ring and subsequent rearrangement, to afford *o*-quinonemethide intermediate **20**. Electrocyclic ring closure of **20** can complete favourably with solvent water capture to yield the observed pyran **7**. A competing reaction pathway, electron ejection into solution (photoionization) which leads to the formation of bixanthyl **41** also occurs on irradiation of **26**. The proposed mechanism for the photoisomerization is further supported by the photochemistry of **44**, whose photodegradation mechanism is found to be via *ortho*-dibenzo-quinone intermediate **46**, which has been directly observed by UV-Vis spectrophotometry. The photoisomerization reaction appears to be general for xanthene systems.

4.5 Experimental

4.5.1 General

A general description of various instruments, techniques and procedures used in these studies is available in Chapter Two.

4.5.2 Materials

Xanthene (**26**) and dibenzo-p-dioxin (**44**) were purchased from Aldrich and recrystallized several times prior to photochemical studies. 9-Methyl-xanthene (**42**) was made by reduction of 9-methyl-xanthene-9-ol, which in turn was obtained from the reaction of xanthone with CH_3MgCl. All compounds were checked for purity by GC and ^1H NMR prior to photochemical study.

9,9'-Bixanthyl (41). A sample of this material was prepared by photolysis of 200 mg of **26** and 800 mg of p-nitrobenzoic acid in 100 mL H_2O and 100 mL CH_3CN (pH adjusted to 12) for 2.5 h at 350 nm. After photolysis, the solution was saturated with NaCl and extracted with CH_2Cl_2 (3 x 100 mL). Evaporation of the solvent and separation by prep TLC (silica; 2:1 hexanes-CH_2Cl_2) gave 70 mg of **41** which was re-crystallized from 95% EtOH to give a colourless crystal. mp 201-204°C (lit.[118] 205-207°C). ^1H NMR δ 7.30-6.55 (m, 16H, ArH), 4.18 (s, 2H, ArCH); ^{13}C NMR δ 49.6, 115.9, 121.9, 122.6, 128.1, 129.2, 153.1; IR (cm^{-1}) (mineral oil) 1600 (m), 1570 (m), 1480 (s), 1300 (s), 1260 (s); MS (EI) m/z (rel int) 362 (M^+) (<5), 181 (100), 182 (15). Anal. Cal. for $C_{26}H_{18}O_2$: C, 86.16; H, 5.01. Found: C, 85.76: H, 5.01 (chemical analysis could not be improved beyond this point, even after successive recrystallizations, probably due to thermal decomposition). Spectroscopic data was identical to that reported by Badejo et. al.[118] However, to ensure that the structure of **41** was indeed a dimer bonded at the 9,9'-positions (as opposed to an isomer, which cannot be ruled out with the

spectroscopic data available) the X-ray crystal structure was solved from single crystals grown from MeOH-toluene. A total of 928 reflections were collected and used for structure refinement. The structure was solved using MULTAN[94] and refined using least squares using SHELX-76.[95] Illustrations were drawn using ORTEP[96] as shown in Figure 4.1. The summary of crystallographic data was given in Table 4.1.

9-Methylxanthene (42). To 8 g (44 mmol) of xanthone dissolved in 200 mL dry THF solution under N_2 (at -5°C) was slowly added 26.7 mL of MeMgCl solution (3 M in THF) over a 30 min period. The reaction mixture was allowed to warm up to room temperature (1h). The reaction was then quenched with 100 g ice-water and neutralized to pH = 7.0 with 2% HCl. After extraction with CH_2Cl_2 (3 x 100 mL), the combined organic layers were dried over $MgSO_4$ and evaporated under reduced pressure to give rise to an oily residue. The crude oil was used without further purification. To a magnetically stirred solution of 1.5 g $LiAlH_4$ and 2.5 g $AlCl_3$ in 200 mL anhydrous ether was added 2 g of the crude oil in 100 mL dry ether. After reflux for 1 h, work up as above gave an oil which was purified by bulb-to-bulb distillation, bp 94-96°C (2 torr) (lit.[119] 95-97°C, 0.3 torr), to give **42** with yield of 1.5 g (75%); ^{1}H NMR δ 7.29-6.98 (m, 8H, ArH), 4.05 (q, J = 8.5 Hz, 1H, ArCH), 1.43 (d, J = 8.5 Hz, 3H, CH_3); mass spectrum (EI) m/z (rel int) 196 (M^+) (13), 181 (M^+-CH_3) (100), 152 (13), 91 (7), 77(5). The ^{1}H

NMR and MS data were consistent with those reported in literature.

9,9'-Dideuterioxanthene. This material was prepared from xanthone by reduction with $LiAlD_4/AlCL_3$ in dry THF. The isolated material was identical to xanthene in all respects except for the absence of methylene signals in the ^1H NMR (estimated isotopic purity >98%).

4.5.3 Product studies

General procedures for preparative and analytical photolysis and dark control runs have been described in Chapter Two.

Photolysis of 26 in H_2O-CH_3CN. In a typical semi-preparative photolysis, 100 mg of substrate **26** was dissolved in 60 mL of CH_3CN and then diluted with 140 mL of H_2O. The solution was then irradiated at 254 nm. After photolysis, the solution was saturated with NaCl and extracted with 3 x 100 mL of CH_2Cl_2. The combined organic layers were dried over $MgSO_4$ and evaporated to give a crude product mixture which was separated on prep TLC (silica; CH_2Cl_2) to give **1, 7, 40-41.** Products **1, 7, 41** were identified by comparison with authentic samples prepared above. Phenol **40** had an ^1H NMR identical to that of an authentic sample. For analytical runs, a solution of 20 mg of **26** in 200 mL of solvent was irradiated and aliquots were removed at different photolysis times for analysis by GC (after normal work up as described above).

Photolysis of 26 in 100% MeOH or 100% 2-PrOH. The procedure was identical to above except direct evaporation of the solvent was carried out. Photolysis of **26** in 100% MeOH gave **5**, **7** and **40**, as determined by prep TLC, GC/MS and ^{1}H NMR. Photolysis of **26** in 100% 2-PrOH gave **40** as the only significant product.

Photolysis of 26 with p-Nitrobenzoic Acid (PNBA). In a typical experiment, a solution of 100 mg substrate and 2 g p-nitrobenzoic acid in 200 mL H_2O-CH_3CN (pH adjusted to 7 with NaOH) was irradiated at 350 nm for 60 min. After standard workup as mentioned above, the product **41** was isolated (yields 20-40%), and identified by ^{1}H NMR, MS and by comparison with similar data from an authentic sample.

Photolysis of 26 in Hexane. A solution of 20 mg substrate in 200 mL hexane was irradiated at 254 nm for 60 min. After removal of solvent, the starting material was recovered unchanged.

Photolysis of 42 in H_2O-CH_3CN. A solution of 100 mg of **42** (t_r = 3.87 min, 180°C) dissolved in 100 mL CH_3CN and 100 mL H_2O was irradiated for 3 h. After the normal work up, **29-32** and **43** were identified by GC/MS and partial ^{1}H NMR spectra: **29** (t_r = 5.44 min, 180°C) MS (CI) m/z 197 ($M^+ + 1$); ^{1}H NMR (partial) δ 1.59 (d, J = 8 Hz, 3H, CH_3), 5.28 (q, J = 8 Hz, 1H, ArCH); **43** (t_r = 4.15 min) MS (CI) m/z 199 ($M^+ + 1$); ^{1}H NMR (partial) δ 1.40 (d, J = 8 Hz, 3H, CH_3), 4.0 (q, J = 8 Hz, 1H, ArCH); **30** (t_r = 4.34 min) MS (CI) m/z 197 ($M^+ + 1$); ^{1}H

NMR (partial) δ 5.22 (dd, J = 7.5 and 14 Hz, 2H, $=CH_2$), 6.80 (dd, J = 7.4 and 14 Hz, 1H, ArCH=); **31** (t_r = 4.98 min; identical with an authentic sample) MS (CI) m/z 179 ($M^+ + 1$); **32** (t_r = 7.3 min) MS (CI) m/z 197 ($M^+ + 1$), ^{1}H NMR (partial) δ 2.7 (s, 4H, $ArCH_2CH_2Ar$).

Photolysis of 44 in Various Solvents. In a typical experiment, 100 mg **44** in 200 mL solvent(s) was irradiated for 1-2h. After the normal work-up described as above, the product mixture was subjected to GC and ^{1}H NMR analysis. Product **45** was identified by comparison with an authentic sample. For analytical runs, 20 mg of **44** in a 100 mL solution was photolysed and aliquots were removed and analyzed by GC (after normal work up).

4.5.4 Quantum Yield Measurements

Quantum yields were measured using 280 nm excitation from the output of an Oriel 200 W Hg lamp filtered through an Applied Photophysics monochromator and a 254-400 bandpass filter. Solutions (10^{-3} M) were prepared in 3 mL quartz cuvettes and purged with a stream of argon prior to photolysis. Potassium ferrioxalate was used for chemical actinometry.[97] The details of this technique are described in Appendix C. After photolysis, the sample was saturated with NaCl and then extracted several times CH_2Cl_2. The conversion (kept <15%) and yields were analyzed by GC. Excellent material balances were observed, as determined using naphthalene as an internal standard. GC responses of starting materials and

products were essentially identical, except for **41**, where a correction factor for GC response was applied.

4.5.5 Fluorescence Measurements

Fluorescence emission spectra (uncorrected) were taken in 3.0 mL quartz cuvettes at about 10^{-4} M using a Perkin-Elmer MRF 66 spectrophotometer at ambient temperature. The fluorescence quantum yield of **26** in 1:1 H_2O-CH_3CN was measured using diphenyl ether (Φ_f = 0.03 in cyclohexane)[99] as secondary fluorescence standard. Optical densities at λ_{ex} = 260 nm were matched prior to measurement. Fluorescence lifetimes were measured at room temperature on a standard single photon counting instrument (Photo Technology International (PTI) LS-1 spectrofluorimeter equipped with single photon electronics) using a hydrogen spark lamp as excitation source. Decays were analyzed using software supplied by PTI and were also first order ($\chi^2 < 1.4$).

4.5.6. Triplet State Sensitization

For a typical experiment, a solution of 2 mg **26** in 1:1 acetone-H_2O (150 mL) was irradiated at 300 nm for 30 min with argon purge. At 300 nm, the sensitizer acetone absorbed over 95% irradiation. After photolysis, the solution was condensed, saturated with NaCl (2 g), and then extracted with CH_2Cl_2 (3 x 100 mL). The combined organic layers were evaporated and the residue analyzed by

GC and ^{1}H NMR. In all runs, no photoproducts were formed and the starting materials were recovered completely unchanged.

CHAPTER FIVE: Summary and Future Work

5.1 General Remarks

This thesis presented the exploratory studies of three classes of photoreactions and the interpretation of the corresponding mechanisms. The most interesting issues addressed in this thesis were structure-reactivity relationships and pH and solvent effects on photochemical mechanisms. For instance, structure vs reactivity studies revealed that the interaction of two reactive groups within the same molecule (bifunctional substrate) promoted interesting photochemical cyclization reactions, as demonstrated in the photocyclization of **1** (see Chapter Two). It was found that a unique assembly of phenoxy and hydroxymethyl functional groups was a necessary requirement for photocyclization of **22** (see Chapter Three). Also, biphenyl alcohol **1** and related derivatives (**5-6, 19**), with twisted ground state geometry, were found to take full advantage of enhanced planarity and the electron-rich phenolate ion in the lowest excited states to accomplish a new photocyclization reaction (see Chapter Two). The corresponding thermal counterpart to this reaction requires much harsher condition for the thermal cyclization. The studies also showed that the pH of the medium not only significantly affected the product quantum yields (see Chapter Two), but altered the primary photochemical process (see Chapter Three). As for the solvent effect, we have shown that use of water - a poor hydrogen donor, but a highly polar medium

- can remarkably enhance photochemical reactions, either by stabilizing the reactive transition state or affecting fates of photogenerated reactive intermediates (see Chapter Four). In addition, unusual rearrangements of the phenyl/phenoxyl biradical and a novel photochemical approach to reactive intermediates such as *o*-dibenzo-quinonemethide or o-dibenzoquinone were also disclosed. The research presented in this thesis opens up several new areas for the future work, especially the photochemistry of biphenyl systems as will be discussed below.

5.2 Suggestions for Future Studies

As mentioned previously, the current study covered several important areas of current interest in mechanistic organic photochemistry and physical organic chemistry, namely the photogeneration and reactivity of cationic, radical and neutral reactive intermediates. With the advent of laser flash photolysis techniques which have recently become more accessible, there has been more and more research directed towards obtaining the transient absorption spectra of these elusive species and to investigate their reaction dynamics. In view of this trend it would be worthwhile to study all of the above photoreactions via laser flash photolysis. In addition, three other areas seem to hold promise, as outlined below.

First, as discussed previously, *o*-quinonemethide **20** has not been described in the literature yet. This elusive intermediate is probably very short-lived (in the picosecond time domain), due to the rapid ring-closure to give pyran **7**. Thus

direct evidence is needed to prove its existence. Picosecond laser flash photolysis might provide a useful approach to detect its transient absorption, which should be in visible region (400-450 nm). The ideal precursors to generate this species would be alcohol **1** and pyran **7** since their photochemistry has been shown to be very straightforward (eq. 5.1). In order to maximize the quantum efficiency as well as its lifetime, the solvent should be polar and of very weak nucleophilicity, such as 1,1,1,3,3,3-hexafluoroisopropanol (HFIP).

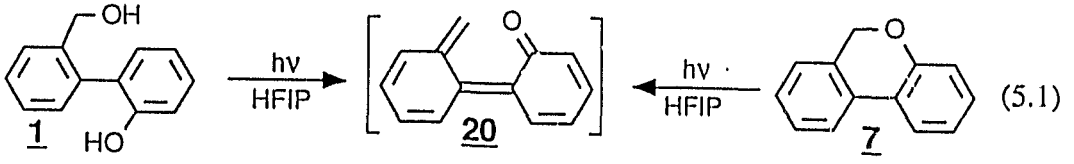

1 **20** **7** (5.1)

Secondly, in order to test the proposed *charge transfer* mechanism and to examine the substituent effect on the efficiency for photosolvolyses of biphenyls, 2-(3'- or 4'-substituted phenyl)benzyl alcohols **55-58** are ideal precursors in this

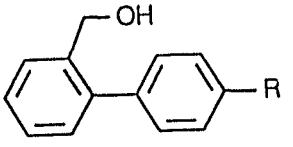

55 R = OMe
56 R = OH

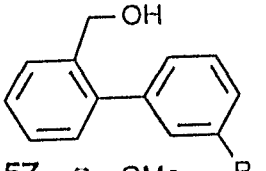

57 R = OMe
58 R = OH

regard. These alcohols, like some simple benzyl alcohols,[22,23,29] might exhibit

appreciable photosolvolytic reactivity and substituent effects. For example, in the photosolvolyses of simple methoxybenzyl alcohols, a "*meta*-effect" has been observed.[6,22,23] For the biphenyl system, 2-(2'-hydroxyphenyl)benzyl alcohol (1) has been shown to undergo efficient photosolvolysis, whereas 2-(2'-methoxyphenyl)benzyl alcohol (4) does not exhibit any enhanced photosolvolytic efficiency. The reason for this might be due to steric hindrance towards approach to a more planar geometry. Therefore it will be of interest to examine if substituents such as OMe or OH placed at the 3'- or 4'- positions can impose any charge transfer or electron-donating effect on photosolvolysis in substrates **55-58**. In addition, a logical extension of this work is to study intramolecular photoredox reactions of biphenyls with the nitro group at the at 3' or 4'-position. Simple *meta*- or *para*-nitro-benzyl alcohols have been shown to undergo intramolecular photoredox reaction in aqueous solution (eq. 5.2 and 5.3).[120] Thus, 3'- or 4'- nitro-substituted biphenyls **59** and **60** might also exhibit similar photochemistry.

Finally, as demonstrated in the photoisomerization of **26** and derivative **42**, photogenerated phenyl/phenoxy biradicals can induce a novel rearrangement. This new pathway for such biradicals may be generally applicable to other xanthene derivatives. Thus, further studies in these systems might provide more information on structure vs reactivity of phenyl/phenoxy biradicals.

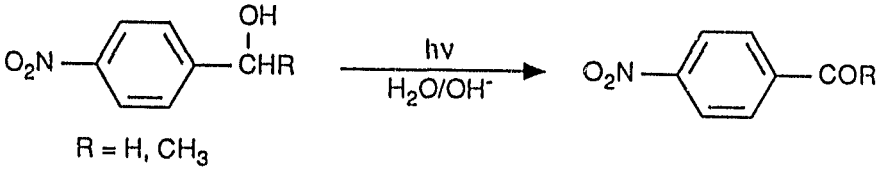
OH
O_2N
CHR
hν
H_2O/OH^-
O_2N
COR
R = H, CH_3

(5.2)

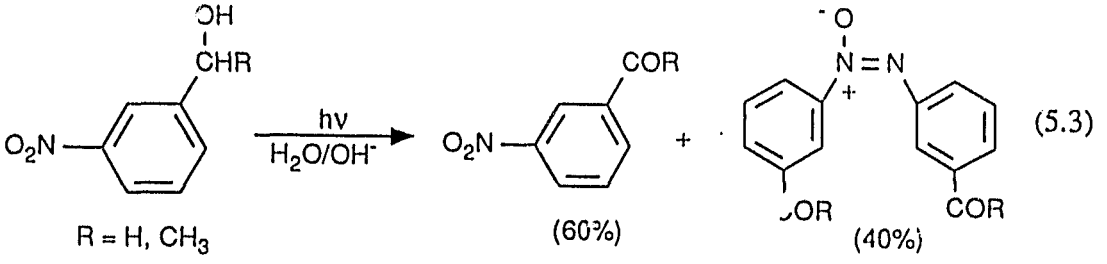
OH
CHR
O_2N
hν
H_2O/OH^-
R = H, CH_3
O_2N
COR
(60%)
+
O
N=N
+
COR
OR
(40%)

(5.3)

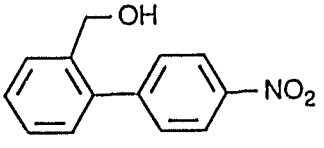
OH
NO_2

59

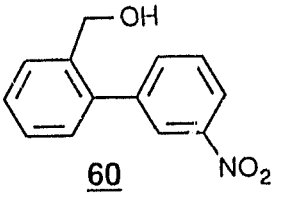
OH
NO_2

60

APPENDIX A

SELECTED BOND LENGTHS AND ANGLES OF ALCOHOLS 1 AND 6

Table A-1 Interatomic Distances (Å) of Crystal Structure of **1**.

Atoms	Distance	Atoms	Distnce
C (2) -C (1)	1.403 (16)	C (8) -C (7)	1.392 (13)
C (6) -C (1)	1.425 (13)	C (12) -C (7)	1.392 (13)
C (1) -C (1)	1.406 (13)	C (9) -C (8)	1.395 (15)
C (3) -C (2)	1.404 (13)	C (13) -C (8)	1.475 (13)
C (4) -C (3)	1.302 (15)	C (10) -C (9)	1.376 (17)
C (5) -C (4)	1.421 (15)	C (11) -C (10)	1.428 (16)
C (6) -C (5)	1.387 (13)	C (12) -C (11)	1.315 (18)
C (7) -C (6)	1.504 (9)	O (2) -C (13)	1.459 (13)

Estimated standard deviations are given in parentheses.

Table A-2 Interatomic Distances (Å) of Crystal Structure of **6**.

Atoms	Distance	Atoms	Distnce
C (2) -C (1)	1.409 (3)	C (12) -C (7)	1.4052 (3)
C (6) -C (1)	1.402 (3)	C (9) -C (8)	1.394 (3)
C (13) -C (1)	1.542 (3)	O (1) -C (8)	1.370 (2)
C (3) -C (2)	1.403 (3)	C (10) -C (9)	1.397 (3)
C (7) -C (2)	1.506 (3)	C (11) -C (10)	1.397 (4)
C (4) -C (3)	1.383 (3)	C (12) -C (11)	1.371 (3)
C (5) -C (4)	1.374 (4)	C (14) -C (13)	1.517 (4)
C (6) -C (5)	1.385 (4)	C (15) -C (13)	1.529 (4)
C (8) -C (7)	1.394 (3)	C (2) -C (13)	1.449 (3)

Estimated standard deviations are given in parentheses.

Table A-3 Bond Angles of Crystal Structure of **1**

Atoms	Angle	Atoms	Angle
C(6) -C(1) -C(2)	117.1(9)	C(12) -C(7) -C(6)	119.9(9)
C(1) -C(1) -C(2)	123.0(9)	C(12) -C(7) -C(8)	117.2(10)
C(6) -C(1) -C(6)	119.8(9)	C(9) -C(8) -C(7)	120.2(10)
C(3) -C(2) -C(1)	118.9(10)	C(13) -C(8) -C(7)	116.4(9)
C(4) -C(3) -C(2)	125.2(10)	C(13) -C(8) -C(9)	123.2(10)
C(5) -C(4) -C(3)	116.8(10)	C(10) -C(9) -C(8)	122.7(10)
C(6) -C(5) -C(4)	121.2(10)	C(11) -C(10) -C(9)	113.8(11)
C(5) -C(6) -C(1)	120.1(10)	C(12) -C(11) -C(10)	124.3(12)
C(7) -C(6) -C(1)	120.4(9)	C(11) -C(12) -C(7)	121.0(10)
C(7) -C(6) -C(5)	119.2(9)	O(2) -C(12) -C(7)	107.7(9)
C(8) -C(7) -C(6)	122.9(9)		

Estimated standard deviations are given in parentheses.

Table A-4 Bond Angles of Crystal Structure of 6

Atoms	Angle	Atoms	Angle
C(6) -C(1) -C(2)	117.6(2)	C(9) -C(8) -C(7)	120.8(2)
C(13) -C(1) -C(2)	123.7(2)	C(1) -C(8) -C(7)	117.2(2)
C(13) -C(1) -C(6)	118.7(2)	C(1) -C(8) -C(9)	122.0(2)
C(3) -C(2) -C(1)	119.0(2)	C(10) -C(9) -C(8)	119.8(2)
C(7) -C(2) -C(1)	127.2(2)	C(11) -C(10) -C(9)	119.7(2)
C(7) -C(2) -C(3)	113.9(2)	C(12) -C(11) -C(10)	120.3(2)
C(4) -C(3) -C(2)	113.9(2)	C(11) -C(12) -C(7)	121.8(2)
C(5) -C(4) -C(3)	119.1(2)	C(14) -C(13) -C(1)	112.3(2)
C(6) -C(5) -C(4)	119.7(2)	C(15) -C(13) -C(1)	113.5(2)
C(5) -C(6) -C(1)	122.4(2)	C(15) -C(13) -C(14)	109.4(2)
C(8) -C(7) -C(2)	122.9(2)	O(2) -C(13) -C(1)	108.9(2)
C(12) -C(7) -C(2)	118.9(2)	O(2) -C(13) -C(14)	108.6(2)
C(12) -C(7) -C(8)	117.8(2)	O(15) -C(13) -C(15)	103.8(2)

Estimated standard deviations are given in parentheses.

APPENDIX B

SELECTED BOND LENGTHS AND ANGLES OF 9,9'-BIXANTHYL (41)

Table B-1 Interatomic Distances (Å) of Crystal Structure of **41**.

Atoms	Distance	Atoms	Distnce
C (11) -C (1)	1.337 (4)	C (7) -C (6)	1.369 (6)
C (12) -O (1)	1.379 (4)	C (8) -C (7)	1.383 (6)
C (2) -C (1)	1.371 (5)	C (13) -C (8)	1.396 (5)
C (11) -C (1)	1.391 (5)	C (10) -C (9)	1.506 (5)
C (3) -C (2)	1.386 (5)	C (13) -C (9)	1.509 (5)
C (4) -C (3)	1.378 (6)	C (9) -C (9)	1.584 (7)
C (10) -C (4)	1.405 (5)	C (9) -C (9)	1.386 (5)
C (6) -C (5)	1.386 (6)	C (11) -C (10)	1.379 (5)
C (12) -C (5)	1.384 (5)		

Estimated standard deviations are given in parentheses.

Table B-2 Bond Angles of Crystal Structure of **41**

Atoms	Angle	Atoms	Angle
C(12) -C(1) -C(11)	118.1(3)	C(11) -C(10) -C(4)	117.3(3)
C(11) -C(1) -C(2)	119.7(4)	C(11) -C(10) -C(9)	120.(3)
C(3) -C(2) -C(1)	119.8(4)	C(1) -C(11) -C(1)	115.6 (3)
C(4) -C(3) -C(2)	120.5(4)	C(10) -C(11) -C(1)	122.5(3)
C(10) -C(4) -C(3)	120.8(4)	C(10) -C(11) -C(1)	121.9(3)
C(12) -C(5) -C(6)	119.2(4)	C(5) -C(12) -C(1)	115.9(3)
C(7) -C(6) -C(5)	121.0(4)	C(13) -C(12) -C(1)	122.5(3)
C(8) -C(7) -C(6)	119.6(4)	C(13) -C(12) -C(5)	121.6(3)
C(13) -C(8) -C(7)	120.9(4)	C(9) -C(13) -C(8)	121.6(3)
C(13) -C(9) -C(10)	110.4(4)	C(12) -C(13) -C(8)	117.7(3)
C(9) -C(10) -C(4)	122.4(4)	C(12) -C(13) -C(9)	120.4(3)

Estimated standard deviations are given in parentheses.

APPENDIX C

POTASSIUM FERRIOXALATE AS A CHEMICAL ACTINOMETER

The potassium ferrioxalate chemical actinometer, used to measure light intensity (i.e., the number of incident photons), was developed by Parker and Hatchard.[97] Irradiation of $K_3Fe(C_2O_4)_3$ dissolved in dilute sulfuric acid leads to the reduction of the ion into Fe^{2+} along with oxidation of an oxalate ion. The product ferreous ion formed during photolysis is analyzed by measuring the absorbance of its highly coloured $Fe(phen)_3^{2+}$ (where phen = 1, 10-phenanthroline) complex. The quantum yields of this photoreaction have been accurately determined at various excitation wavelengths (over 250 -500 nm) by a number of authors.[97] A typical procedure for light intensity measurement is given below.

3.0 mL (V_1) of the stock solution of 0.006 M $K_3Fe(C_2O_4)_3$ in 0.1 N sulfuric acid was transferred into two UV cuvettes. One of these was irradiated at 280 nm for 5.0 min (Δt) under a stream of argon. The other was put under the dark without irradiation and serves as a blank. Both solutions were worked up in the same manner as follows. 1.0 mL (V_2) of each solution was taken from the cuvettes into a 10 mL (V_3) volumetric flask. 2.0 mL of a 0.1% (weight) solution of 1,10-phenanthroline in water and 0.5 mL of a buffer solution (prepared from 41.0 g $NaOAc.3H_2O$ and 5 mL H_2SO_4 in 1 L) was added to this flask. The volume was adjusted into 10.0 mL with distilled water and the solutions were mixed and let stand for half of hour. The absorbance of the irradiated and blank solutions was

then determined at 510 nm. The difference (ΔA) was employed to calculate the number of einsteins of incident light absorbed by potassium ferrioxalate (where $\varepsilon = 1.11 \times 10^4$ and $\Phi_{Fe2+} = 1.25$ at 280 nm).[97] When all photolysis was carried out using 3.0 mL of solution, the light intensity calculated is per cuvette per min, as shown in the following equation.

$$\text{einsteins/cuvette/min} = \frac{\Delta A \; V_1 \; V_3}{\varepsilon \; \Phi_{Fe2+} \; V_2 \; \Delta t}$$

References

1. S. J. Cristol and T. H. Bindel, *Org. Photochem.*, **6**, 327 (1983).
2. P. Wan and D. Shukla, *Trends in Organic Chemistry*, in preparation.
3. A. Hantzsch and G. Osswald, *Ber.*, **33**, 278 (1900).
4. J. Lifschitz, *Ber.*, **52**, 1919 (1919).
5. J. Lifschitz and C. L. Joffe, *Z. Physik. Chem.*, **97**, 426 (1921).
6. H. E. Zimmerman and V. R. Sandel, *J. Am. Chem. Soc.*, **85**, 915 (1963).
7. R. Grinter, E. Heilbronner, T. Petrzilka and P. Seiler, *Tetrahedron Lett.*, **35**, 3845 (1968).
8. P. V. Seiler and J. Wirz, *Tetrahedron Lett.*, 1683 (1971).
9. P. V. Seiler and J. Wirz, *Helv. Chim. Acta.*, **55**, 2693 (1972).
10. S. J. Cristol and G. C. Schloemer, *J. Am. Chem. Soc.*, **94**, 5916 (1972).
11. S. J. Cristol, R. P. Mitchell, *J. Org. Chem.*, **40**, 667 (1975).
12. S. J. Cristol and R. P. Mitchell, *J. Am. Chem. Soc.*, **100**, 850 (1978).
13. (a) D. A. Jaeger, *J. Am. Chem. Soc.*, **98**, 6401 (1976); (b) S. J. Cristol, M. B. Ali and I. V. Sankar, *J. Am. Chem. Soc.*, **111**, 8207 (1989) and references cited herein; (c) H. Morrison, *Rev. Chem. Intermed.*, **8**, 125 (1987).
14. P. J. Kropp, *Acc. Chem. Res.*, **17**, 131 (1984).
15. P. J. Kropp and R. L. Adkins, *J. Am. Chem. Soc.*, **113**, 2709 (1991).
16. P. J. Kropp, P. R. Worsham, R. I. Davidson and T. H. Jones, *J. Am. Chem. Soc.*, **104**, 3972 (1982).

17. D. S. Reddy, G. P. Sollott and P. E. Eaton, *J. Org. Chem.*, **54**, 722 (1989).

18. P. Wan, K. Yates and M. K Boyd, *J. Org. Chem.*, **50**, 93 (1985).

19. P. Wan, *J. Org. Chem.*, **50**, 2853 (1985).

20. C. -G. Huang, K. A. Beveridge and P. Wan, *J. Am. Chem. Soc.*, In press (1991).

21. C. -I. Lin, P. Singh and E. F. Ullman, *J. Am Chem. Soc.*, **98**, 6711 (1976).

22. N. J. Turro and P. Wan, *J. Photochem.*, **28**, 93 (1985).

23. P. Wan and B. Chak, *J. Chem. Soc, Perkin Trans. II*, 1751 (1986).

24. For a general definition and discussion of energy surfaces and adiabatic/diabatic photoreactions, see: N. J. Turro, *Molecular Photochemistry*; Benjamin/Cummings: Menlo Park, 1978.

25. R. E. Minto and P. K. Das, *J. Am Chem. Soc.* **111**, 5471 (1989).

26. R. A. McClelland, N. Bannait and S. Steenken, *J. Am Chem. Soc.* **111**, 2929 (1989).

27. P. Wan and D. Shukla, Unpublished results.

28. P. Wan and E. Krogh, *J. Chem. Soc., Chem. Commun.*, 1027 (1985).

29. P. Wan and E. Krogh, *J. Am Chem. Soc.*, **111**, 4887 (1989).

30. E. Gaillard, M. A. Fox and P. Wan, *J. Am Chem. Soc.*, **111**, 2180 (1989).

31. S. L. Mecklenburg and E. F. Hilinski, *J. Am Chem. Soc.*, **111**, 5471 (1989).

32. R. A. McClelland, N. Mathivanan and S. Steenken, *J. Am Chem. Soc.*, **111**, 4857 (1989).

33. (a) D. M. Hall, "*Progress in Stereochemistry*", edited by B. J. Aylett and M. M. Harris, vol **4**, Butterworth, London, 1969. (b) R. M. Hochstrasser and H. N. Surg, *J. Chem. Phys.*, **66**, 3265 (1977).

34. R. M. G. Roberts, *Mag. Reso. Chem.*, **23**, 54 (1985).

35. F. Foweather and M. Traetteberg, *Acta. Crystallogr.*, **3**, 81 (1950).

36. P. Wan and C. -G. Huang, unpublished results.

37. P. J. Wagner, *J. Am Chem. Soc.*, **89**, 2820 (1967).

38. A. Imamura and R. Hoffmann, *J. Am Chem. Soc.*, **90**, 5379 (1968).

39. T. C. Werner, in *Modern Fluorescence Spectroscopy*, E. L. Wehry (ed.), Plenum Press, New York, 1976, p287.

40. H. E. Zimmerman and D. S. Crumrine, *J. Am Chem. Soc.*, **92**, 498 (1972).

41. K. Mislow and A. J. Gorden, *J. Am Chem. Soc.*, **85**, 3521 (1962).

42. Y. Takei, T. Yamaguchi, Y. Osamura, K. Fuke and K. Kaya, *J. Phys. Chem.*, **92**, 577 (1988).

43. W. H. Laarhoven, in *Organic Photochemistry*, edited by A. Padwa, vol **10**, Marcel Dekker, New York, 1989.

44. P. Fornier de Violet, R. Bonneau, R. Lapouyade, R. Koussini and W. R. Ware, *J. Am Chem. Soc.*, **100**, 6683 (1978).

45. R. Lapouyade, C. Manigand and A. Nourmamode, *Can. J. Chem.*, **63**, 2192 (1985).

46. S. Lazare, R. Lapouyade and R. Bonneau, *J. Am Chem. Soc.*, **107**, 6604

(1985).

47. R. Lapouyade, R. Koussini, A. Nourmamode and C. Courseille, *J. Chem. Soc. Chem. Comm.*, 740 (1980).

48. A. Bowd, D. A. Swan and J. H. Turnbull, *J. Chem. Soc., Chem. Comm.*, 797 (1975).

49. A. Bowd, J. H. Turnbull and J. D. Coyle, *J. Chem. Research (S)*, 202 (1980).

50. A. Padwa, M. J. Pulwer and R. J. Rosenthal, *Tetrahedron Lett.*, **24**, 983 (1983).

51. A. Padwa, C. Doubleday and A. Mazzu, *J. Org. Chem.*, **42**, 3271 (1977).

52. J. De Jong and J. H. Boyer, *J. Chem. Soc., Chem. Comm.*, 961 (1971).

53. J. S. Swenton, T. J. Ikeler and G. Le Roy Smyser, *J. Org. Chem.*, **38**, 1157 (1973).

54. (a) A. J. Lin, L. A. Cosby, C. W. Shansky and A. C. Sartorelli, *J. Med. Chem.*, **15**, 1247 (1972); (b) A. J. Lin, C. W. Shansky and A. C. Sartorelli, *J. Med. Chem.*, **17**, 558 (1974); (c) H. W. Moore, *Science*, **197**, 527 (1977).

55. (a) G. Desimoni and G. Tacconi, *Chem. Rev.*, **75**, 651 (1975); (b) A. B. Donald, *J. Org. Chem.*, **35**, 3666 (1970); (c) T. Inoue, S. Inoue and K. Sato, *Chem. Lett.*, 653 1989); (d) K. Kostas and W. M. Harold, *J. Am. Chem. Soc.*, **112**, 5372 (1990); (e) J. T. John, *J. Org. Chem.*, **50**, 1695 (1984).

56. R. S. Becker and J. Michl, *J. Am. Chem. Soc.*, **88**, 5931 (1966).

57. A. Padwa, A. Au, G. A. Lee and W. Owens, *J. Org. Chem.*, **43**, 303 (1978).

58. A. Padwa and G. A. Lee, *J. Chem. Soc., Chem. Comm.*, 795 (1972).

59. A. Padwa, A. Au, G. A. Lee and W. Owens, *J. Org. Chem.*, **40** 1142 (1975).

60. C. Lenoble and R. S. Becker, *J. of Photochem.*, **33**, 187 (1986).

61. P. Wan and C. -G. Huang, *J. Chem. Soc., Chem. Comm.*, 1193 (1988).

62. C. -G. Huang and P. Wan, *J. Org. Chem.*, **56**, 4846 (1991).

63. A. G. Schultz and L. Motyka, in *Organic Photochemistry*, edited by A. Padwa, vol **6**, Marcel Dekker, New York, 1983.

64. W. Carthers, *Chem. Commun.*, 202 (1966).

65. H. Shizuka, Y. Takayama, I. Tanaka and T. Morita, *J. Am. Chem. Soc.*, **92**, 7270 (1970).

66. E. W. Forster, K. H. Grellmann and H. Linschitz, *J. Am. Chem. Soc.*, **95**, 3108 (1973).

67. K. -P. Zeller and H. Petersen, *Synthesis*, 532 (1975).

68. J. A. Elix and D. P. Murphy, *Aust. J. Chem.*, **28**, 1559 (1975).

69. W. A. Henderson and A. Zweig, *Tetrahedron Lett.*, 625 (1969).

70. M. S. Kharasch, G. Stampa and W. Nudenberg, *Sciences*, **116**, 309 (1952).

71. D. P. Kelly, J. T. Pinhey and R. D. G. Rigby, *Tetrahedron Lett.*, 5953 (1966).

72. H. Stegenmeyer, *Naturwiss.*, **22**, 582 (1966).

73. H. I. Joschek and S. I. Miller, *J. Am. Chem. Soc.*, **88**, 3269 (1966).

74. Y. Ogata, K. Takagi and I. Ishino, *Tetrahedron*, **26**, 2703 (1970).

75. H. J. Hageman and W. G. B. Huysmans, *Tetrahedron*, **26**, 2045 (1970).

76. H. J. Hageman and W. G. B. Huysmans, *Recueil*, **91**, 528 (1972).

77. C. G. Huang, D. Shukla and P. Wan, *J. Org. Chem.*, in press (1991).

78. P. Wan and C. -G. Huang, unpublished results.

79. J. P. Delvin, *Can. J. Chem.*, **53**, 343 (1975).

80. G. W. Kenner, M. A. Murray and C. M. B. Taylor, *Tetrahedron*, **1**, 259 (1957).

81. P. M. Brown, J. Russell, R. H. Thompson and A. G. Wylie, *J. Chem. Soc. (C)*, 842 (1968).

82. H. Masada and Y. Murotani, *Bull. Chem. Soc. Jpn.*, **53**, 1181 (1980).

83. see reference 34, page..

84. P. Wan and C. -G. Huang, unpublished results.

85. L. M. Tolbert and J. E. Haubrich, *J. Am. Chem. Soc.*, **112**, 8163 (1990) and references quoted therein.

86. J. F. Ireland and P. A. H. Wyatt, *Adv. Phys. Org. Chem.*, **12**, 131 (1976).

87. I. Y. Martynov, *Russ. Chem. Rev.*, **46**, 7 (1977).

88. W. Klöpfer, *Adv. Photochem.*, **10**, 311 (1977).

89. J. F. Ireland and P. A. H. Wyatt, *J. Chem. Soc. Faraday*, **68**, 1053 (1972).

90. J. C. Haylock, *J. Chem. Soc.*, 4897 (1963).

91. E. S. Mansueto and C. A. Wight, *J. Am. Chem. Soc.*, **111**, 1900 (1989).

92. J. R. Lakowicz, *Principles of Fluorescence Spectroscopy;* Plenum Press, New York, 1983.

93. (a) S. L. Murov, *Handbook of Photochemistry*, M. Dekker, New York, 1973. (b) J. C. Scaiano (ed.), *Handbook of Organic Photochemistry*, Vol. 1, CRC Press: Boca Raton, 1989.

94. P. Main, *Multan: Programme for the Automatic Solution of Crystal Structures from X-ray Diffraction Data by Multiple Starting Point Tangent Formula;* University of York: York, England, 1978.

95. G. M. Sheldrick, *SHELX-76, Program for Crystal Structure Determination;* University of Cambridge: Cambridge, England, 1976.

96. C. K. Johnson, ORTEPII, Report ORNL-5138; Oak Redge National Laboratory: Oak Ridge, TN, 1976.

97. C. G. Hatchard and C. A. Parker, *Proc. R. Soc. London, Ser, A*, 235, 518 (1956).

98. Refer to reference 23 (similar results were obtained by using 2,5-dimethoxylbenzyl alcohol (Φ = 0.31) as secondary standard).

99. I. B. Berlman, *Handbook of Fluorescence Spectra of Aromatic Molecules*, 2nd, Academic Press, New York, 1971, p185.

100. G. W. K. Cavill, F. M. Dean. J. F. E. Keenan, A. McGookin, A. Robertson and G. B. Smith, *J. Chem. Soc.*, 1544 (1958).

101. J. Bartl, S. Steenken, H. Mayr and R. A. McClelland, *J. Am Chem. Soc.*, **112**, 6918 (1990).

102. J. W. Thompson and J. Gaudino, *J. Org. Chem.*, **49**, 5237 (1984).

103. J. Fu, M. J. Sharp and V. Snieckus, *Tetrahedron Letters*, **29**, 5459 (1988) and references quoted therein.

104. T. Iihaman, J. Fu, M. Bourguinon and V. Snieckus, *Synthesis*, 184 (1989).

105. J. F. W. McOmie and D. E. West, *Org. Synth. Coll Vol V*, 412 (1973).

106. S. Muralidharan and P. Wan, *J. Chem. Soc., Chem. Commun.*, 1142 (1987).

107. D. Shukla, F. de Rege, P. Wan and L. Johnston, *J. Phys. Chem.*, in press, 1991.

108. P. Wan and D. Budac, personnel communication.

109. D. S. Frohlinde and F. Erhardt, *Ann.*, **671**, 92 (1964).

110. C. J. R. Adderley and F. R. Hewgill, *J. Chem. Soc. (C)*, 1434 (1968).

111. C. Grundmann, *Syn. Commun.*, 644 (1977).

112. H. D. Becker and K. Gustafsson, *Tetrahedron Letters*, **52**, 4883 (1983).

113. H. D. Becker, *J. Org. Chem.*, **34**, 169 (1989).

114. G. Trampe, J. Mattay and S. Steenken, *J. Phys. Chem.*, **93**, 7157 (1989).

115. E. Vauthey, E. Haselbach and P. Suppan, *Helv. Chim. Acta.*, **70**, 347 (1987).

116. M. O. Delcourt and M. Rossi, *J. Phys. Chem.*, **86**, 3233 (1983).

117. R. Masse and B. Pelletier, *Chemosphere*, **16**, 7 (1987).

118. I. T. Badejo, R. Karaman, A. A. Pinkerton and J. L. Fry, *J. Org. Chem.*, **55**,

4327 (1990).

119. *Dictionary of Organic Compounds*, 5th ed., Chapman and Hall, New York, 1982.